

Integrable Dynamics in Projective Geometry via Dimers and Triple Crossing Diagram Maps on the Cylinder

Niklas Christoph AFFOLTER^{abc}, Terrence GEORGE^d and Sanjay RAMASSAMY^e

- a) *Technische Universität Berlin, Institute of Mathematics,
Strasse des 17. Juni 136, 10623 Berlin, Germany*
- b) *Département de mathématiques et applications, École Normale Supérieure,
CNRS, PSL University, 45 rue d'Ulm, 75005 Paris, France*
- c) *Institute of Discrete Mathematics and Geometry, TU Wien,
Wiedner Hauptstraße 8–10/104, 1040 Wien, Austria*
E-mail: niklas.affolter@tuwien.ac.at
URL: <https://sites.google.com/view/niklasaffolter/>
- d) *Department of Mathematics, UCLA, 520 Portola Plaza, Los Angeles, CA 90095, USA*
E-mail: tegeorge@math.ucla.edu
URL: <https://terrencegeorge.github.io>
- e) *Université Paris-Saclay, CNRS, CEA, Institut de Physique Théorique,
91191 Gif-sur-Yvette, France*
E-mail: sanjay.ramassamy@ipht.fr
URL: <https://www.normalesup.org/~ramassamy/>

Received December 23, 2024, in final form May 20, 2025; Published online June 03, 2025

<https://doi.org/10.3842/SIGMA.2025.040>

Abstract. We introduce twisted triple crossing diagram maps, collections of points in projective space associated to bipartite graphs on the cylinder, and use them to provide geometric realizations of the cluster integrable systems of Goncharov and Kenyon constructed from toric dimer models. Using this notion, we provide geometric proofs that the pentagram map and the cross-ratio dynamics integrable systems are cluster integrable systems. We show that in appropriate coordinates, cross-ratio dynamics is described by geometric R -matrices, which solves the open question of finding a cluster algebra structure describing cross-ratio dynamics.

Key words: discrete integrable systems; dimer model; cluster algebras; pentagram map; triple crossing diagram maps

2020 Mathematics Subject Classification: 37J70; 82B20; 13F60

1 Introduction

A widely studied class of discrete systems which are integrable both in the algebro-geometric sense and in the Liouville sense is the cluster integrable systems of Goncharov and Kenyon [23]. Cluster integrable systems are constructed from the dimer model on bipartite graphs on the torus coming from statistical mechanics. The class of cluster integrable systems was shown to contain many other integrable systems [14], several of which have geometric origins as moduli spaces of points in projective space. The most prominent example of such an integrable system is the pentagram map, discovered by Schwartz [44]. However, proofs of the coincidence of such

a geometric integrable system with some cluster integrable system are essentially algebraic; they involve constructing isomorphisms between the two integrable systems using coordinates.

The main idea of this paper is that one can actually provide a more geometric identification by making use of a generalization of the recently introduced triple crossing diagram maps (TCD maps) [1, 2], which we call *twisted TCD maps*. We develop the general theory of twisted TCD maps and show that any cluster integrable system can be realized as a geometric integrable system. A key role is played by the monodromy matrix, which provides a robust and systematic way to compute the conserved quantities (Hamiltonians and Casimirs) of these geometric integrable systems and relate them to the conserved quantities of cluster integrable systems.

We then use the theory to show that the pentagram map and the cross-ratio dynamics integrable system of [4] are cluster integrable systems. For cross-ratio dynamics, this is a completely new result and this answers an open question asked in [4]. For the pentagram map, its cluster algebra structure was identified with that of a dimer model in [1]. In this paper, we illustrate the power of the framework of twisted TCD maps by providing a new derivation of the Hamiltonians and Casimirs of the pentagram map. This new derivation is faster than the classical ones [41, 46] once we have the theory of twisted TCD maps. We expect that the geometric integrable systems arising from twisted TCD maps should encompass a large part (if not all) of the class of Y-meshes of [21], which is one of the broadest generalizations of the pentagram map.

1.1 Twisted TCD maps

The phase space of the cluster integrable system is an \mathcal{X} cluster variety constructed from bipartite graphs in the torus as follows (see Section 2 for more details). Let Γ be a bipartite graph in the torus $\mathbb{T} := \mathbb{R}^2/\mathbb{Z}^2$ satisfying a certain minimality condition. Associated to Γ is the space $\mathcal{L}_\Gamma := H^1(\Gamma, \mathbb{C}^\times)$ of weights on it, where a weight $[\text{wt}]$ is a cohomology class assigning to every homology class $[L] \in H_1(\Gamma, \mathbb{Z})$ a nonzero complex number $[\text{wt}]([L])$. Two such graphs are *move-equivalent* if they are related by the two moves shown on the left and middle of Figure 4. Move-equivalence classes of (minimal) bipartite graphs are classified by convex integral polygons N in the plane; if Γ is in the move-equivalence class of N , we write $N(\Gamma) = N$. Each move $\Gamma \rightarrow \Gamma'$ induces a birational map of weights $\mathcal{L}_\Gamma \rightarrow \mathcal{L}_{\Gamma'}$; for the spider move, the map is given by the mutation formula for cluster X -variables [13] or y -variables [15] depending on the authors. Gluing all the \mathcal{L}_Γ in the move-equivalence class, we get the \mathcal{X} cluster variety \mathcal{X}_N . Goncharov and Kenyon identified a Poisson structure on \mathcal{X}_N , generalizing the cluster Poisson structure of [16]. Associated to $(\Gamma, [\text{wt}])$ is a periodic finite-difference operator $K(z, w)$ called the Kasteleyn matrix whose determinant $P(z, w)$ is a bivariate polynomial whose coefficients are weighted enumerations of dimer covers with prescribed homology. The curve defined by this polynomial is called the *spectral curve*. Goncharov and Kenyon showed that \mathcal{X}_N is a Liouville integrable system whose Hamiltonians and Casimirs are coefficients of the polynomial defining the spectral curve. We will henceforth call them the GK Poisson structures, Casimirs and Hamiltonians.

A twisted TCD map lives in the infinite cylinder $\widehat{\mathbb{A}} := \mathbb{R}^2/\mathbb{Z}(0, 1)$. By using the contraction-uncontraction move, we may assume that every black vertex in Γ has degree 3. Let $\Gamma_{\widehat{\mathbb{A}}}$ denote the infinite periodic graph that is the preimage of Γ under the quotient map $\widehat{\mathbb{A}} \rightarrow \mathbb{T}$. A *TCD map* is a function $P: W(\Gamma_{\widehat{\mathbb{A}}}) \rightarrow \mathbb{CP}^d$ assigning to every white vertex in $\Gamma_{\widehat{\mathbb{A}}}$ a point in \mathbb{CP}^d such that for every black vertex b incident to white vertices w_1, w_2, w_3 , the points P_{w_1}, P_{w_2} and P_{w_3} are contained in a line $\mathbb{CP}^1 \subseteq \mathbb{CP}^d$ [2]. These maps are a version of the vector-relation configurations of [1] better adapted to geometric dynamics. A TCD map P is called *twisted* if there is an $M \in \text{PGL}_{d+1}$, called the *monodromy matrix*, such that $P_{w+(1,0)} = M(P_w)$, where $w + (1, 0)$ denotes the translate of w . A twisted TCD map defines a weight $[\text{wt}]$ on Γ as follows. Let L be a closed loop in Γ such that $[L] \in \{0\} \times \mathbb{Z}$, i.e., which has zero homology in the

horizontal direction. Let $\tilde{L} = w_1 \rightarrow b_1 \rightarrow w_2 \rightarrow b_2 \rightarrow \cdots \rightarrow w_n \rightarrow b_n \rightarrow w_1$ denote any lift of L to $\Gamma_{\hat{\mathbb{A}}}$ such that $w_i \neq w_{i+1}$ for every i . Let w'_i denote the third white vertex incident to b_i that is not in $\{w_i, w_{i+1}\}$. Then,

$$[\text{wt}]([L]) := \pm \text{mr}(P_{w_1}, P_{w'_1}, P_{w_2}, P_{w'_2}, \dots, P_{w_n}, P_{w'_n}),$$

where \pm denotes an explicit sign, and

$$\text{mr}(P_1, \dots, P_{2m}) := \frac{\prod_{i=1}^m (P_{2i-1} - P_{2i})}{\prod_{i=1}^m (P_{2i} - P_{2i+1})}$$

is a PGL_{d+1} -invariant generalizing the cross-ratio called the *multi-ratio*. Note that PGL_{d+1} -invariance of the multi-ratio and the twisted condition imply that $[\text{wt}]([L])$ is independent of the choice of lift \tilde{L} . The two moves in Figure 4 induce transformations of TCD maps that give rise to the birational maps of weights described above; see Figure 9.

In Section 3.1, we construct from a weighted bipartite graph on the torus $(\Gamma, [\text{wt}])$ a matrix $\Pi(w)$. In Section 4.1, we use Kasteleyn theory in the cylinder to construct from $(\Gamma, [\text{wt}])$ and a choice of zig-zag path a TCD map P on $\hat{\mathbb{A}}$. Our first main result is the following.

Theorem 1.1 (cf. Theorem 4.6). *The TCD map P is a twisted TCD map with monodromy $-\Pi(1)$.*

In other words, the construction of $[\text{wt}]$ from a twisted TCD map by taking multi-ratios has a (left) inverse. Hamiltonians and Casimirs in geometric integrable systems are typically constructed as invariants of the monodromy matrix M [16, 34, 41, 46]. By definition, the GK Hamiltonians and Casimirs are coefficients of the spectral curve. Therefore, the following theorem turns out to be the key to proving that Hamiltonians and Casimirs in geometric integrable systems coincide with their GK counterparts.

Theorem 1.2 (cf. Theorem 3.6). *The spectral curve of the dimer model on an arbitrary minimal graph Γ on the torus is given by*

$$\{(z, w) \in (\mathbb{C}^\times)^2 \mid \det(zI + \Pi(w)) = 0\}.$$

The matrix $-\Pi(w)$ is closely related to the boundary measurement matrix for networks on cylinders of [16, 18], as detailed in Remark 3.3. In a recent preprint of which we learned during the completion of this work, Izosimov [28] made precise the connection between the integrable systems of [23] and [16]. In particular, his main result provides a representation of the dimer spectral curve similar to Theorem 1.2. We note that analogous representations have appeared in physics in the special case of the periodic Toda chain [11] and in mathematical physics via representation-theoretic arguments [14].

1.2 The pentagram map

Our first application is to the pentagram map, a discrete dynamical system discovered by Richard Schwartz [44], proved to be Liouville and discrete integrable in [41, 42] and algebro-geometric integrable in [46]. Glick [20] discovered an underlying cluster algebra structure (see also [45]). Gekhtman, Shapiro, Tabachnikov and Vainstein [16] generalized the pentagram map and related it to the integrable systems associated to weighted networks in a torus [18]. The pentagram map was further generalized to the noncommutative setting [40] and to general algebraically closed fields [49].

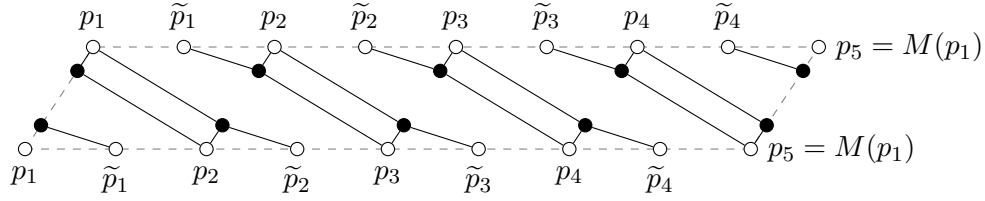


Figure 1. Twisted TCD map for the pentagram map with $n = 4$, where $\tilde{p}_i := \overline{p_{i-1}p_i} \cap \overline{p_{i+1}p_{i+2}}$.

A *twisted n -gon* in \mathbb{CP}^2 is a pair (p, M) where $p: \mathbb{Z} \rightarrow \mathbb{CP}^2$ and $M \in \text{PGL}_3$ is a projective transformation called *monodromy* such that $p_{i+n} = M(p_i)$ for all $i \in \mathbb{Z}$. The phase space of the pentagram map is the moduli space \mathcal{T}_n of twisted n -gons satisfying a nondegeneracy condition. The rational map $T: \mathcal{T}_n \rightarrow \mathcal{T}_n$ defined by $(p, M) \mapsto (q, M)$, where $q_i = \overline{p_{i-1}p_{i+1}} \cap \overline{p_i p_{i+2}}$ is called the *pentagram map*.

In Section 5, we construct a twisted TCD map on a bipartite torus graph denoted Ξ_n for the pentagram map (see Figure 1 for the twisted TCD map when $n = 4$). The coordinates of Schwartz [45] and Glick [20] can be obtained from the twisted TCD map by taking weights of appropriate cycles. Using the correspondence between twisted TCD maps and the \mathcal{X} cluster variety \mathcal{X}_{Ξ_n} associated to the graph Ξ_n , we show the following.

Theorem 1.3 (cf. Proposition 5.3 and Theorem 5.6). *The map sending the twisted TCD map P to the twisted n -gon p induces a Poisson birational map $\pi_n: \mathcal{X}_{\Xi_n}^\lambda \rightarrow \mathcal{T}_n$ that restricts to a birational isomorphism between symplectic leaves on the two sides. The GK Hamiltonians are the pullbacks of the pentagram map Hamiltonians by π_n .*

Here, $\mathcal{X}_{\Xi_n}^\lambda$ is a level set of \mathcal{X}_{Ξ_n} where we set a GK Casimir equal to $\lambda \in \mathbb{C}^\times$ and by a birational isomorphism, we mean a birational map that preserves the symplectic structure. Almost all of Theorem 1.3 is well known; see [14, 16, 22]. However, the precise correspondence between the OST Hamiltonians and GK Hamiltonians for general n has not been clarified before; the case $n = 5$ appears in [22]. Our motivation for including it is that twisted TCD maps give a quick proof, and the same type of argument will be used to prove the analogous results for the cross-ratio dynamics integrable system for which these results are new.

1.3 Cross-ratio dynamics

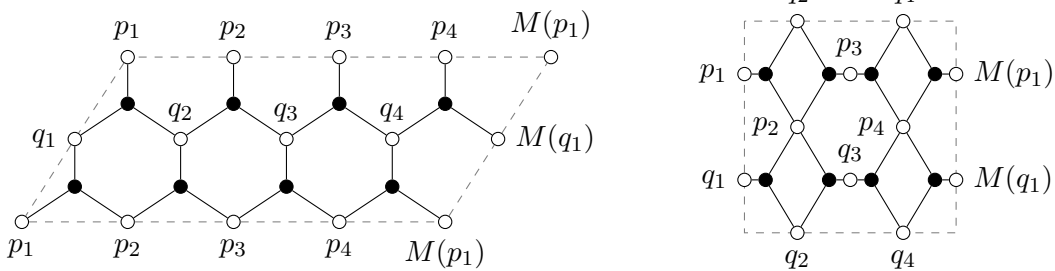


Figure 2. Twisted TCD maps for cross-ratio dynamics when $n = 4$. The graph on the left is Δ_4 and the one on the right is Γ_4 .

Let $(\alpha_j)_{j \in \mathbb{Z}}$ be a bi-infinite sequence of elements of \mathbb{C}^\times and consider maps $f: \mathbb{Z}^2 \rightarrow \mathbb{CP}^1$ such that for every $(i, j) \in \mathbb{Z}^2$, we have

$$\frac{(f_{i,j} - f_{i+1,j})(f_{i+1,j+1} - f_{i,j+1})}{(f_{i+1,j} - f_{i+1,j+1})(f_{i,j+1} - f_{i,j})} = \alpha_j, \quad (1.1)$$

where we denote by $f_{i,j}$ the value taken by f at $(i,j) \in \mathbb{Z}^2$. Such a map is a special case of a discrete version of the Schwarzian KdV equation [39], or a special case of a *discrete isothermic surface* [6] restricted to the sphere S^2 . In both cases it was shown that these maps are a discrete integrable system in the sense that they admit a discrete Lax representation. An interesting question is: Given all the α_j , what is the space of solutions of (1.1)? To answer this, consider each column i of \mathbb{Z}^2 as a *discrete curve* $f_i: \mathbb{Z} \rightarrow \mathbb{CP}^1$. The discrete curve corresponding to two adjacent columns f_i and f_{i+1} are called $\vec{\alpha}$ -related, where $\vec{\alpha}$ is the vector of all α_j . In the case when α_j is independent of j , the curve f_{i+1} is called a *Darboux transform* [24] of f_i in the discrete differential geometry community, see also [8]. If we know f_i and one point of f_{i+1} , then equation (1.1) determines all of f_{i+1} . As a consequence, there is a complex one-parameter freedom for each additional column of \mathbb{Z}^2 .

However, this changes if one considers *periodic* maps, that is maps $\mathbb{Z} \times \mathbb{Z}/n\mathbb{Z} \rightarrow \mathbb{CP}^1$ that satisfy equation (1.1) for some $n \in \mathbb{N}$. These periodic discrete curves can be seen as *closed n -gons* in \mathbb{CP}^1 . In this case, if we know f_i then there are only two possible solutions for f_{i+1} , because f_{i+1} has to be periodic as well. Thus if we know both f_{i-1} as well as f_i and assume that $f_{i+1} \neq f_{i-1}$, then f_{i+1} is determined *uniquely*. Special attention has been paid to the case that α_j does not depend on j . In this case, periodic solutions to equation (1.1) have been studied as *periodic discrete conformal maps* [25] with respect to algebro-geometric integrability. Also in this case, the map $(f_{i-1}, f_i) \mapsto (f_i, f_{i+1})$ is called *cross-ratio dynamics* [4]. Cross-ratio dynamics can also be generalized from closed n -gons to *twisted n -gons*, that is curves $f_i: \mathbb{Z} \rightarrow \mathbb{CP}^1$ such that $f_i(j+n) = M(f_i(j))$ for all $j \in \mathbb{Z}$ and for some length $n \in \mathbb{N}$ and monodromy $M \in \text{PGL}_2$.

We now transition to the notation of [4]. Let $p_i := f_0(i)$ and $q_i := f_1(i)$ for $i \in \mathbb{Z}$. The phase space of the cross-ratio dynamics integrable system is the moduli space $\mathcal{U}_{n,\vec{\alpha}}$ of pairs (p, q) of $\vec{\alpha}$ -related nondegenerate twisted n -gons modulo PGL_2 . Arnold, Fuchs, Izmistiev and Tabachnikov [4] identified a Poisson structure on $\mathcal{U}_{n,\vec{\alpha}}$ and proved integrability in the sense of Liouville. Indeed, they provide Poisson brackets that are preserved by the dynamics as well as integrals of motion that are Casimirs and Hamiltonians. We will henceforth call them the AFIT Poisson structures, Casimirs and Hamiltonians.

In Section 7, we give two different constructions of twisted TCD maps for cross-ratio dynamics, one on a hexagonal lattice denoted Δ_n and the other on a square lattice denoted Γ_n (see Figure 2 for the case $n = 4$). The map sending the twisted TCD map to the pair of twisted n -gons (p, q) induces a birational map $\pi_{\vec{\alpha}}: \mathcal{X}_{N_{\Theta_n}, \vec{\alpha}}^\lambda \rightarrow \mathcal{U}_{n,\vec{\alpha}}$, where $\mathcal{X}_{N_{\Theta_n}, \vec{\alpha}}^\lambda$ denotes a closed subvariety of the space of dimer weights for Θ_n , where $\Theta \in \{\Gamma, \Delta\}$. We summarize several results of Section 7 in the following theorem.

Theorem 1.4. *Let $n \geq 2$, let $\vec{\alpha} \in (\mathbb{C} \setminus \{0\})^n$, and let $\Theta \in \{\Gamma, \Delta\}$. The map $\pi_{\vec{\alpha}}$ is a Poisson birational map from $\mathcal{X}_{N_{\Theta_n}, \vec{\alpha}}^\lambda$ to $\mathcal{U}_{n,\vec{\alpha}}$ that restricts to a birational isomorphism between symplectic leaves on the two sides. The GK Hamiltonians are related to the pullbacks of the AFIT Hamiltonians by $\pi_{\vec{\alpha}}$ by an invertible linear transformation.*

An explicit geometric bridge between cross-ratio dynamics and the dimer model is given by the following result.

Theorem 1.5 (cf. Theorems 7.9 and 7.14). *Let $n \geq 2$, let $\vec{\alpha} \in (\mathbb{C} \setminus \{0\})^n$, and let $\Theta \in \{\Gamma, \Delta\}$. Pairs of $\vec{\alpha}$ -related twisted polygons of length n arise as twisted TCD maps on $\Theta_{n,\mathbb{A}}$ taking values in \mathbb{CP}^1 and cross-ratio dynamics arises as an explicit sequence of local moves on these twisted TCD maps.*

An important note regarding Theorem 1.5 is that the first local move in the sequence depends on a parameter and that parameter depends globally on the initial pair of $\vec{\alpha}$ -related twisted polygons. In this sense, the sequence of transformations could be termed a *semi-local*

transformation. Furthermore, combining Theorem 1.4 with Theorem 1.5, we obtain an alternative proof of the conservation of the AFIT Hamiltonians (stated as Corollary 7.10), since the dynamics on TCD maps is conjugated to the dimer integrable dynamics of [23]. A more explicit statement of Theorem 1.5 is given by Theorem 7.9.

As a first corollary of Theorem 1.5, we find that the evolution of certain coordinates under cross-ratio dynamics is given by a so-called *geometric R -matrix transformation*. Geometric R -matrices have been introduced in representation theory in relation with geometric crystals [5, 12, 30, 32] and are so named because they are birational maps that tropicalize to combinatorial R -matrices [31]. They first received an interpretation in terms of semi-local transformations of electrical networks [35, 36, 37] then in terms of semi-local transformations for dimer models [9, 19, 26, 27]. Transforming our graphs Γ_n , we recover the graphs of [26] whose semi-local transformation is described by a geometric R -matrix transformation, hence the following result.

Corollary 1.6 (cf. Proposition 6.2). *The evolution of some coordinates under cross-ratio dynamics is given by a geometric R -matrix transformation.*

Recently, it was observed that another geometric dynamics, polygon recutting, was also governed by geometric R -matrices [29].

As a second corollary, we answer an open question of [4] asking for an interpretation of cross-ratio dynamics in terms of cluster algebras. Indeed, all but the first and the last operations for TCD maps of Theorem 1.5 have a cluster algebra interpretation [1, 2]. Actually, Inoue–Lam–Pylyavskyy showed in [27] that this sequence of operations, including the first and the last one, could be interpreted as cluster algebra mutations provided one considers a decorated version of the bipartite graph.

Corollary 1.7. *The evolution of some coordinates under cross-ratio dynamics can be written as an explicit composition of cluster algebra mutations.*

Geometric R -matrix transformations give rise to the class of generalized cluster transformations that were systematically studied in [19]. In Section 7.3, we describe explicitly the group of all generalized cluster transformations associated with the Newton polygon Δ_n .

As noted by [4], cross-ratio dynamics bears a lot of resemblances with the pentagram map. There is however a notable difference with cross-ratio dynamics. For the pentagram map and its generalizations, the dynamics is local in the sense that one can construct a point of the twisted n -gon q knowing only a bounded number of points of the twisted n -gon p . For cross-ratio dynamics the dynamics is global, one needs to know all the points of p to construct any given point of q .

We end the introduction by remarking that it is mysterious to us that cross-ratio dynamics can be realized as a cluster integrable system in at least two different ways. The two realizations have different Casimirs and reveal different symmetries of the system. We believe this phenomenon deserves further study.

Organization of the paper

In Section 2, we recall the Goncharov–Kenyon integrable system [23] associated with the dimer model on the torus. In Section 3, we consider the dimer model on the cylinder, construct the matrix $\Pi(w)$ and prove Theorem 1.2. We introduce in Section 4 the notion of twisted TCD maps associated to a bipartite graph on the cylinder. In Section 5, we realize the pentagram map as a twisted TCD map and show that it coincides with a cluster integrable system. In Section 6, we provide the necessary background on cross-ratio dynamics and its integrability following mostly [4]. In Section 7, we realize the cross-ratio dynamics integrable system as a cluster

integrable system in two different ways, and describe the sequence of local moves for twisted TCD maps that realize cross-ratio dynamics, as stated in Theorem 1.5. Section 7.2 shows Corollary 1.6 on the relation with geometric R -matrices. Finally Appendix A presents some results used in Sections 3 and 4 related to the classical notion of Schur complement.

2 The cluster integrable system

In this section, we recall the integrable system associated with the dimer model on a weighted graph on a torus. For further details, see [23].

2.1 The dimer model in a torus

Let $\Gamma = (B \cup W, E)$ be a bipartite graph embedded in a torus \mathbb{T} such that $|B| = |W|$ and such that the faces of Γ , that is, the connected components of the complement of Γ , are topological disks. We denote by F the set of faces of Γ . An *edge weight* on Γ is a function $\text{wt}: E \rightarrow \mathbb{C}^\times$. Two edge weights wt_1 and wt_2 are said to be *gauge equivalent* if there is a function $g: B \cup W \rightarrow \mathbb{C}^\times$ such that for every edge $e = bw$ with $b \in B$, $w \in W$, we have $\text{wt}_2(e) = \text{wt}_1(e)g(w)g(b)^{-1}$. Let \mathcal{L}_Γ denote the space of edge weights modulo gauge equivalence and denote by $[\text{wt}]$ the gauge equivalence class of the weight wt .

To rephrase the above in the language of algebraic topology, we consider the graph Γ to be a cell complex whose 0- and 1-cells are $B \cup W$ and E , respectively. Considering each edge $e = bw$ to be oriented from b to w , we have the nonzero cellular chain groups

$$C_0(\Gamma, \mathbb{Z}) = \mathbb{Z}B \oplus \mathbb{Z}W, \quad C_1(\Gamma, \mathbb{Z}) = \mathbb{Z}E,$$

with boundary homomorphism $\partial: C_1(\Gamma, \mathbb{Z}) \rightarrow C_0(\Gamma, \mathbb{Z})$ given by $\partial(e) = w - b$, so that $H_1(\Gamma, \mathbb{Z}) = \ker \partial$. Dually, we have cellular cochain groups $C^q(\Gamma, \mathbb{C}^\times) := \text{Hom}_{\mathbb{Z}}(C_q(\Gamma, \mathbb{Z}), \mathbb{C}^\times)$, for $q \in \{0, 1\}$, with coboundary homomorphism $\delta: C^0(\Gamma, \mathbb{C}^\times) \rightarrow C^1(\Gamma, \mathbb{C}^\times)$ given by $\delta(g)(e) = \frac{g(w)}{g(b)}$. Since an edge weight is a 1-cochain and two edge weights are gauge equivalent if and only if they differ by a 1-coboundary, we have

$$\mathcal{L}_\Gamma = H^1(\Gamma, \mathbb{C}^\times) := C^1(\Gamma, \mathbb{C}^\times) / \delta(C^0(\Gamma, \mathbb{C}^\times)).$$

Then, $[\text{wt}]$ is the cohomology class represented by the cochain wt .

For $[L] \in H_1(\Gamma, \mathbb{Z})$, we denote by $[\text{wt}]([L])$ the result of evaluating the cohomology class $[\text{wt}]$ on the homology class $[L]$ yielding an alternating product of edge weights around L (the product is alternating due to our choice of orientation of edges from b to w). Explicitly, if the L is the 1-cycle $w_1 \xrightarrow{e_1} b_1 \xrightarrow{e_2} w_2 \xrightarrow{e_3} b_2 \xrightarrow{e_4} \dots \xrightarrow{e_{2n-2}} w_n \xrightarrow{e_{2n-1}} b_n \xrightarrow{e_{2n}} w_1 \in H_1(\Gamma, \mathbb{Z})$, we have

$$[\text{wt}]([L]) = \prod_{i=1}^n \frac{\text{wt}(e_{2i})}{\text{wt}(e_{2i-1})}.$$

Since $\mathcal{L}_\Gamma = \text{Hom}_{\mathbb{Z}}(H_1(\Gamma, \mathbb{Z}), \mathbb{C}^\times)$ is an algebraic torus, the algebra $\mathcal{O}_{\mathcal{L}_\Gamma}$ of regular functions on \mathcal{L}_Γ is generated by the characters $\chi_{[L]}$ for $[L] \in H_1(\Gamma, \mathbb{Z})$ defined by $\chi_{[L]}([\text{wt}]) := [\text{wt}]([L])$.

We now give a description of $\mathcal{O}_{\mathcal{L}_\Gamma}$ in terms of a basis. For a face f of Γ , let ∂f denote the counterclockwise oriented cycle given by the walk along the boundary of f and define the *face weight* $X_f := \chi_{[\partial f]}$. Let a and b denote two cycles in Γ such that their homology classes $[a]$ and $[b]$ generate $H_1(\mathbb{T}, \mathbb{Z})$. Then

$$\mathcal{O}_{\mathcal{L}_\Gamma} = \mathbb{C}[X_f^{\pm 1}, \chi_{[a]}^{\pm 1}, \chi_{[b]}^{\pm 1}] / (1 - \prod_{f \in F} X_f),$$

where the relation $\prod_{f \in F} X_f = 1$ comes from the relation $\sum_{f \in F} [\partial f] = 0$ in $H_1(\Gamma, \mathbb{Z})$. While this set of generators is natural, both from the point of view of cluster algebras and topology, we will see in the examples of the pentagram map and cross-ratio dynamics that other generators are often more convenient to work with.

Zig-zag paths and the Newton polygon. A *zig-zag* path in Γ is a path that turns maximally left at white vertices and maximally right at black vertices. Let \mathcal{Z} denote the set of zig-zag paths of Γ . Each zig-zag path $\beta \in \mathcal{Z}$ defines a homology class $[\beta] \in H_1(\mathbb{T}, \mathbb{Z})$. Label the zig-zag paths $\beta_1, \beta_2, \dots, \beta_{|\mathcal{Z}|}$ so that the $[\beta_i]$ regarded as vectors in $H_1(\mathbb{T}, \mathbb{Z}) \otimes \mathbb{R} \cong \mathbb{R}^2$ are in counterclockwise order. We construct a closed convex integral polygon $N(\Gamma)$ (or just N when Γ is clear from the context) by placing the $[\beta_i]$ such that the head of $[\beta_i]$ is the tail of $[\beta_{i+1}]$. Each edge of Γ is contained in two zig-zag paths that traverse the edge in opposite directions, so we have $\sum_{\beta \in \mathcal{Z}} [\beta] = 0$, which shows that N constructed as above is a closed polygon. N is unique up to translation and is called the Newton polygon of Γ . The name Newton polygon will be justified at the end of this section by the fact that this polygon arises as the Newton polygon of the characteristic polynomial of the dimer model on Γ .

A graph Γ is said to be *minimal* if any lift of a zig-zag path to the universal cover of \mathbb{T} has no self intersections and any lifts of two zig-zag paths to the universal cover of \mathbb{T} do not form parallel bigons (pairs of zig-zag paths oriented the same way intersecting twice). Hereafter, when considering a graph Γ in \mathbb{T} , we assume that it is minimal unless stated otherwise. By construction, the set of primitive edge vectors of the Newton polygon of a minimal graph Γ is in bijection with \mathcal{Z} , but this bijection is not canonical when there is more than one zig-zag path with a given homology class.

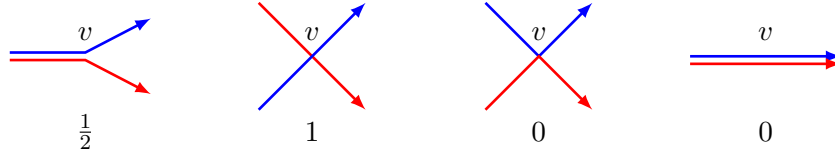


Figure 3. Local rules for computing ϵ_Γ . L_1 and L_2 are the blue and red cycles, respectively.

Conjugate surface and Poisson structure. Thickening the edges of Γ , we obtain a ribbon graph. Equivalently a ribbon graph is a graph along with the data of a cyclic order of edges around each vertex. The ribbon graph obtained from Γ has the cyclic order induced from the embedding in \mathbb{T} . Let $\widehat{\Gamma}$ be the ribbon graph obtained from Γ by reversing the cyclic order at all black vertices. The boundary components of $\widehat{\Gamma}$ are in bijection with the zig-zag paths of Γ . Gluing in disks along these boundary components of $\widehat{\Gamma}$, we obtain a surface \widehat{S} , called the *conjugate surface*, along with an embedding of Γ in \widehat{S} . Let $\epsilon_{\widehat{S}}$ denote the intersection form on $H_1(\widehat{S}, \mathbb{Z})$ defined as follows. If L_1 and L_2 are two cycles on \widehat{S} intersecting transversely, then

$$\epsilon_{\widehat{S}}([L_1], [L_2]) := \sum_{p \in L_1 \cap L_2} \epsilon_p(L_1, L_2),$$

where $\epsilon_p(L_1, L_2)$ is the local intersection index, with sign chosen so that it is positive if L_2 crosses L_1 at p from its right side to its left side. Note that the definition of $\epsilon_{\widehat{S}}([L_1], [L_2])$ is independent of the choice of cycles representing $[L_1]$ and $[L_2]$. The embedding $\iota: \Gamma \hookrightarrow \widehat{S}$ induces the homomorphism of homology groups $\iota_*: H_1(\Gamma, \mathbb{Z}) \rightarrow H_1(\widehat{S}, \mathbb{Z})$. We define the alternating form ϵ_Γ on $H_1(\Gamma, \mathbb{Z})$ by $\epsilon_\Gamma([L_1], [L_2]) := \epsilon_{\widehat{S}}(\iota_*[L_1], \iota_*[L_2])$. The pairing ϵ_Γ has the following local description which is useful for computations (see [23, Appendix]): $\epsilon_\Gamma([L_1], [L_2]) = \sum_{v \in B} \epsilon_v(L_1, L_2) - \sum_{v \in W} \epsilon_v(L_1, L_2)$, where $\epsilon_v(L_1, L_2)$ is defined in Figure 3. In particular, if f and f' are two faces having a single edge in common and f lies to the left of that edge when traversed from its black endpoint to its white endpoint, then $\epsilon_\Gamma([\partial f], [\partial f']) = 1$.

For $[L_1], [L_2] \in H_1(\Gamma, \mathbb{Z})$, define the Poisson bracket

$$\{\chi_{[L_1]}, \chi_{[L_2]}\}_\Gamma := \epsilon_\Gamma([L_1], [L_2]) \chi_{[L_1]} \chi_{[L_2]}.$$

By linearity and Leibniz's rule, we obtain a Poisson bracket on $\mathcal{O}_{\mathcal{L}_\Gamma}$. The faces of Γ in \widehat{S} become the zig-zag paths of Γ in \mathbb{T} , so we have $\{\chi_{[L_1]}, \chi_{[L_2]}\} = 0$ for all $[L_2] \in H_1(\Gamma, \mathbb{Z})$ if and only if $[L_1] \in \bigoplus_{\beta \in \mathcal{Z}} \mathbb{Z} \cdot [\beta]$. Therefore, the center of the Poisson algebra $\mathcal{O}_{\mathcal{L}_\Gamma}$ is the subalgebra

$$\mathbb{C}[C_\beta^{\pm 1}] / \left(1 - \prod_{\beta \in \mathcal{Z}} C_\beta\right),$$

generated by the functions $C_\beta := \chi_{[\beta]}, \beta \in \mathcal{Z}$. Elements of the center of a Poisson algebra are called *Casimirs*.

2.2 Local and semi-local transformations

There are two local modifications of bipartite graphs called *elementary transformations*. An elementary transformation $s: \Gamma \rightarrow \Gamma'$ induces a unique up to isotopy homeomorphism of conjugate surfaces $\hat{s}: \widehat{S}_\Gamma \rightarrow \widehat{S}_{\Gamma'}$ [23, Lemma 4.1], which in turn induces an isomorphism $\hat{s}_*: H_1(\Gamma, \mathbb{Z}) \rightarrow H_1(\Gamma', \mathbb{Z})$. For $[L'] \in H_1(\Gamma', \mathbb{Z})$, let $[L] = (\hat{s}_*)^{-1}([L'])$. Associated to the elementary transformation s is a Poisson birational map of weights $\mu_s: \mathcal{L}_\Gamma \rightarrow \mathcal{L}_{\Gamma'}$:

1. *The spider move s at face f* : We define

$$\mu_s^*(\chi_{[L']}) = \begin{cases} X_f^{-1} & \text{if } [L] = [\partial f], \\ \chi_{[L]} (1 + X_f^{-\text{sign } \epsilon_\Gamma([L], \partial f)})^{-\epsilon_\Gamma([L], \partial f)} & \text{otherwise.} \end{cases}$$

This is illustrated on the left side of Figure 4.

2. *Contracting/expanding degree two vertices*: We define $\mu_s^*(\chi_{[L']}) = \chi_{[L]}$. This is illustrated in the middle of Figure 4.

In other words, the spider move at f inverts the face weight at f and multiplies the face weights of a face f' adjacent to f by some power of $1 + X_f$ or of $(1 + X_f^{-1})^{-1}$. Such a transformation on face weights corresponds to the mutation rule for coefficient variables in cluster algebras [13, 15] and indeed one can associate a cluster algebra to a dimer model on a torus [23]. Contracting/expanding degree two vertices does not change the face weights.

Elementary transformations do not change homology classes of zig-zag paths, and therefore the Newton polygon. Gluing the Poisson affine varieties \mathcal{L}_Γ for all Γ minimal with $N(\Gamma) = N$ using these Poisson birational maps, we obtain the Poisson space \mathcal{X}_N called the *dimer cluster Poisson variety* associated to N . \mathcal{X}_N is a cluster Poisson variety as defined by Fock and Goncharov [13], and will be the phase space of the cluster integrable system. Each \mathcal{L}_Γ such that Γ is minimal with $N(\Gamma) = N$ is Zariski-dense inside \mathcal{X}_N .

Inserting/removing a bigon. The right side of Figure 4 shows the insertion of a bigon between vertices $w \in W$ and $b \in B$ belonging to a common face f , with parameter u . This divides f into three new faces, the bigon f_b and the face f_l (resp. f_r) to the left (resp. right) of f_b when traversing the bigon from w to b . Let Γ_b denote the graph obtained. The embedding $i_b: \Gamma \hookrightarrow \Gamma_b$ induces a homomorphism $(i_b)_*: H_1(\Gamma, \mathbb{Z}) \rightarrow H_1(\Gamma_b, \mathbb{Z})$. We define the induced map of weights $\mu_u: \mathcal{L}_\Gamma \rightarrow \mathcal{L}_{\Gamma_b}$ on a basis as follows: If $[L]$ is topologically nontrivial in $H_1(\mathbb{T}, \mathbb{Z})$ or is the boundary of a face of Γ set $\mu_u^*(\chi_{(i_b)_*[L]}) = \chi_{[L]}$. Define also $\mu_u^*(X_{f_l}) = u$ and $\mu_u^*(X_{f_b}) = -1$. Note that the second equation implies that in any cocycle, the weights of the two edges of the bigon sum to zero. On the other hand, if we have a bigon with $X_{f_b} = -1$, we may remove it.

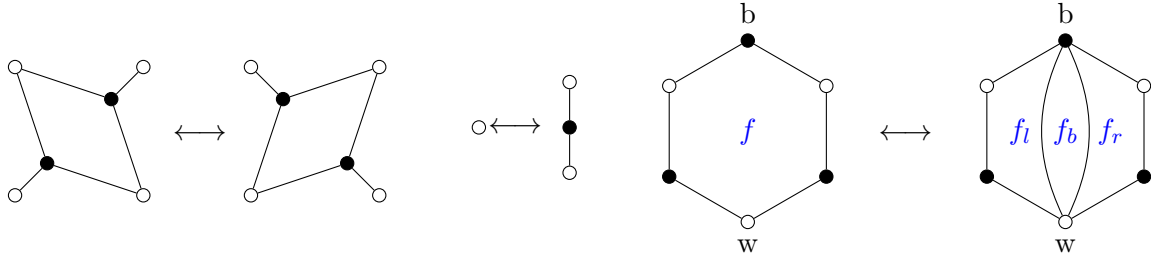


Figure 4. On the left, the spider move. In the middle, contracting/expanding a degree two vertex. On the right, adding/removing a bigon inside a face.

This induces a map of weights $\mu'_b: \{X_{f_b} = -1\} \rightarrow \mathcal{L}_\Gamma$ given by $(\mu'_b)^*(\chi_{[L]}) = \chi_{(i_b)_*[L]}$, where $\{X_{f_b} = -1\}$ denotes the subvariety in \mathcal{L}_{Γ_b} . In other words, the insertion of a bigon with parameter u inside a face f assigns to the faces f_l , f_b and f_r the respective weights u , -1 and $-\frac{X_f}{u}$, while the deletion of a bigon f_b with face weight -1 assigns to the resulting face the product of the weights of the three faces that got merged.

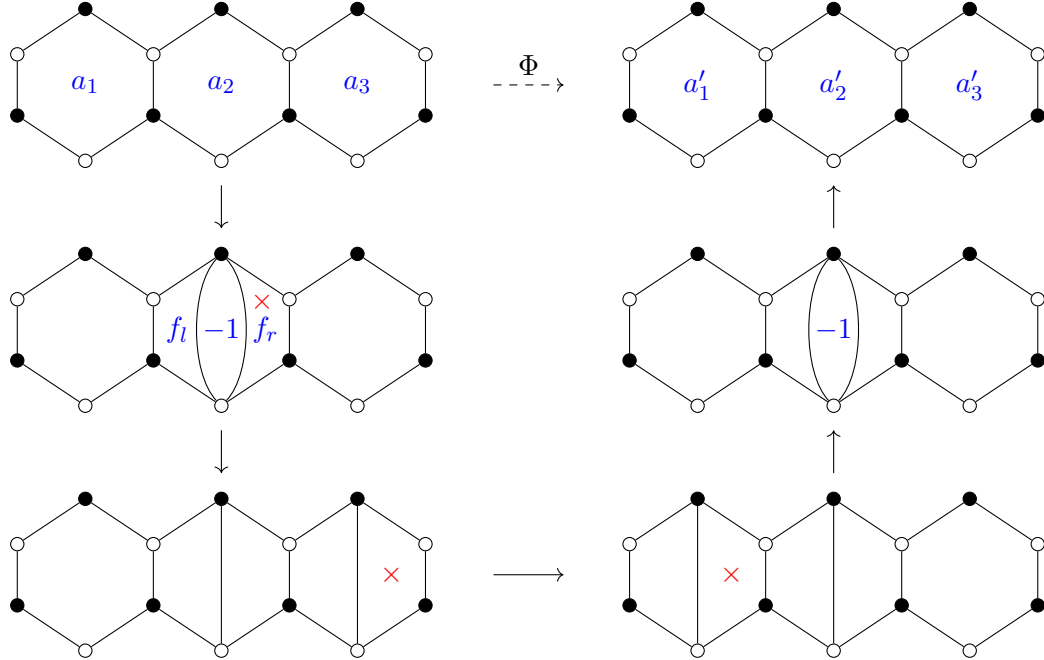


Figure 5. The sequence of operations corresponding to the geometric R -matrix transformation when $n = 3$. For each of the six pictures, the left and right sides are identified. Here we have $k = 2$, so that we add the bigon in the second hexagon. The red crosses indicate the faces at which we perform the next spider move. The face weights are depicted in blue.

Geometric R -matrices. We now recall the dimer interpretation of geometric R -matrix transformations given in [26, Section 11] as a composition of bigon insertion/removal and spider moves. We call this a semi-local move, because the choice of the parameter u associated with the bigon insertion is a function of weights of faces that may be arbitrarily far away from the bigon. Consider a bipartite graph embedded on a surface, which possesses a cyclic chain of n hexagons (see the first picture of Figure 5 for an example with $n = 3$). The two edges of each hexagon which separate it from the neighboring hexagons must form an opposite pair of edges. Denote by a_1, \dots, a_n the face weights of the hexagons. Fix k between 1 and n and add a bigon between the two vertices of the k th hexagon that are not part of the neighboring two hexagons.

We impose the weight of the bigon to be -1 and we denote by f_r and $f_l = -\frac{a_k}{f_r}$ the weight of the two newly created quadrilaterals, as on the right picture of Figure 4. For now f_r is an unknown. We then perform a sequence of n spider moves, starting at the face of weight f_r and moving in the direction of increasing values of k . At the end of this sequence of spider moves, we come back to a situation where the k th hexagon has a bigon. It follows from [26] that the closing condition for the weight of this bigon to be -1 is linear in f_r . We set f_r to be the unique solution of this equation. We finally delete the bigon, obtaining again a cyclic chain of n hexagons, the weights of which we denote by a'_1, \dots, a'_n . Formulas (11.1) and (11.2) of [26] lead to the following result.

Theorem 2.1 ([26]). *With the setting defined above, the values a'_1, \dots, a'_n are independent of the choice of the starting position k and are given for every $1 \leq i \leq n$ by*

$$a'_i = \frac{\sum_{t=0}^{n-1} \prod_{s=0}^{t-1} a_{i+s}}{\sum_{t=1}^n \prod_{s=1}^t a_{i+s}}, \quad (2.1)$$

where indices are taken modulo n .

We point out that the formula we stated above slightly differs from the one obtained from [26] in that our indices are increasing while theirs are decreasing ($i + s$ instead of $i - s$). This comes from having the opposite convention for mutation rules, which results from different convention in the definitions of zig-zag paths and of dimer face weights. We also note that the framework of [26] was a bit more restrictive than the one we are considering, since they were assuming that on each side of the cyclic chain of hexagons there were other chains of hexagons. Here we are only assuming that no face immediately above or below the cyclic chain of n hexagons may be one of these n hexagons. The proof of [26] holds verbatim in this framework. Finally, we point out that the map sending (a_1, \dots, a_n) to (a'_1, \dots, a'_n) is an involution [26]. We denote this map by Φ .

2.3 Dimer covers and Kasteleyn theory

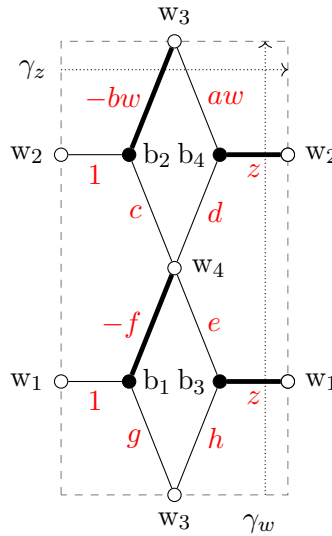


Figure 6. Edge weight, Kasteleyn sign, cochain ϕ and M_0 (thick edges) on Γ_2 .

A *dimer cover* M of Γ is a subset of E such that each vertex of Γ is incident to exactly one edge in M . Let \mathcal{M} denote the set of dimer covers of Γ . If we fix a reference dimer cover M_0 ,

then we can associate to each dimer cover a homology class

$$M \mapsto [M - M_0] \in H_1(\mathbb{T}, \mathbb{Z}),$$

where, as before, we orient $e = bw$ from b to w . Given $[\text{wt}] \in \mathcal{L}_\Gamma$, each dimer cover also gets a *weight* $[\text{wt}](M - M_0)$. If Γ is minimal, we can describe the Newton polygon in terms of dimer covers.

Proposition 2.2 ([23, Theorem 3.12]). *For a minimal bipartite graph Γ in \mathbb{T} , we have*

$$N(\Gamma) = \text{Convex-hull}\{[M - M_0] \mid M \text{ is a dimer cover of } \Gamma\},$$

up to a translation.

Let R be a fundamental rectangle of \mathbb{T} and let γ_z, γ_w be cycles in \mathbb{T} such that $[\gamma_z], [\gamma_w]$ generate $H_1(\mathbb{T}, \mathbb{Z})$. We choose γ_z, γ_w parallel to the sides of R as shown in Figure 6. Isotoping if necessary, we assume that the edges of Γ intersect γ_z, γ_w transversely. Applying $\text{Hom}_{\mathbb{Z}}(\cdot, \mathbb{C}^\times)$ to the surjection $H_1(\Gamma, \mathbb{Z}) \rightarrow H_1(\mathbb{T}, \mathbb{Z})$, we get an inclusion $H^1(\mathbb{T}, \mathbb{C}^\times) \hookrightarrow H^1(\Gamma, \mathbb{C}^\times)$. Let $[\phi'] \in H^1(\Gamma, \mathbb{C}^\times)$ be in the image of $H^1(\mathbb{T}, \mathbb{C}^\times)$. In other words, $X_f([\phi']) = 1$ for all $f \in F$. We choose a cochain ϕ representing $[\phi']$ as follows: Let $z := [\phi']([\gamma_z])$, $w = [\phi']([\gamma_w])$, and define

$$\phi(e) := z^{(e, \gamma_w)} w^{(e, -\gamma_z)},$$

where (\cdot, \cdot) is the intersection index, i.e., the sum of the local intersection indices defined in the previous subsection.

The cohomology class $[\kappa] \in H^1(\Gamma, \mathbb{C}^\times)$ is called a *Kasteleyn sign* if the following conditions hold:

- (1) $X_{[L]}([\kappa]) = \pm 1$ for all $[L] \in H_1(\Gamma, \mathbb{Z})$;
- (2) $X_f([\kappa]) = (-1)^{\frac{|\partial f|}{2} + 1}$ for all $f \in F$, where $|\partial f|$ is the number of edges in ∂f .

Let $\kappa: E \rightarrow \mathbb{C}^\times$ be a cochain representing the Kasteleyn sign $[\kappa]$. We define the *Kasteleyn matrix*

$$K(z, w): \mathbb{C}[z^{\pm 1}, w^{\pm 1}]^B \rightarrow \mathbb{C}[z^{\pm 1}, w^{\pm 1}]^W$$

by

$$K(z, w)_{w,b} := \sum_{e=bw \in E} \text{wt}(e) \kappa(e) \phi(e),$$

where the sum is over edges between b and w .

Theorem 2.3 ([33]). *We have*

$$\frac{1}{\text{wt}(M_0) \kappa(M_0) \phi(M_0)} \det K(z, w) = \sum_{M \in \mathcal{M}} \text{sign}([M - M_0]) [\text{wt}]([M - M_0]) [\phi]([M - M_0]),$$

where $\text{sign}([M - M_0])$ is a sign that depends on $[\kappa]$ and on the homology class $[M - M_0]$ in $H_1(\mathbb{T}, \mathbb{Z})$ and that is irrelevant for our purposes.

Moreover,

$$P(z, w) := \frac{1}{\text{wt}(M_0) \kappa(M_0) \phi(M_0)} \det K(z, w)$$

is called the *characteristic polynomial* and $\Sigma := \{(z, w) \in (\mathbb{C}^\times)^2 \mid P(z, w) = 0\}$ is called the *spectral curve* of $(\Gamma, [\text{wt}])$. Although $K(z, w)$ depends on the choice of cochains representing $[\text{wt}]$ and $[\kappa]$, the spectral curve is independent of these choices. Moreover $N(\Gamma)$ is the Newton polygon of $P(z, w)$, that is, the convex hull of the pairs $(i, j) \in \mathbb{Z}^2$ such that $z^i w^j$ has a nonzero coefficient in $P(z, w)$.

Example 2.4. Consider the graph Γ_2 with edge weights, Kasteleyn sign, ϕ and reference dimer cover M_0 chosen as in Figure 6. The Kasteleyn matrix is

$$K(z, w) = \begin{bmatrix} b_1 & b_2 & b_3 & b_4 \\ 1 & 0 & z & 0 \\ 0 & 1 & 0 & z \\ g & -bw & h & aw \\ -f & c & e & d \end{bmatrix} \begin{matrix} w_1 \\ w_2 \\ w_3 \\ w_4 \end{matrix},$$

and the spectral curve is

$$P(z, w) = \frac{1}{bfz^2w} (-dh + (dg + ch)z - cz^2 + aew + (be + af)zw + bfz^2w). \quad (2.2)$$

Hamiltonians. Let N° denote the interior of N . For $[\gamma] \in N^\circ \cap H_1(\mathbb{T}, \mathbb{Z})$, let

$$H_{[\gamma]} := \sum_{M \in \mathcal{M}: [M - M_0] = [\gamma]} [\text{wt}]([M - M_0])$$

denote the coefficient of $[\phi]([\gamma])$ (up to a sign) in $P(z, w)$.

A space equipped with a Poisson bracket is a *Liouville integrable system* if the generic level sets of the Casimirs are symplectic leaves of some dimension $2m$, which possess m mutually Poisson-commuting *Hamiltonians* which are functionally independent.

Proposition 2.5 ([23, Theorem 1.2]). *The generic level sets of the Casimirs are symplectic leaves of \mathcal{X}_N . The quantities $H_{[\gamma]}$ for $[\gamma] \in H_1(\mathbb{T}, \mathbb{Z}) \cap N^\circ$ mutually Poisson-commute, making these symplectic leaves into Liouville integrable systems with Hamiltonians $H_{[\gamma]}$.*

3 The dimer model in a cylinder

In this section, we consider balanced cylinder graphs, which are bipartite graphs on a cylinder satisfying certain conditions. In Section 3.1, we construct a matrix $\Pi(w)$ from a dimer model on a balanced cylinder graph. Then in Section 3.2, we prove Theorem 1.2 relating the spectrum of $\Pi(w)$ to the spectral curve of the dimer model on the torus graph obtained by gluing the two boundaries of the balanced cylinder graph. Finally, in Section 3.3, we show that this result holds for a large class of torus graphs, namely minimal graphs.

Let $\Gamma_{\mathbb{A}} = (B \cup W, E)$ be a bipartite graph embedded in a cylinder \mathbb{A} satisfying the following conditions:

1. Every vertex on the boundary of \mathbb{A} is white and of degree 1.
2. Let S and T denote the boundary white vertices on the two components of the boundary of \mathbb{A} , called the *source* and *target* vertices, respectively. Let $W_{\text{int}} = W \setminus (S \cup T)$ denote the set of internal white vertices. We assume that $|S| = |T|$ and $|B| = |W| - |S|$.
3. $\Gamma_{\mathbb{A}}$ has a dimer cover M_0 that uses all the vertices in S and none of the vertices in T .
4. The faces of $\Gamma_{\mathbb{A}}$ (including boundary faces) are topological disks.

Here by a dimer cover of $\Gamma_{\mathbb{A}}$, we mean a matching that uses all the vertices in B and in a $|B|$ -element subset of W exactly once. Note that assumptions 1 and 3 imply that the black vertices incident to the white vertices in S are all different.

We call graphs $\Gamma_{\mathbb{A}}$ satisfying these conditions *balanced cylinder graphs*.

An edge weight on $\Gamma_{\mathbb{A}}$ is a function $\text{wt}: E \rightarrow \mathbb{C}^\times$. Two edge weights wt_1 and wt_2 are gauge equivalent if there is a function $g: B \cup W \rightarrow \mathbb{C}^\times$ satisfying $g(w) = 1$ for all $w \in S \cup T$ such that for every edge $e = bw$ with $b \in B$, $w \in W$, we have $\text{wt}_2(e) = g(b)^{-1} \text{wt}_1(e) g(w)$. In other words we only allow gauge transformations at interior vertices. The space of edge weights modulo gauge transformations is the relative cohomology group $H^1(\Gamma_{\mathbb{A}}, S \cup T, \mathbb{C}^\times)$. This relative cohomology group is generated by functions of cycles in $\Gamma_{\mathbb{A}}$ and of paths in $\Gamma_{\mathbb{A}}$ starting and ending at $S \cup T$. As before, we denote by $[\text{wt}]$ the cohomology class represented by wt .

Let \mathcal{M} denote the set of dimer covers of $\Gamma_{\mathbb{A}}$. For $M \in \mathcal{M}$, we define its weight to be $\text{wt}(M) = \prod_{e \in M} \text{wt}(e)$. For $M \in \mathcal{M}$, let ∂M denote the set of boundary white vertices incident to M . For example, $\partial M_0 = S$.

3.1 Kasteleyn theory in \mathbb{A}

Suppose $\Gamma_{\mathbb{A}}$ is a balanced cylinder graph. Let γ_z be a simple path connecting the two boundaries of the cylinder and directed from the boundary containing T towards the boundary containing S . Write $h = |S| = |T|$. Denote by w_1, \dots, w_h the vertices of T labelled consecutively and by w'_1, \dots, w'_h the vertices of S labelled consecutively. The orientations of the boundaries induced by these labelings are prescribed to be compatible with the orientation of the cylinder. We also prescribe that γ_z starts between w_h and w_1 and ends between w'_h and w'_1 . For any face $f \in F$, denote by T_f (resp. S_f) the subset of $i \in \{1, \dots, h\}$ such that the boundary segment $w_i w_{i+1}$ (resp. $w'_i w'_{i+1}$) is adjacent to f .

An element $[\kappa] \in H^1(\Gamma_{\mathbb{A}}, S \cup T, \mathbb{C}^\times)$ is called a Kasteleyn sign if the following conditions hold:

- (1) $\chi_{[L]}([\kappa]) = \pm 1$ for all $[L] \in H_1(\Gamma_{\mathbb{A}}, S \cup T, \mathbb{Z})$;
- (2) there exists $(\sigma_1, \dots, \sigma_h) \in \{0, 1\}^h$ such that for every $f \in F$,

$$X_f([\kappa]) = (-1)^{\frac{|\partial f|}{2} + 1 + \sum_{i \in T_f} \sigma_i + \sum_{i \in S_f} 1 - \sigma_i}.$$

As an example of the second condition, if all the σ_i are zero and $|S_f| \leq 1$ for every $f \in F$ (see, for example, Figure 6), then $X_f([\kappa]) = (-1)^{\frac{|\partial f|}{2}}$ if f is adjacent to the boundary containing S , otherwise $X_f([\kappa]) = (-1)^{\frac{|\partial f|}{2} + 1}$. The existence of a Kasteleyn sign is shown in [10, Proposition 2.1]. Note that this definition of Kasteleyn signs for balanced cylinder graphs makes them compatible with concatenation or with gluing the two boundaries to obtain a torus graph. The signs are admittedly complicated but they can mostly be ignored for the purposes of this paper.

We define the *Kasteleyn matrix* of $\Gamma_{\mathbb{A}}$:

$$K_{\mathbb{A}}(w): \mathbb{C}[w^{\pm 1}]^B \rightarrow \mathbb{C}[w^{\pm 1}]^W, \quad K_{\mathbb{A}}(w)_{w,b} := \sum_{e=bw \in E} \text{wt}(e) \kappa(e) w^{(e, -\gamma_z)}.$$

We have the following version of Kasteleyn's theorem.

Theorem 3.1 ([10, Theorem 2.4]). *Let $I \subset S \cup T$ such that $|I| = |S|$, and let $K_{\mathbb{A}, I}(w)$ denote the submatrix of the Kasteleyn matrix with rows indexed by white vertices in $I \cup W_{\text{int}}$ and columns indexed by black vertices in B . Then we have*

$$\frac{1}{\text{wt}(M_0) \kappa(M_0) w^{(M_0, -\gamma_z)}} \det K_{\mathbb{A}, I}(w) = \sum_{\partial M = I} \text{sign}([M - M_0]) [\text{wt}]([M - M_0]) w^{([M - M_0], -\gamma_z)},$$

where $[M - M_0]$ is the relative homology class in $H_1(\mathbb{A}, \partial \mathbb{A}, \mathbb{Z})$ defined by the relative cycle $M - M_0$ and $\text{sign}([M - M_0])$ is a sign that depends on $[\kappa]$ and on the relative homology class $[M - M_0]$ and that is irrelevant for our purposes.

Let B_S denote the set of black vertices incident to S . We denote by b_i the black vertex in B_S that is connected to the white vertex w'_i in S . B_S is matched to S by M_0 . Up to performing gauge transformations at B_S to ensure that the edges connecting B_S to S have $\kappa = 1$, the Kasteleyn matrix $K_{\mathbb{A}}(w)$ of $\Gamma_{\mathbb{A}}$ has the block matrix form

$$K_{\mathbb{A}}(w) = \begin{bmatrix} B_S & B \setminus B_S \\ \begin{bmatrix} I & 0 \\ K_1 & K_2 \\ K_3 & K_4 \end{bmatrix} & \begin{bmatrix} S \\ T \\ W_{\text{int}} \end{bmatrix} \end{bmatrix}. \quad (3.1)$$

For generic $[wt]$ and for generic $w \in \mathbb{C}^\times$, the submatrix K_4 is invertible using Theorem 3.1 with $I = S$, since M_0 is a dimer cover with $\partial M_0 = S$ that will appear as a summand in $\det K_4 = \det K_{\mathbb{A},S}(w)$. We will now resort to the notion of Schur complement and we refer the reader to Appendix A for some background on this. Define the Schur complement

$$L := K_{\mathbb{A}}(w)/K_4 = \begin{bmatrix} I \\ K_1 \end{bmatrix} - \begin{bmatrix} 0 \\ K_2 \end{bmatrix} K_4^{-1} K_3 = \begin{bmatrix} I \\ \Pi(w) \end{bmatrix}, \quad (3.2)$$

where $\Pi(w) := K_1 - K_2 K_4^{-1} K_3$. To get an explicit formula for the entries of $\Pi(w)$, notice that for $w'_i \in S$, $w_j \in T$, the square submatrix $L_{S \setminus \{w'_i\} \cup \{w_j\}}$ of L with rows indexed by $S \setminus \{w'_i\} \cup \{w_j\}$ is the Schur complement $K_{\mathbb{A}, S \setminus \{w'_i\} \cup \{w_j\}}(w)/K_4$. Using $\det K_4 = \det K_{\mathbb{A},S}(w)$ and Theorem A.1, we have

$$\Pi(w)_{w_j, b_i} = (-1)^{|S|-i} \det L_{S \setminus \{w'_i\} \cup \{w_j\}} = (-1)^{|S|-i} \frac{\det K_{\mathbb{A}, S \setminus \{w'_i\} \cup \{w_j\}}(w)}{\det K_{\mathbb{A},S}(w)}. \quad (3.3)$$

The $\Pi(w)$ matrix has the following multiplicativity property which will be very useful later for computations.

Proposition 3.2. *Suppose $\Gamma_{\mathbb{A}}$ is a balanced cylinder graph obtained by gluing balanced cylinder graphs Γ_i for $i = 1, \dots, n$ from left to right, so that $S(\Gamma_i)$ is identified with $T(\Gamma_{i+1})$. Assume that the Kasteleyn signs on the Γ_i induce a Kasteleyn sign on $\Gamma_{\mathbb{A}}$ (which is the case if they use the same $(\sigma_1, \dots, \sigma_h)$ for their definition). Then,*

$$\Pi(\Gamma_{\mathbb{A}})(w) = (-1)^{n-1} \Pi(\Gamma_1)(w) \Pi(\Gamma_2)(w) \cdots \Pi(\Gamma_n)(w).$$

Here, $S(\Gamma_i)$ and $T(\Gamma_{i+1})$ denote the source vertices of Γ_i and target vertices of Γ_{i+1} , respectively.

Proof. We may assume that $n = 2$, the general case will follow by induction. For $i \in \{1, 2\}$, denote by B_S^i , B^i , S^i , T^i and W_{int}^i the sets of vertices associated with Γ_i . Then we have the following form for the Kasteleyn matrices of Γ_1 and Γ_2 :

$$K(\Gamma_1)(w) = \begin{bmatrix} B_S^1 & B^1 \setminus B_S^1 \\ \begin{bmatrix} I & 0 \\ K_1 & K_2 \\ K_3 & K_4 \end{bmatrix} & \begin{bmatrix} S^1 \\ T^1 \\ W_{\text{int}}^1 \end{bmatrix} \end{bmatrix}, \quad K(\Gamma_2)(w) = \begin{bmatrix} B_S^2 & B^2 \setminus B_S^2 \\ \begin{bmatrix} I & 0 \\ K'_1 & K'_2 \\ K'_3 & K'_4 \end{bmatrix} & \begin{bmatrix} S^2 \\ T^2 \\ W_{\text{int}}^2 \end{bmatrix} \end{bmatrix}.$$

Observing that $S^1 = T^2$, we have the following Kasteleyn matrix for $\Gamma_{\mathbb{A}}$:

$$K(\Gamma_{\mathbb{A}})(w) = \begin{bmatrix} B_S^2 & B_S^1 & B^2 \setminus B_S^2 & B^1 \setminus B_S^1 \\ \begin{bmatrix} I & 0 & 0 & 0 \\ 0 & K_1 & 0 & K_2 \\ K'_1 & I & K'_2 & 0 \\ K'_3 & 0 & K'_4 & 0 \\ 0 & K_3 & 0 & K_4 \end{bmatrix} & \begin{bmatrix} S^2 \\ T^1 \\ T^2 \\ W_{\text{int}}^2 \\ W_{\text{int}}^1 \end{bmatrix} \end{bmatrix}.$$

Thus,

$$-\Pi(\Gamma_{\mathbb{A}})(w) = \begin{bmatrix} K_1 & 0 & K_2 \end{bmatrix} \begin{bmatrix} I & K'_2 & 0 \\ 0 & K'_4 & 0 \\ K_3 & 0 & K_4 \end{bmatrix}^{-1} \begin{bmatrix} K'_1 \\ K'_3 \\ 0 \end{bmatrix}.$$

Since

$$\begin{bmatrix} I & K'_2 & 0 \\ 0 & K'_4 & 0 \\ K_3 & 0 & K_4 \end{bmatrix}^{-1} = \begin{bmatrix} I & -K'_2 K'^{-1}_4 & 0 \\ 0 & K'^{-1}_4 & 0 \\ -K_4^{-1} K_3 & K_4^{-1} K_3 K'_2 K'^{-1}_4 & K_4^{-1} \end{bmatrix},$$

we conclude that $-\Pi(\Gamma_{\mathbb{A}})(w) = \Pi(\Gamma_1)(w)\Pi(\Gamma_2)(w)$. \blacksquare

When $w = 1$, we abbreviate $K_{\mathbb{A}}(1)$ (resp. $\Pi(1)$) to $K_{\mathbb{A}}$ (resp. Π).

Remark 3.3. The matrix $\Pi(w)$ is related to the boundary measurement matrix of [16] constructed from networks on cylinders. The reference dimer cover M_0 makes $\Gamma_{\mathbb{A}}$ into a directed network \mathcal{N} as follows. Orient each edge $e = bw$ contained in M_0 from w to b , and assign it weight $\frac{1}{\text{wt}(e)}$, and each edge not contained in M_0 from b to w and assign it weight $\text{wt}(e)$. Each directed path in \mathcal{N} gets a weight that is the product of weights of all edges appearing in it. Then using Theorem 3.1 and formula (3.3), we have for $w'_i \in S$, $w_j \in T$,

$$\begin{aligned} \Pi(w)_{w_j, b_i} &= (-1)^{|S|-i} \frac{\det K_{\mathbb{A}, S \setminus \{w'_i\} \cup \{w_j\}}(w)}{\det K_{\mathbb{A}, S}(w)} \\ &= (-1)^{|S|-i} \frac{\text{wt}(M_0) \kappa(M_0) w^{(M_0, -\gamma_z)}}{\det K_{\mathbb{A}, S}(w)} \frac{\det K_{\mathbb{A}, S \setminus \{w'_i\} \cup \{w_j\}}(w)}{\text{wt}(M_0) \kappa(M_0) w^{(M_0, -\gamma_z)}} \\ &= (-1)^{|S|-i} \frac{\text{wt}(M_0) \kappa(M_0) w^{(M_0, -\gamma_z)}}{\det K_{\mathbb{A}, S}(w)} \\ &\quad \times \left(\sum_{\partial M = S \setminus \{w'_i\} \cup \{w_j\}} \text{sign}([M - M_0]) [\text{wt}]([M - M_0]) w^{([M - M_0], -\gamma_z)} \right). \end{aligned} \quad (3.4)$$

Notice that if M is a dimer cover with $\partial M = S \setminus \{w'_i\} \cup \{w_j\}$, then $M - M_0$ is the union of some directed cycles and a single directed simple path in \mathcal{N} from w'_i to w_j . The multiplicative factor is ± 1 if M_0 is the only dimer cover M' with $\partial M' = S$. If there is another dimer cover M' with $\partial M' = S$, then $M' - M_0$ is a collection of directed cycles in \mathcal{N} that can be attached to any directed path from w'_i to w_j to get a new directed path from w'_i to w_j . Expanding the multiplicative factor

$$\begin{aligned} &\frac{\text{wt}(M_0) \kappa(M_0) w^{(M_0, -\gamma_z)}}{\det K_{\mathbb{A}, S}(w)} \\ &= \frac{\text{sign}([0])}{1 + \left(\sum_{\substack{M' \neq M_0 \\ \partial M' = S}} \text{sign}([M' - M_0]) \text{sign}([0]) [\text{wt}]([M' - M_0]) w^{([M' - M_0], -\gamma_z)} \right)} \end{aligned}$$

as a geometric series, we see that on the right-hand side of equation (3.4), we have a (signed) partition function for (not necessarily simple) directed paths from w'_i to w_j along with collections of directed cycles. The boundary measurement matrix of [16] is also a matrix whose entries are signed partition functions for directed paths from w'_i to w_j . Therefore, the matrix $\Pi(w)$ is the boundary measurement matrix of [16] up to signs. A careful choice of κ is required to make the signs match up; this was worked out recently in [28]. This is the reason for calling S and T the source and target vertices, respectively.

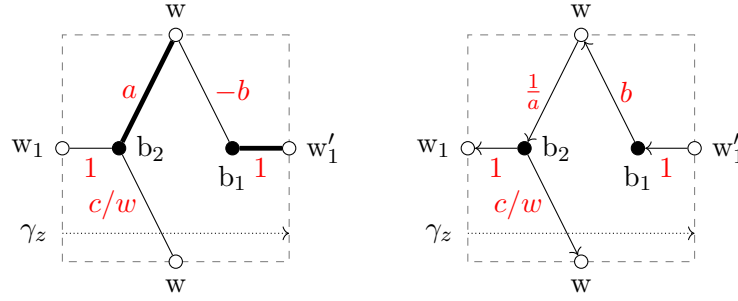


Figure 7. On the left, a bipartite graph $\Gamma_{\mathbb{A}}$ on a cylinder with the dimer cover M_0 in bold. On the right, the associated network \mathcal{N} .

Example 3.4. Consider the bipartite graph shown in Figure 7. We compute

$$K_{\mathbb{A}}(w) = \begin{bmatrix} b_1 & b_2 \\ 1 & 0 \\ 0 & 1 \\ -b & a + \frac{c}{w} \end{bmatrix} \begin{matrix} w'_1 \\ w_1 \\ w \end{matrix}, \quad \Pi(w) = \left[-\frac{b}{a + \frac{c}{w}} \right].$$

There are two dimer covers with $\partial M = \{w'_1\}$ with weights a and $\frac{c}{w}$, respectively. Notice that $w'_1 \rightarrow b_1 \rightarrow w \rightarrow b_2 \rightarrow w_1$ is a directed simple path from w'_1 to w_1 with weight $\frac{b}{a}$ and that $w \rightarrow b_2 \rightarrow w$ is a directed cycle in \mathcal{N} with weight $\frac{c}{aw}$. Moreover, any directed path from w'_1 to w_1 is obtained by attaching a finite number of copies of the cycle to the simple path at b_2 . Therefore, we see that

$$\Pi_{w_1, b_1}(w) = -\left(\frac{1}{1 + \frac{c}{aw}} \right) \frac{b}{a} = -\frac{b}{a} \sum_{k \geq 0} (-1)^k \left(\frac{c}{aw} \right)^k$$

is the (signed) partition function for all paths from w'_1 to w_1 .

Example 3.5. Let $\Gamma_{2, \mathbb{A}}$ denote the balanced cylinder graph obtained by gluing the top and bottom sides of the rectangle on Figure 6 (here we should take $z = 1$ on the picture). Gluing also the left and right sides yields the torus graph Γ_2 . The targets are the two white vertices w_1 and w_2 on the left boundary, while the sources are their copies on the right boundary that we denote by w'_1 and w'_2 . The set B_S is $\{b_3, b_4\}$. The Kasteleyn matrix (with blocks as in (3.1) and with $w = 1$) is

$$K_{\mathbb{A}} = \begin{bmatrix} b_3 & b_4 & b_1 & b_2 \\ \hline 1 & 0 & 0 & 0 \\ 0 & 1 & 0 & 0 \\ \hline 0 & 0 & 1 & 0 \\ 0 & 0 & 0 & 1 \\ \hline h & a & g & -b \\ e & d & -f & c \end{bmatrix} \begin{matrix} w'_1 \\ w'_2 \\ w_1 \\ w_2 \\ w_3 \\ w_4 \end{matrix},$$

and

$$\Pi = \frac{1}{bf - cg} \begin{bmatrix} ch + be & ac + bd \\ eg + fh & dg + af \end{bmatrix}. \quad (3.5)$$

3.2 Spectral curve of a torus graph constructed from a cylinder graph

We now show how the spectral curve of the torus graph obtained by gluing the two boundaries of a balanced cylinder graph can be obtained from the Π matrix of the cylinder graph.

Theorem 3.6. *Let $\Gamma_{\mathbb{A}}$ be a balanced cylinder graph and assume that by gluing the two boundaries of $\Gamma_{\mathbb{A}}$ we obtain a torus graph Γ . Write $\Pi(w)$ for $\Pi(\Gamma_{\mathbb{A}})(w)$. Then $\Sigma = \{(z, w) \in (\mathbb{C}^\times)^2 \mid \det(zI + \Pi(w)) = 0\}$ is the spectral curve.*

Due to the construction of Section 3.3 this result holds in particular when $\Gamma_{\mathbb{A}}$ is obtained from an arbitrary minimal torus graph Γ cut along a zig-zag path.

Proof. In Γ , split the white vertices that are in the image of S and T under the projection of $\Gamma_{\mathbb{A}}$ to \mathbb{T} , so that we now have two copies of these white vertices which we identify with S and T , respectively, connected by degree two black vertices. Let Γ_{ST} denote the torus graph obtained. Let B_{ST} denote the newly created degree two black vertices. Perturb γ_w so that it goes transversely through all the edges connecting B_{ST} with T (see the right picture of Figure 8). We extend the Kasteleyn sign κ on Γ to Γ_{ST} by defining $\kappa(e) = 1$ if e is an edge between B_{ST} and T and $\kappa(e) = -1$ if e is an edge between B_{ST} and S . The Kasteleyn matrix $K(z, w)$ of Γ_{ST} has the block matrix form

$$K(z, w) = \begin{bmatrix} B(\Gamma_{\mathbb{A}}) & B_{ST} \\ K_{\mathbb{A}}(w) & \begin{bmatrix} -I \\ zI \\ 0 \end{bmatrix} \end{bmatrix} \begin{bmatrix} S \\ T \\ W_{\text{int}} \end{bmatrix}.$$

Defining $K_4(w)$ to be the square submatrix of $K(z, w)$ with rows indexed by W_{int} and columns indexed by $B(\Gamma_{\mathbb{A}}) \setminus B_S$, we have the Schur complement

$$K(z, w)/K_4(w) = \begin{bmatrix} B_S & B_{ST} \\ I & \begin{bmatrix} -I \\ zI \end{bmatrix} \end{bmatrix} \begin{bmatrix} S \\ T \end{bmatrix}.$$

By Theorem A.1, we get $\det K(z, w) = \det K_4(w) \det(zI + \Pi(w))$. ■

Example 3.7. Consider again the graph Γ_2 from Figure 6 for which we have

$$\Pi(w) = \frac{1}{-cg + bfw} \begin{bmatrix} ch + bew & (ac + bd)w \\ eg + fh & dg + afw \end{bmatrix}$$

from (3.5). We have

$$\det(zI + \Pi(w)) = \frac{1}{-cg + bfw} (-dh + (dg + ch)z - cz^2 + aew + (be + af)zw + bfz^2w),$$

which agrees with (2.2).

3.3 Torus to cylinder

In this subsection, we show that Theorem 3.6 actually applies to any minimal bipartite graph on the torus. We outline a general procedure to construct a balanced cylinder graph $\Gamma_{\mathbb{A}}$ from a minimal graph Γ in a torus \mathbb{T} . This procedure is a generalization of Example 3.5, in which the balanced cylinder graph $\Gamma_{2,\mathbb{A}}$ is obtained from the minimal torus graph Γ_2 by cutting along the vertical side of the fundamental rectangle, which is parallel to the zig-zag path ζ_2 .

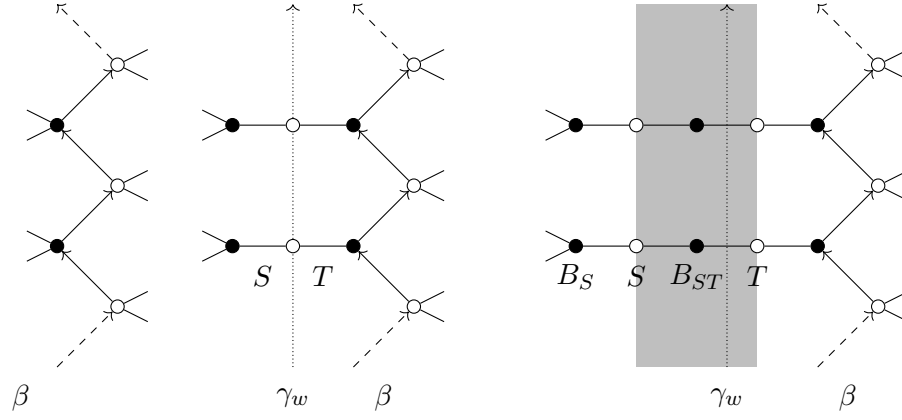


Figure 8. On the left is a zig-zag path β on a torus graph Γ . In the middle is the graph resulting from splitting the black vertices on β . On the right is the torus graph Γ_{ST} obtained from further splitting the white vertices lying on γ_w . Removing the shaded region from Γ_{ST} , we get the cylinder graph $\Gamma_{\mathbb{A}}$.

Let β be a zig-zag path in Γ . Without loss of generality, we assume that there are no 2-valent black vertices in β . Changing the fundamental domain if necessary, we can assume that $[\beta] = [\gamma_w]$. Split each black vertex in β to create a 2-valent white vertex, in such a way that one of the newly created black vertices is trivalent, having as neighbors the newly created white vertex as well as the two white vertices on β that were adjacent to the black vertex before the split. See the left and middle pictures of Figure 8. The homology class $[\gamma_w]$ has a representative cycle γ_w in \mathbb{T} that goes through each of the newly created 2-valent white vertices and does not intersect Γ anywhere else. Cutting \mathbb{T} along γ_w , we obtain a cylinder \mathbb{A} and a graph $\Gamma_{\mathbb{A}}$ embedded in it. The 2-valent white vertices become S and T , where T is connected to β (see the middle picture of Figure 8). We label the vertices of T in clockwise order as w_1, \dots, w_h , where $h = |T|$. Since $|B(\Gamma)| = |W(\Gamma)|$, we have $|B(\Gamma_{\mathbb{A}})| = |W(\Gamma_{\mathbb{A}})| - |S|$. Since Γ is minimal, there is a dimer cover M_0 in Γ that contains half the edges in β (see, for example, [23, Theorem 3.12]), which becomes a dimer cover in $\Gamma_{\mathbb{A}}$ such that $\partial M_0 = S$. For every $1 \leq i \leq h$ let f_i be the face of $\Gamma_{\mathbb{A}}$ adjacent to the boundary segment $w_i w_{i+1}$ on the T side. The Kasteleyn signs κ on Γ induce Kasteleyn signs on $\Gamma_{\mathbb{A}}$ provided we set $\sigma_i = 1$ if and only if $X_{f_i}([\kappa]) = (-1)^{\frac{|\partial f_i|}{2}}$ for every $1 \leq i \leq h$.

4 TCD maps on cylinders

In this section, we describe the cokernel of the Kasteleyn matrix K from a projective point of view in terms of *triple crossing diagram maps*, which we abbreviate to TCD maps. Our presentation of TCD maps is self-contained but we refer to [1, 2] for more details on TCD maps. We then define the notion of twisted TCD maps on a cylinder and compute the monodromy of such twisted TCD maps.

TCD maps are introduced in [2, 3] as a special case of the vector-relation configurations of [1]. The spider move for TCD maps first appeared in [1] while the resplit move is introduced in [2, 3]. The geometric R -matrix move for TCD maps is a novel contribution of the present paper.

4.1 TCD maps

Let $\Gamma_{\mathbb{A}}$ be a balanced cylinder graph. Assume that the black vertices of $\Gamma_{\mathbb{A}}$ are all of degree 2 or 3, which we can always do using expansion moves. A TCD map is a collection of points $(P_w)_{w \in W} \in \mathbb{CP}^{|W|-|B|-1}$ such that the following two conditions hold:

- for each $b \in B$ of degree 3, the three points P_w for w incident to b are distinct and are all contained in a line;
- for each $b \in B$ of degree 2, the two points P_w for w incident to b are equal.

Strictly speaking, the black vertices of a TCD should all be of degree 3 [48], but for the purposes of this article, it will be convenient to also allow black vertices of degree 2. The above definition of a TCD map was given in [2] for any bipartite graph with black vertices of degree 2 or 3, not necessarily a balanced cylinder graph. However starting in the next paragraph we use the Kasteleyn matrix hence we have to restrict the level of generality to consider only balanced cylinder graphs.

Recall that for a linear map f between two vector spaces E and F , the *cokernel* of f is defined as $F/\text{im } f$. Given a generic weight wt on $\Gamma_{\mathbb{A}}$, we obtain a TCD map as follows: consider the exact sequence

$$0 \rightarrow \mathbb{C}^B \xrightarrow{K_{\mathbb{A}}} \mathbb{C}^W \rightarrow \text{coker } K_{\mathbb{A}} \rightarrow 0,$$

where $\text{coker } K_{\mathbb{A}}$ is $(|W| - |B|)$ -dimensional. Let e_w be the unit basis vector corresponding to w in $\mathbb{C}^{W(\Gamma_{\mathbb{A}})}$ and let $v_w \in \text{coker } K_{\mathbb{A}}$ be the image of e_w . Then the projectivizations P_w of the vectors v_w define a TCD map. Clearly the definition is invariant under gauge equivalence. On the other hand, given a TCD map, we recover the edge weights modulo gauge transformations from the equations of the lines associated to the black vertices (see Lemma 4.3 below).

Remark 4.1. Note that the cokernel is only defined up to isomorphism. Different choices for a representative of the isomorphism class of the cokernel give different TCD maps related by projective transformations.

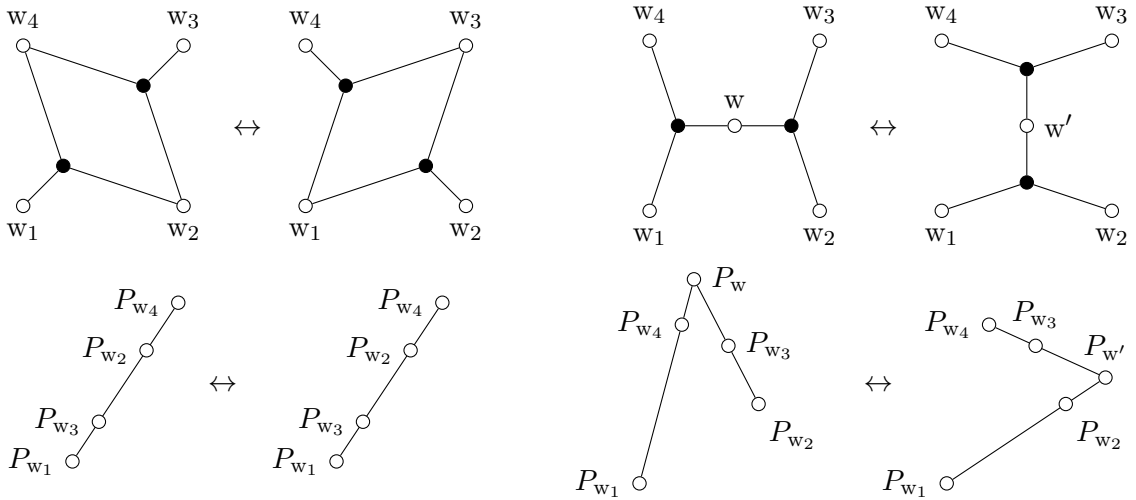


Figure 9. Elementary transformations allowed in TCD maps: spider move (left) and resplit (right).

The advantage of working with a graph $\Gamma_{\mathbb{A}}$ having trivalent black vertices is that we can keep track of both the geometric dynamics and the invariants while performing local moves. For TCD maps, there are two allowed elementary transformations, the spider move and the resplit, see Figure 9. In a generic situation, the points associated to white vertices after one of these two moves are determined by the combinatorics. Indeed, points do not change when performing the spider move. Furthermore, if the ambient projective space is of dimension at least 2, the new point appearing in the resplit is determined as the intersection of the two lines represented by the two black vertices. One can give a formula for it using multi-ratios.

The *multi-ratio* of $2m$ points $P_1, P_2, \dots, P_{2m} \in \mathbb{CP}^n$ with $n \geq 1$ is defined by

$$\text{mr}(P_1, \dots, P_{2m}) = \frac{\prod_{i=1}^m (P_{2i-1} - P_{2i})}{\prod_{i=1}^m (P_{2i} - P_{2i+1})}.$$

Such a definition makes sense by taking an affine chart of \mathbb{CP}^n (and is independent of the choice of such a chart) by pairing up each term in the numerator with a collinear term in the denominator, which is possible whenever one of the following two conditions is satisfied:

- (1) for every $1 \leq i \leq m$ the points P_{2i-1} , P_{2i} and P_{2i+1} are aligned;
- (2) for every $1 \leq i \leq m$ the points P_{2i} , P_{2i+1} and P_{2i+2} are aligned.

The *cross-ratio* of four aligned points $P_1, P_2, P_3, P_4 \in \mathbb{CP}^n$ with $n \geq 1$ is defined by

$$\text{cr}(P_1, P_2, P_3, P_4) = \text{mr}(P_1, P_2, P_3, P_4).$$

If the ambient dimension is at least 2, then the points involved in a resplit satisfy the classical Menelaus' theorem (see for, e.g., [38]):

$$\text{mr}(P_{w_1}, P_w, P_{w_2}, P_{w_3}, P_{w'}, P_{w_4}) = -1, \quad (4.1)$$

where the white vertices are labeled as on the right-hand side of Figure 9. In \mathbb{CP}^1 however, there is no incidence geometry. In this case, we *define* the new white vertex in the resplit via equation (4.1). Equation (4.1) has the symmetries of the octahedron.

Lemma 4.2. *Let $n \geq 1$ and let P_1, \dots, P_6 be six points in \mathbb{CP}^n . For every permutation σ of $\{1, \dots, 6\}$ such that $\sigma(i+3) = \sigma(i) + 3 \pmod{6}$ for every $1 \leq i \leq 6$, we have*

$$\text{mr}(P_1, P_2, P_3, P_4, P_5, P_6) = -1 \quad \Leftrightarrow \quad \text{mr}(P_{\sigma(1)}, P_{\sigma(2)}, P_{\sigma(3)}, P_{\sigma(4)}, P_{\sigma(5)}, P_{\sigma(6)}) = -1.$$

Proof. The permutations σ such that $\sigma(i+3) = \sigma(i) + 3 \pmod{6}$ for every i form the symmetry group of the octahedron, namely they leave invariant the collection of pairs of opposite points $\{\{P_1, P_4\}, \{P_2, P_5\}, \{P_3, P_6\}\}$. This subgroup is generated by σ_1 , σ_2 and σ_3 , where $\sigma_1(i) = i + 1 \pmod{6}$ for every i , $\sigma_2(i) = 7 - i$ for every i and σ_3 is the transposition $(1, 4)$.

Observe that σ_1 changes a multi-ratio to its inverse, while σ_2 leaves it invariant. In the case of σ_3 , solving the linear equation $\text{mr}(P_1, \dots, P_6) = -1$ for P_1 and reinserting it in $\text{mr}(P_4, P_2, P_3, P_1, P_5, P_6)$ yields the value -1 . ■

Another useful property of TCD maps is that the face weights can be recovered as multi-ratios as stated in the following lemma.

Lemma 4.3 ([1, Proposition 2.6]). *For a loop*

$$L = w_1 \rightarrow b_1 \rightarrow w_2 \rightarrow b_2 \rightarrow \dots \rightarrow w_n \rightarrow b_n \rightarrow w_1$$

such that $w_i \neq w_{i+1}$ for every i , let w'_i denote the third white vertex incident to b_i that is not in $\{w_i, w_{i+1}\}$. Then we have

$$[\text{wt}]([L]) = [\kappa]([L])^{-1} \text{mr}(P_{w_1}, P_{w'_1}, P_{w_2}, P_{w'_2}, \dots, P_{w_n}, P_{w'_n}).$$

4.2 TCD map on $\Gamma_{\hat{\mathbb{A}}}$ from Γ

Let $\Gamma_{\mathbb{A}}$ be a balanced cylinder graph.

Lemma 4.4. *Suppose there exists a dimer cover M_1 of $\Gamma_{\mathbb{A}}$ such that $\partial M_1 = T$. Then the matrix Π in (3.2) is invertible for generic weights on $\Gamma_{\mathbb{A}}$.*

Proof. Since $\det K_4 = \det K_{\mathbb{A},S}$, using Theorem A.1, we get

$$\det \Pi = \frac{\det K_{\mathbb{A},T}}{\det K_{\mathbb{A},S}}.$$

The existence of M_1 with $\partial M_1 = T$ and Theorem 3.1 with $I = T$ gives $\det K_{\mathbb{A},T} \neq 0$ for generic weights. \blacksquare

Hereafter, we assume that there is a dimer cover M_1 of $\Gamma_{\mathbb{A}}$ such that $\partial M_1 = T$ and that weights on $\Gamma_{\mathbb{A}}$ are generic.

Let \mathbb{T} be the torus obtained by gluing together the two boundary components of \mathbb{A} in such a way that the two endpoints of γ_z are identified and that each vertex in S is identified with a vertex in T . Let γ_w be the image in \mathbb{T} of the boundaries of \mathbb{A} and let Γ be the image in \mathbb{T} of $\Gamma_{\mathbb{A}}$. Let $\hat{\mathbb{A}} := H_1(\mathbb{T}, \mathbb{R})/\mathbb{Z}[\gamma_w]$ denote the infinite cylinder covering \mathbb{A} . Note that $\hat{\mathbb{A}} = \bigcup_{k \in \mathbb{Z}} \mathbb{A} + k[\gamma_z]$, that is $\hat{\mathbb{A}}$ is obtained by gluing together infinitely many copies of \mathbb{A} . Let

$$\Gamma_{\hat{\mathbb{A}}} = (B(\Gamma_{\hat{\mathbb{A}}}) \cup W(\Gamma_{\hat{\mathbb{A}}}), E(\Gamma_{\hat{\mathbb{A}}}))$$

denote the preimage of Γ under the covering map $\hat{\mathbb{A}} \rightarrow \mathbb{T}$. Fix a white vertex $w \in W(\Gamma_{\hat{\mathbb{A}}})$ and choose a large enough m so that w is in $\mathbb{A}_m := \bigcup_{k \in [-m, m] \cap \mathbb{Z}} (\mathbb{A} + k\gamma_z) \subset \hat{\mathbb{A}}$. Let $\Gamma_{\mathbb{A}_m} := \Gamma_{\hat{\mathbb{A}}} \cap \mathbb{A}_m$.

Lemma 4.5. *We have $\text{coker } K_{\mathbb{A}_m} \cong \text{coker } K_{\mathbb{A}} \cong \mathbb{C}^{|W(\Gamma_{\mathbb{A}})| - |B(\Gamma_{\mathbb{A}})|}$ for all $m \geq 0$. Moreover with these identifications, the image of e_w in $\mathbb{C}^{|W(\Gamma_{\mathbb{A}})| - |B(\Gamma_{\mathbb{A}})|}$ under the cokernel map of $K_{\mathbb{A}_m}$ is independent of m , where e_w is the unit basis vector corresponding to w in $\mathbb{C}^{W(\Gamma_{\mathbb{A}_m})}$.*

Proof. Suppose $m > m'$. $K_{\mathbb{A}_m}$ has the block form

$$K_{\mathbb{A}_m} = \begin{bmatrix} B(\Gamma_{\mathbb{A}_{m'}}) & B(\Gamma_{\mathbb{A}_m}) \setminus B(\Gamma_{\mathbb{A}_{m'}}) \\ K_{\mathbb{A}_{m'}} & * \\ 0 & K' \end{bmatrix} \begin{matrix} W(\Gamma_{\mathbb{A}_{m'}}) \\ W(\Gamma_{\mathbb{A}_m}) \setminus W(\Gamma_{\mathbb{A}_{m'}}) \end{matrix},$$

where K' is invertible by existence of M_0 and M_1 , and Theorem 3.1. Therefore, $K_{\mathbb{A}_m}/K' = K_{\mathbb{A}_{m'}}$ and so the second statement follows from Theorem A.2. By Theorem A.2 with $m' = 0$, we get $\text{coker } K_{\mathbb{A}_m} \cong \text{coker } K_{\mathbb{A}} \cong \mathbb{C}^{|W(\Gamma_{\mathbb{A}})| - |B(\Gamma_{\mathbb{A}})|}$ for all $m \geq 0$. \blacksquare

We define a TCD map $P: W(\Gamma_{\hat{\mathbb{A}}}) \rightarrow \mathbb{CP}^{|W(\Gamma_{\mathbb{A}})| - |B(\Gamma_{\mathbb{A}})| - 1}$ in the following way. For $w \in W(\Gamma_{\hat{\mathbb{A}}})$, we choose m sufficiently large so that $w \in W(\Gamma_{\mathbb{A}_m})$. Let v_w denote the image of e_w in $\mathbb{C}^{|W(\Gamma_{\mathbb{A}})| - |B(\Gamma_{\mathbb{A}})|}$ as in Lemma 4.5, and define $P_w \in \mathbb{CP}^{|W(\Gamma_{\mathbb{A}})| - |B(\Gamma_{\mathbb{A}})| - 1}$ to be the projectivization of v_w . Lemma 4.5 guarantees that the definition is independent of the choice of m .

4.3 Monodromy of a TCD map on $\Gamma_{\hat{\mathbb{A}}}$

A pair (P, M) where $P: W(\Gamma_{\hat{\mathbb{A}}}) \rightarrow \mathbb{CP}^{|W(\Gamma_{\mathbb{A}})| - |B(\Gamma_{\mathbb{A}})| - 1}$ is a TCD map and the operator $M \in \text{PGL}^{|W(\Gamma_{\mathbb{A}})| - |B(\Gamma_{\mathbb{A}})|}$ is called a *twisted TCD map* if $M(P_w) = P_{w+\gamma_z}$ for all $w \in W(\Gamma_{\hat{\mathbb{A}}})$. M is called the *monodromy* of P .

Now suppose $P: W(\Gamma_{\hat{\mathbb{A}}}) \rightarrow \mathbb{CP}^{|W(\Gamma_{\mathbb{A}})| - |B(\Gamma_{\mathbb{A}})| - 1}$ is a TCD map on $\Gamma_{\hat{\mathbb{A}}}$ as in Section 4.2. Let $[\Pi]$ denote the class of Π in $\text{PGL}^{|W(\Gamma_{\mathbb{A}})| - |B(\Gamma_{\mathbb{A}})|}$, where Π is the matrix in (3.2).

Theorem 4.6. *The map P is a twisted TCD map. The $\mathrm{PGL}_{|W(\Gamma_{\mathbb{A}})|-|B(\Gamma_{\mathbb{A}})|}$ matrix class $[-\Pi]$ is the monodromy of P in the basis $\{v_w\}_{w \in T}$.*

Proof. The existence of the dimer cover M_1 implies that the matrix Π is invertible (Lemma 4.4). Let $T = \{w_1, \dots, w_h\}$ be the set of target vertices in $W(\Gamma_{\mathbb{A}})$ so that $S = \{w_1 + \gamma_z, \dots, w_h + \gamma_z\}$ is the set of source vertices. Since each boundary white vertex of $\Gamma_{\mathbb{A}}$ has degree 1, we have a unique black vertex $b_i \in B_S$ incident to $w_i + \gamma_z \in S$ in $\Gamma_{\mathbb{A}}$. Therefore, we have a canonical isomorphism $\mathbb{C}^S \cong \mathbb{C}^{B_S}$, $e_{w_i + \gamma_z} \mapsto e_{b_i}$.

By Theorem A.2, we have $\mathrm{coker} \begin{bmatrix} I \\ \Pi \end{bmatrix} \cong \mathrm{coker} K_{\mathbb{A}}$ such that the cokernel map $\mathbb{C}^S \oplus \mathbb{C}^T \rightarrow \mathrm{coker} \begin{bmatrix} I \\ \Pi \end{bmatrix} \cong \mathrm{coker} K_{\mathbb{A}}$ is $e_w \mapsto v_w$. Consider the following exact sequence:

$$0 \rightarrow \mathbb{C}^{B_S} \xrightarrow{\begin{bmatrix} I \\ \Pi \end{bmatrix}} \mathbb{C}^S \oplus \mathbb{C}^T \xrightarrow{[-\Pi \ I]} \mathbb{C}^T \rightarrow 0.$$

When we write $-\Pi$ above the third arrow, we are abusing notation and mean the composition $\mathbb{C}^S \cong \mathbb{C}^{B_S} \xrightarrow{-\Pi} \mathbb{C}^T$. By the universal property of the cokernel, we have a canonical isomorphism of $\mathrm{coker} K_{\mathbb{A}}$ with \mathbb{C}^T such that $v_{w_i} = e_{w_i}$ for $w_i \in T$ and $v_{w_i + \gamma_z} = -\Pi e_{w_i + \gamma_z}$ for $w_i + \gamma_z \in S$. Translation by γ_z gives us an isomorphism $\mathbb{C}^T \cong \mathbb{C}^S$ sending e_{w_i} to $e_{w_i + \gamma_z}$. Therefore, $v_{w_i + \gamma_z} = -\Pi v_{w_i}$ for $i = 1, 2, \dots, h$, where again we are abusing notation by calling $-\Pi$ the composition $\mathbb{C}^T \cong \mathbb{C}^S \xrightarrow{-\Pi} \mathbb{C}^T$ which sends v_{w_i} to $v_{w_i + \gamma_z}$.

The same argument applied to the translated graph $\Gamma_{\mathbb{A} + k\gamma_z}$ gives $v_{w_i + (k+1)\gamma_z} = -\Pi v_{w_i + k\gamma_z}$. This implies $v_{w_i + k\gamma_z} = (-\Pi)^k v_{w_i}$ for all $k \in \mathbb{Z}$. For $w \in W(\Gamma_{\mathbb{A}})$, since $\{v_{w_i}\}$ is a basis of $\mathrm{coker} K_{\mathbb{A}}$, there exist $a_i \in \mathbb{C}$ such that $v_w = \sum_{i=1}^h a_i v_{w_i}$. Then we have

$$(-\Pi)^k v_w = \sum_{i=1}^h a_i (-\Pi)^k v_{w_i} = \sum_{i=1}^h a_i v_{w_i + k\gamma_z} = v_{w + k\gamma_z},$$

where the last equality follows from $K_{\mathbb{A}} = K_{\mathbb{A} + k\gamma_z}$. Any white $w' \in W(\Gamma_{\mathbb{A}})$ is of the form $w + m\gamma_z$ for some $w \in W(\Gamma_{\mathbb{A}})$. Then $w' + \gamma_z = w + (m+1)\gamma_z$, so that we have

$$v_{w'} = (-\Pi)^m v_w, \quad v_{w' + \gamma_z} = (-\Pi)^{m+1} v_w,$$

and therefore $v_{w' + \gamma_z} = -\Pi v_{w'}$. Projectivizing, we get the statement of the proposition. \blacksquare

In the second half of the paper, the setting of twisted TCD maps will be used to study dynamical systems on spaces of twisted polygons.

Definition 4.7. Let $d \geq 1$ and let $n \geq 3$. A *twisted n -gon in dimension d* is a pair (p, M) where $p: \mathbb{Z} \rightarrow \mathbb{CP}^d$ and $M \in \mathrm{PGL}_{d+1}$ is a projective transformation called *monodromy* such that $p_{i+n} = M(p_i)$ for all $i \in \mathbb{Z}$.

The group PGL_{d+1} acts on the space of twisted n -gons in dimension d by

$$A \cdot (p_1, p_2, \dots, p_n, M) = (A(p_1), A(p_2), \dots, A(p_n), AMA^{-1}). \quad (4.2)$$

For each dynamical system considered, we will impose some additional nondegeneracy conditions for the twisted n -gons, which will be specific to each dynamics.

5 The pentagram map

Our exposition follows [41, 49]. Let $n \geq 4$. A twisted n -gon in dimension 2 is said to be *nondegenerate* if in each 5-tuple $(p_i, p_{i+1}, p_{i+2}, p_{i+3}, p_{i+4})$ of consecutive points, no three points are collinear, except possibly p_i, p_{i+2}, p_{i+4} .

Let $\tilde{\mathcal{T}}_n$ denote the space of nondegenerate twisted n -gons. $\tilde{\mathcal{T}}_n$ is an open subvariety of $(\mathbb{CP}^2)^n \times \mathrm{PGL}_3$, and PGL_3 acts on it by (4.2). The quotient $\mathcal{T}_n := \tilde{\mathcal{T}}_n / \mathrm{PGL}_3$ is the moduli space parameterizing projective equivalence classes of nondegenerate twisted n -gons. For $(p, M) \in \tilde{\mathcal{T}}_n$, the *left and right corner invariants* are defined by

$$\begin{aligned} x_i &:= \mathrm{cr}(p_{i-2}, p_{i-1}, \overline{p_{i-2}p_{i-1}} \cap \overline{p_{i+1}p_{i+2}}, \overline{p_{i-2}p_{i-1}} \cap \overline{p_i p_{i+1}}), \\ y_i &:= \mathrm{cr}(\overline{p_{i-2}p_{i-1}} \cap \overline{p_{i+1}p_{i+2}}, \overline{p_{i-1}p_i} \cap \overline{p_{i+1}p_{i+2}}, p_{i+2}, p_{i+1}), \end{aligned}$$

where \overline{ab} denotes the projective line spanned by $a, b \in \mathbb{CP}^2$. The corner invariants define a morphism

$$(x, y): \tilde{\mathcal{T}}_n \rightarrow (\mathbb{C} \setminus \{0, 1\})^{2n}, \quad (p, M) \mapsto (x_1, \dots, x_n, y_1, \dots, y_n). \quad (5.1)$$

Since the x_i, y_i 's are cross-ratios, they are PGL_3 -invariant. Therefore, the morphism (5.1) descends to a morphism $(x, y): \mathcal{T}_n \rightarrow (\mathbb{C} \setminus \{0, 1\})^{2n}$, which is an isomorphism [45]. The Poisson brackets

$$\{x_i, x_{i+1}\}_{\mathcal{T}_n} := -x_i x_{i+1}, \quad \{y_i, y_{i+1}\}_{\mathcal{T}_n} := y_i y_{i+1}, \quad (5.2)$$

make \mathcal{T}_n a Poisson variety. Here, we only give the nonzero values obtained by pairing two coordinate functions.

The rational map $T: \mathcal{T}_n \rightarrow \mathcal{T}_n$ defined by $(p, M) \mapsto (q, M)$, where $q_i = \overline{p_{i-1}p_{i+1}} \cap \overline{p_i p_{i+2}}$ is called the *pentagram map*. In the coordinates (x, y) , the rational map T is given by [41, Lemma 2.4]

$$T^* x_i = x_i \frac{1 - x_{i-1} y_{i-1}}{1 - x_{i+1} y_{i+1}}, \quad T^* y_i = y_{i+1} \frac{1 - x_{i+2} y_{i+2}}{1 - x_i y_i}.$$

5.1 Integrability of the pentagram map

We recall the following well known result from the theory of algebraic groups (see, for example, [47, Theorem 3.2.3]). If we have an action of a torus \mathbb{C}^\times on a vector space V , then $V = \bigoplus_{k \in \mathbb{Z}} V_k$ can be decomposed into the *weight subspaces* corresponding to the *characters* of \mathbb{C}^\times , where a character $\chi: \mathbb{C}^\times \rightarrow \mathbb{C}^\times$ is just a Laurent monomial $\chi(w) = w^k$, $k \in \mathbb{Z}$, and the weight subspace of $\chi(w) = w^k$ is defined as

$$V_k := \{v \in V \mid w \cdot v = w^k v \text{ for } w \in \mathbb{C}^\times\}.$$

If $v \in V_k$, then we say that v has *weight* k .

Now consider the (rational) action of \mathbb{C}^\times on \mathcal{T}_n : $R_w(x, y) = (w^{-1}x, wy)$, $x = (x_1, \dots, x_n)$, $y = (y_1, \dots, y_n)$, and let R_w^* denote the induced action on the vector space $\mathbb{C}[x, y]$:

$$R_w^*(f(x, y)) = f(R_{w^{-1}}(x, y)).$$

Define $O_n := \prod_{i=1}^n x_i$ and $E_n := \prod_{i=1}^n y_i$. Then, O_n and E_n have weights n and $-n$, respectively. For $(p, M) \in \mathcal{T}_n$, let $M(w)$ denote the monodromy matrix of $R_w(p, M)$, and let

$$P(z, w) := \det(zI - M(w)).$$

In [45], it is shown that

$$\begin{aligned} \left(\frac{w^n O_n^2 E_n}{\det M(w)^{-1}} \right)^{\frac{1}{3}} \mathrm{tr} M(w)^{-1} &= 1 + \sum_{k=1}^{\lfloor \frac{n}{2} \rfloor} O_k w^k, \\ \left(\frac{O_n E_n^2}{w^n \det M(w)} \right)^{\frac{1}{3}} \mathrm{tr} M(w) &= 1 + \sum_{k=1}^{\lfloor \frac{n}{2} \rfloor} E_k w^{-k}, \end{aligned} \quad (5.3)$$

where O_k, E_k , $k = 1, \dots, \lfloor \frac{n}{2} \rfloor$, are polynomials in $\mathbb{C}[x, y]$.

Theorem 5.1 ([41]). *We have*

1. For n even, $\{\cdot, \cdot\}_{\mathcal{T}_n}$ has corank 4, and the subalgebra of Casimirs is generated by $O_{\frac{n}{2}}, E_{\frac{n}{2}}, O_n, E_n$.
2. For n odd, $\{\cdot, \cdot\}_{\mathcal{T}_n}$ has corank 2, and the subalgebra of Casimirs is generated by O_n, E_n .
3. For $k = 1, 2, \dots, \lfloor \frac{n-1}{2} \rfloor$, the functions O_k and E_k mutually commute and form a maximal set of functionally independent Hamiltonians, making the Poisson variety \mathcal{T}_n a Liouville integrable system.

Moreover, the pentagram map T is discrete integrable in the following sense:

4. T is Poisson.
5. The Hamiltonians and the Casimirs are invariant under T .

5.2 Pentagram TCD maps

Let $n \geq 4$. Let Ξ_n denote the torus graph obtained by gluing in cyclic order the graphs H_i in Figure 10 for $i = 1, 2, \dots, n$ and contracting two-valent black vertices (see Figure 11 for a picture of Ξ_4). Let N_{Ξ_n} denote the Newton polygon of Ξ_n . When n is even, there are 6 zig-zag paths and the Newton polygon is as shown on left hand side of Figure 13, and when n is odd, there are 4 zig-zag paths and the Newton polygon as shown on the right hand side of Figure 13.

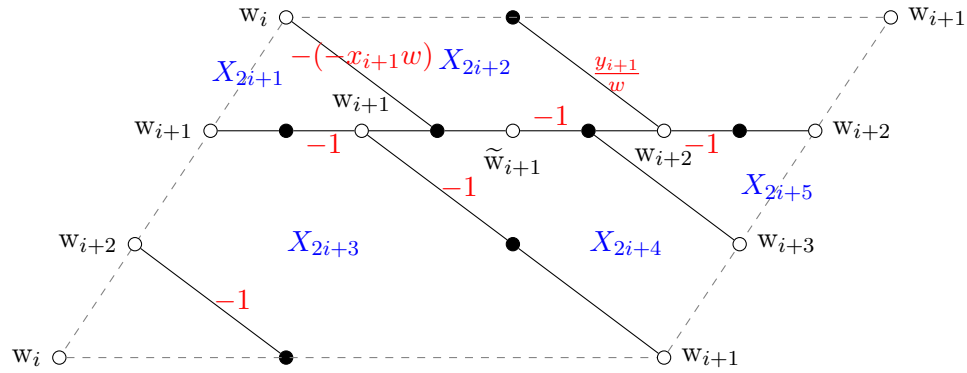


Figure 10. The building block graph H_i . In the edge label $-(-x_{i+1}w)$, the edge weight is $-x_{i+1}$ and the other $-$ is the Kasteleyn sign. We have given white vertices that are identified upon contracting 2-valent black vertices the label, since they are mapped to the same point by the twisted TCD map P .

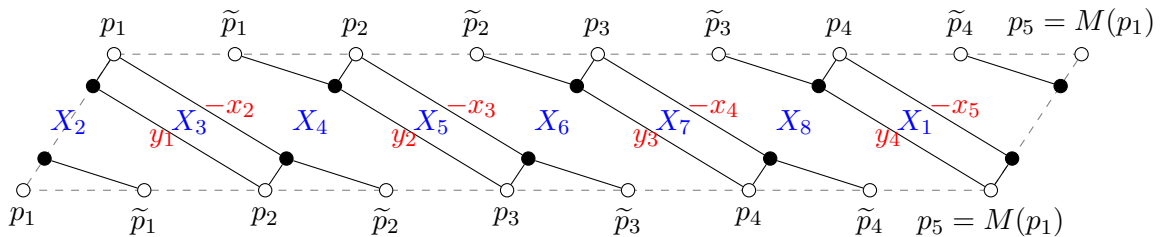


Figure 11. The graph Ξ_4 showing the face weights and the pentagram map TCD. Here $\tilde{p}_i := \overline{p_{i-1}p_i} \cap \overline{p_{i+1}p_{i+2}}$.

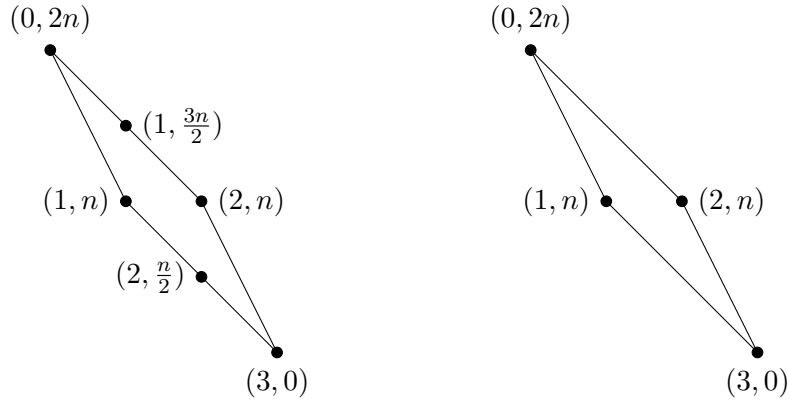


Figure 13. The Newton polygon N_{Ξ_n} of Ξ_n for even n (left) and odd n (right).

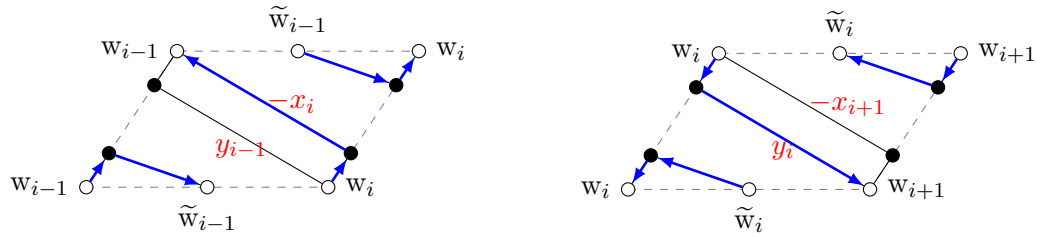


Figure 14. The cycles σ_i (left) and ρ_i (right) (compare with Figure 11 and Figure 12 (6)).

Let $(p, M) \in \mathcal{T}_n$ and let $[\text{wt}] \in \mathcal{X}_{N(\Xi_n)}^\lambda$ such that $(x, y)^{-1} \circ \pi_n([\text{wt}]) = (p, M)$. We choose edge weights and Kasteleyn signs representing $[\text{wt}]$ as in Figure 10. Let $\Xi_{n, \mathbb{A}}$ denote the balanced cylinder graph obtained by concatenating the graphs H_i for $i = 1, 2, \dots, n$ without closing up cyclically. We have $|W(\Xi_{n, \mathbb{A}})| - |B(\Xi_{n, \mathbb{A}})| = 3$. Let $P: W(\Xi_{n, \mathbb{A}}) \rightarrow \mathbb{CP}^2$ denote the twisted TCD map associated to $[\text{wt}]$. We label the vertices of $\Xi_{n, \mathbb{A}}$ as in Figure 10.

Proposition 5.3. *We have*

$$P_{w_i} = p_i, \quad P_{\tilde{w}_i} = \overline{p_{i-1}p_i} \cap \overline{p_{i+1}p_{i+2}},$$

for all $i \in \mathbb{Z}$ modulo the action of PGL_3 .

Proof. Since P is a TCD map, the three white vertices incident to a trivalent black vertex are in a line. Therefore, we have $P_{\tilde{w}_{i+1}} = \overline{P_{w_i}P_{w_{i+1}}} \cap \overline{P_{w_{i+2}}P_{w_{i+3}}}$, and so it suffices to show that $P_{w_i} = p_i$ for all $i \in \mathbb{Z}$. The points p_i are determined modulo PGL_3 by their x_i and y_i coordinates, so it suffices to show that the points P_{w_i} have the same x_i and y_i coordinates. Since $[\text{wt}]$ is defined so that $(x, y)^{-1} \circ \pi_n([\text{wt}]) = (p, M)$, we have $\chi_{[\sigma_i]}([\text{wt}]) = -x_i$. On the other hand,

$$\chi_{[\sigma_i]}([\text{wt}]) = \text{mr}(P_{w_{i-1}}, P_{w_{i-2}}, P_{\tilde{w}_{i-1}}, P_{w_{i+1}}, P_{w_i}, P_{\tilde{w}_i}),$$

so it suffices to show that

$$\begin{aligned} & -\text{mr}(P_{w_{i-1}}, P_{w_{i-2}}, P_{\tilde{w}_{i-1}}, P_{w_{i+1}}, P_{w_i}, P_{\tilde{w}_i}) \\ &= \text{cr}(P_{w_{i-2}}, P_{w_{i-1}}, \overline{P_{w_{i-2}}P_{w_{i-1}}} \cap \overline{P_{w_{i+1}}P_{w_{i+2}}}, P_{\tilde{w}_{i-1}}) \\ &= \text{cr}(P_{w_{i-1}}, P_{w_{i-2}}, P_{\tilde{w}_{i-1}}, \overline{P_{w_{i-2}}P_{w_{i-1}}} \cap \overline{P_{w_{i+1}}P_{w_{i+2}}}), \end{aligned} \tag{5.4}$$

where the cross-ratio on the right hand side of the first line is the definition of x_i , and the second equality is from reordering the terms in the cross-ratio. Expanding both sides of (5.4)

and canceling common terms, we see that (5.4) is equivalent to

$$\text{mr} \left(P_{w_{i-1}}, \overline{P_{w_{i-2}} P_{w_{i-1}}} \cap \overline{P_{w_{i+1}} P_{w_{i+2}}}, P_{\tilde{w}_{i-1}}, P_{w_{i+1}}, P_{w_i}, P_{\tilde{w}_i} \right) = -1,$$

which is Menelaus' theorem applied to the quadrilateral $P_{\tilde{w}_i} P_{w_{i-1}} P_{\tilde{w}_{i-1}} P_{w_{i+1}}$, whose opposite sides intersect at the points P_{w_i} and $\overline{P_{w_{i-2}} P_{w_{i-1}}} \cap \overline{P_{w_{i+1}} P_{w_{i+2}}}$. The proof for y_i is similar. ■

We call the twisted TCD map P the *pentagram TCD map*. It was studied in [1, Section 3.1].

Corollary 5.4. *The monodromy matrix of the twisted TCD map P coincides with the monodromy matrix M of the twisted n -gon (p, M) .*

Now we compute this monodromy matrix. The Kasteleyn matrix of H_i , with rows and columns indexed as in (3.1), is

$$K_{H_i}(w) = \left[\begin{array}{ccc|ccc} 1 & 0 & 0 & 0 & 0 & 0 \\ 0 & 1 & 0 & 0 & 0 & 0 \\ 0 & 0 & 1 & 0 & 0 & 0 \\ \hline 0 & 0 & 0 & 0 & x_{i+1}w & 0 \\ 0 & 0 & 0 & 0 & 0 & 1 \\ 0 & 0 & 0 & -1 & 0 & 0 \\ \hline -1 & 0 & 0 & 0 & 1 & -1 \\ 0 & -1 & 1 & \frac{y_{i+1}}{w} & 0 & 0 \\ 0 & 0 & -1 & 0 & 1 & 0 \end{array} \right] \begin{matrix} w_{i+1} \\ w_{i+2} \\ w_{i+3} \\ w_i \\ w_{i+1} \\ w_{i+2} \\ w_{i+1} \\ w_{i+2} \\ \tilde{w}_{i+1} \end{matrix},$$

using which we get

$$\Pi_{H_i}(w) = \begin{bmatrix} 0 & 0 & x_{i+1}w \\ -1 & 0 & 1 \\ 0 & -\frac{w}{y_{i+1}} & \frac{w}{y_{i+1}} \end{bmatrix}.$$

We have $\det \Pi_{H_i}(w) = \frac{x_{i+1}}{y_{i+1}} w^2$. The monodromy matrix $M(w) = (-1)^n \prod_{i=1}^n \Pi_{H_i}(w)$, so that

$$\det M(w) = (-1)^n \frac{O_n}{E_n} w^{2n}. \quad (5.5)$$

The following lemma is elementary.

Lemma 5.5. *For a 3×3 invertible matrix M , we have*

$$\det(zI - M) = z^3 - \text{tr } M z^2 + \frac{\text{tr } M^{-1}}{\det M^{-1}} z - \det M.$$

Applying Lemma 5.5 to $M(w)$, multiplying by E_n , and using equations (5.3) and (5.5), we get

$$\begin{aligned} E_n P(z, w) &= E_n z^3 - E_n \text{tr } M(w) z^2 + E_n \frac{\text{tr } M(w)^{-1}}{\det M(w)^{-1}} z - E_n \det M(w) \\ &= E_n z^3 \pm \left(1 + \sum_{k=1}^{\lfloor \frac{n}{2} \rfloor} E_k w^{-k} \right) z^2 w^n \pm \left(1 + \sum_{k=1}^{\lfloor \frac{n}{2} \rfloor} O_k w^k \right) z w^n \pm O_n w^{2n}, \end{aligned}$$

where the signs are irrelevant for our purposes. Since the GK Hamiltonians are coefficients of $P(z, w)$, we have proved the following theorem.

Theorem 5.6. *The map π_n identifies the GK Poisson structure, Hamiltonians and Casimirs with those of the pentagram map in Theorem 5.1.*

Remark 5.7. Glick [20] discovered a cluster algebra structure for the pentagram map, where the cluster variables are given by

$$X_{2i} = -\frac{1}{x_i y_i}, \quad X_{2i+1} = -x_{i+1} y_i.$$

On the other hand, the GK cluster variables are the face weights. Since the cycles $-(\sigma_i + \rho_i)$ and $\sigma_{i+1} + \rho_i$ are the faces of Ξ_n , we see that Glick's cluster variables coincide with those of GK.

6 The cross-ratio dynamics integrable system

In this section, we define cross-ratio dynamics on the space of $\vec{\alpha}$ -related pairs of twisted polygons and we recall the integrability results of [4] for that dynamics, generalizing them to the case when α_i may depend on i . All the results that we attribute to [4] in this section were stated and proven by them for constant α , but the proofs carry over easily to the case when α_i depends on i .

6.1 Poisson varieties of twisted polygons in \mathbb{CP}^1

Let $n \geq 2$. A twisted n -gon (p, M) in dimension 1 is called *nondegenerate* if for all $i \in \mathbb{Z}$, we have $p_i \notin \{p_{i+1}, p_{i+2}\}$. Let $\tilde{\mathcal{P}}_n$ denote the space of nondegenerate twisted n -gons. $\tilde{\mathcal{P}}_n$ is an open subvariety of $(\mathbb{CP}^1)^n \times \mathrm{PGL}_2$, and PGL_2 acts on it by (4.2). The quotient $\mathcal{P}_n := \tilde{\mathcal{P}}_n / \mathrm{PGL}_2$ is the moduli space parameterizing projective equivalence classes of nondegenerate twisted n -gons. We will sometimes abuse notation and simply write $p \in \tilde{\mathcal{P}}_n$ instead of $(p, M) \in \tilde{\mathcal{P}}_n$. Given $p \in \tilde{\mathcal{P}}_n$, we define the c -variables

$$c_i := \mathrm{cr}(p_{i-1}, p_i, p_{i+2}, p_{i+1}) \quad \text{for all } i \in \mathbb{Z}. \quad (6.1)$$

Notice that $c_{i+n} = c_i$ for all $i \in \mathbb{Z}$. Since p is nondegenerate, $c_i(p) \notin \{0, \infty\}$, so the c -variables define a morphism

$$c: \tilde{\mathcal{P}}_n \rightarrow (\mathbb{C}^\times)^n, \quad p \mapsto (c_1, c_2, \dots, c_n). \quad (6.2)$$

Since each c_i is a cross-ratio, this morphism is PGL_2 -invariant, and therefore, (6.2) descends to a morphism $c: \mathcal{P}_n \rightarrow (\mathbb{C}^\times)^n$. Given the c -variables and three initial points p_1, p_2, p_3 , the whole polygon is recovered from (6.1). Since any three points can be mapped to any other three points by a projective transformation, the c -variables characterize a polygon up to projective transformations and so c is an isomorphism. The inverse morphism is given explicitly in [4, Section 3.2].

The following lemma gives an explicit representative for the PGL_2 conjugacy class of the monodromy matrix M in terms of the c -variables.

Theorem 6.1 ([4, Lemma 3.2]). *The matrix*

$$M = \begin{bmatrix} 0 & c_1 \\ -1 & 1 \end{bmatrix} \begin{bmatrix} 0 & c_2 \\ -1 & 1 \end{bmatrix} \cdots \begin{bmatrix} 0 & c_n \\ -1 & 1 \end{bmatrix}$$

represents the monodromy matrix.

Let $\vec{\alpha} = (\alpha_i)_{i \in \mathbb{Z}}$ with $\alpha_i \in \mathbb{C} \setminus \{0, 1\}$ such that $\alpha_{i+n} = \alpha_i$. Two twisted polygons $p, q \in \tilde{\mathcal{P}}_n$ are said to be $\vec{\alpha}$ -related, and denoted $p \stackrel{\vec{\alpha}}{\sim} q$ if

$$\mathrm{cr}(p_i, q_i, p_{i+1}, q_{i+1}) = \alpha_i \quad \text{for all } i \in \mathbb{Z}, \quad (6.3)$$

and p and q have the same monodromy. Note that condition (6.3) alone does not imply that p and q have the same monodromy. The relation $\tilde{\sim}$ is PGL_2 -invariant, and therefore, descends to a relation on \mathcal{P}_n .

Let $\tilde{\mathcal{U}}_{n,\vec{\alpha}}$ denote the space of pairs of $\vec{\alpha}$ -related nondegenerate twisted polygons of length n . It is a subvariety of $(\mathbb{P}^1)^{2n} \times \mathrm{PGL}_2$ and PGL_2 acts on it by

$$A \cdot (p_1, \dots, p_n, q_1, \dots, q_n, M) = (A(p_1), \dots, A(p_n), A(q_1), \dots, A(q_n), AMA^{-1}).$$

We define the u -variables by

$$u_i := -\mathrm{cr}(p_i, p_{i+1}, q_i, p_{i-1}) \quad \text{for all } i \in \mathbb{Z}. \quad (6.4)$$

Since p and q are nondegenerate and $\vec{\alpha}$ -related, $u_i \notin \{0, -1, \infty\}$. Therefore, the u -variables define a PGL_2 -invariant morphism $u: \tilde{\mathcal{U}}_{n,\vec{\alpha}} \rightarrow (\mathbb{C} \setminus \{0, -1\})^n$ which descends to a morphism

$$u: \mathcal{U}_{n,\vec{\alpha}} \rightarrow (\mathbb{C} \setminus \{0, -1\})^n,$$

where $\mathcal{U}_{n,\vec{\alpha}} := \tilde{\mathcal{U}}_{n,\vec{\alpha}} / \mathrm{PGL}_2$. When there is no ambiguity on the choice of $\vec{\alpha}$, we will denote $\tilde{\mathcal{U}}_{n,\vec{\alpha}}$ and $\mathcal{U}_{n,\vec{\alpha}}$ simply by $\tilde{\mathcal{U}}_n$ and \mathcal{U}_n . Consider the morphism

$$\rho_{\vec{\alpha}}: \mathcal{U}_n \rightarrow \mathcal{P}_n, \quad (p, q, M) \mapsto (p, M).$$

It follows from [4, Section 4.8] that the diagram

$$\begin{array}{ccc} \mathcal{U}_n & \xrightarrow{\rho_{\vec{\alpha}}} & \mathcal{P}_n \\ \downarrow u & & \downarrow c \\ (\mathbb{C} \setminus \{0, -1\})^n & \xrightarrow{\Lambda_{\vec{\alpha}}} & (\mathbb{C}^\times)^n \end{array}$$

commutes, where the map $\Lambda_{\vec{\alpha}}$ is determined by

$$c_i = \frac{\alpha_i}{(1 + u_i)(1 + \frac{1}{u_{i+1}})}.$$

If we are given the u -variables, we can recover p up to projective transformations as $c^{-1} \circ \Lambda_{\vec{\alpha}}(u_1, \dots, u_n)$, and q is then determined by (6.4). Therefore, the morphism u induces an isomorphism between \mathcal{U}_n and $(\mathbb{C} \setminus \{0, -1\})^n$. The set \mathcal{U}_n is the moduli space parameterizing projective equivalence classes of pairs of $\vec{\alpha}$ -related twisted n -gons. The Poisson bracket

$$\{u_i, u_{i+1}\}_{\mathcal{U}_n} := u_i u_{i+1}, \quad (6.5)$$

makes $(\mathcal{U}_n, \{\cdot, \cdot\}_{\mathcal{U}_n})$ a Poisson variety while the Poisson bracket

$$\{c_i, c_{i+1}\}_{\vec{\alpha}} := c_i c_{i+1} \left(1 - \frac{c_i}{\alpha_i} - \frac{c_{i+1}}{\alpha_{i+1}}\right), \quad \{c_i, c_{i+2}\}_{\vec{\alpha}} := -\frac{1}{\alpha_{i+1}} c_i c_{i+1} c_{i+2},$$

makes $(\mathcal{P}_n, \{\cdot, \cdot\}_{\vec{\alpha}})$ a Poisson variety. For both Poisson brackets, we only give the nonzero values obtained by pairing two coordinate functions. We also define the rescaled coordinates $\bar{c}_i := \frac{c_i}{\alpha_i}$. In these coordinates, the Poisson bracket $\{\cdot, \cdot\}_{\vec{\alpha}}$ takes the simpler form

$$\{\bar{c}_i, \bar{c}_{i+1}\}_{\vec{\alpha}} = \bar{c}_i \bar{c}_{i+1} (1 - \bar{c}_i - \bar{c}_{i+1}), \quad \{\bar{c}_i, \bar{c}_{i+2}\}_{\vec{\alpha}} = -\bar{c}_i \bar{c}_{i+1} \bar{c}_{i+2}.$$

A computation similar to [4, Lemma 4.9] shows that $\rho_{\vec{\alpha}}$ is Poisson. [4, Corollary 2.7] shows that $\rho_{\vec{\alpha}}$ is generically finite of degree 2, that is, for a generic polygon $q \in \mathcal{P}_n$ there are two polygons $p, r \in \mathcal{P}_n$ that are $\vec{\alpha}$ -related to q . Therefore, the maps $C_{\vec{\alpha}}^1: (p, q, M) \mapsto (r, q, M)$ and $C_{\vec{\alpha}}^2: (q, p, M) \mapsto (q, r, M)$ are birational involutions of \mathcal{U}_n , respectively changing the first and the second curve of a pair of $\vec{\alpha}$ -related curves. The space \mathcal{U}_n also has another involution $j: (p, q, M) \mapsto (q, p, M)$ given in coordinates by

$$u_i \mapsto v_i := \frac{1}{u_i} \frac{\alpha_i - 1}{\alpha_{i-1} - 1} = -\mathrm{cr}(q_i, q_{i+1}, p_i, q_{i-1}). \quad (6.6)$$

6.2 Cross-ratio dynamics and integrability

Suppose $(q, M) \in \mathcal{P}_n$ such that $|\rho_{\vec{\alpha}}^{-1}(q, M)| = 2$, and suppose p, r are the two different polygons $\vec{\alpha}$ -related to q . The birational automorphism

$$\nu_{\vec{\alpha}} = j \circ C_{\vec{\alpha}}^1: \mathcal{U}_n \rightarrow \mathcal{U}_n, \quad (p, q, M) \mapsto (q, r, M)$$

is called *cross-ratio dynamics*. It can be described in coordinates as follows.

Proposition 6.2. *Let $(p, q, M) \in \mathcal{U}_n$ and denote respectively by u_i and u'_i the coordinates of (p, q, M) and $(q, r, M) = \nu_{\vec{\alpha}}(p, q, M)$. Then, we have*

$$u'_i = \frac{\sum_{t=0}^{n-1} \prod_{s=0}^{t-1} v_{i+s}}{\sum_{t=1}^n \prod_{s=1}^t v_{i+s}}, \quad (6.7)$$

where the v_i are expressed in terms of the u_i as in formula (6.6).

Proposition 6.2 is new compared to [4] and is proved in Section 7.2 using geometric R -matrices.

For $I \subset [n]$, let $c_I := \prod_{i \in I} c_i$. Similarly, we define \bar{c}_I , α_I , u_I etc. Let $c_{\text{even}} := c_2 c_4 \cdots$ and $c_{\text{odd}} := c_1 c_3 \cdots$ denote the product of the even and odd c variables, respectively. In the same way, we define α_{even} , etc.

A subset $I \subset [i, j]$ is said to be *cyclically sparse* if it contains no pair of consecutive indices where the indices are taken periodic modulo n . Define

$$F_k(c) := \sum_{I \text{ cyclically sparse: } |I|=k} c_I \quad \text{for } k = 0, \dots, \left\lfloor \frac{n}{2} \right\rfloor,$$

$$E_{\vec{\alpha}} := \frac{1}{\bar{c}_{[n]}} \left(\sum_{k=0}^{\left\lfloor \frac{n}{2} \right\rfloor} (-1)^k F_k(\bar{c}) \right)^2.$$

If $\alpha_i = \alpha$ for all i , then we say that p and q are α -related. In this case, we replace $\vec{\alpha}$ with α and write $p \stackrel{\alpha}{\sim} q$, $\{\cdot, \cdot\}_{\alpha}$, ρ_{α} etc. This is the setting of [4], but we defined everything in the more general setting of nonconstant $\vec{\alpha}$ since it is the natural setting from the point of view of the corresponding GK integrable system.

Theorem 6.3 ([4, Main Theorem 1]). *Let $\alpha_i = \alpha$ for all $i \in \mathbb{Z}$. We have*

1. *For n even, $\{\cdot, \cdot\}_{\alpha}$ has corank 2 and the subalgebra of Casimirs is generated by E_{α} and $\frac{c_{\text{even}}}{c_{\text{odd}}}$.*
2. *For n odd, $\{\cdot, \cdot\}_{\alpha}$ has corank 1 and the Casimir is E_{α} .*
3. *For $k = 1, 2, \dots, \left\lfloor \frac{n+1}{2} \right\rfloor - 1$, the functions $\frac{F_k(c)^2}{c_{[n]}}$ mutually commute and form a maximal set of functionally independent Hamiltonians, making the Poisson variety \mathcal{P}_n a Liouville integrable system.*

Moreover, cross-ratio dynamics is discrete integrable in the following sense:

4. ν_{α} is Poisson.
5. The pullbacks of the Hamiltonians and the Casimirs to \mathcal{U}_n by ρ_{α} are invariant under ν_{α} .

The following theorem shows that the Hamiltonians can be obtained from the monodromy matrix.

Theorem 6.4 ([4, Theorem 1]). *We have*

$$\frac{1}{\det M} \operatorname{tr}^2 M = \frac{1}{c_{[n]}} \left(\sum_{k=0}^{\lfloor \frac{n}{2} \rfloor} (-1)^k F_k(c) \right)^2.$$

Remark 6.5. Note that $\operatorname{tr} M$ is not PGL_2 -invariant, but the normalized trace $\frac{\operatorname{tr} M}{\sqrt{\det M}}$ is. However, the normalized trace is not a regular function on \mathcal{P}_n , so we need to square everything to make it so.

To get the Hamiltonians from Theorem 6.4, notice that $F_k(c)$ is the homogeneous degree k component of $\sqrt{c_{[n]}} \frac{\operatorname{tr} M}{\sqrt{\det M}}$ up to a sign. This observation will be very useful to prove the coincidence with the AFIT Hamiltonians of the GK Hamiltonians associated to the TCD maps defined in the next section.

7 TCD maps for cross-ratio dynamics

In this section, we give two different constructions realizing pairs (p, q) of $\vec{\alpha}$ -related curves as twisted TCD maps on the cylinder graph $\Gamma_{n, \hat{\mathbb{A}}}$. We provide a detailed account in Section 7.1 of a TCD map on a hexagonal lattice. In Section 7.2, we show that cross-ratio dynamics, that is the map $\nu_{\vec{\alpha}}: (p, q, M) \mapsto (q, r, M)$, is identified with a certain semi-local move on the TCD map side. This leads to a proof of Proposition 6.2 on the evolution of the u coordinates under cross-ratio dynamics. Finally, in Section 7.4, we give a second TCD map on a square lattice and describe a semi-local move realizing cross-ratio dynamics.

7.1 Hexagonal TCD map

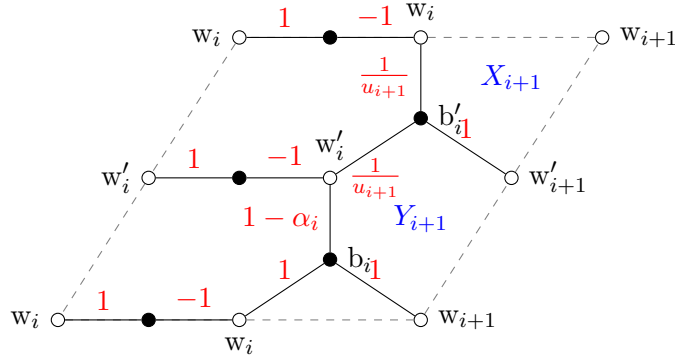


Figure 15. The building block graph K_i .

For $n \geq 2$, let Δ_n denote the torus graph obtained by gluing in cyclic order the graphs K_i in Figure 15 for $i = 1, 2, \dots, n$ and contracting two-valent vertices. See Figure 16 for a picture of Δ_4 .

Let $N_{\Delta_n} := \operatorname{Convex-hull}\{(0, 0), (2, 0), (0, n)\}$ denote the Newton polygon of Δ_n . For even n there are $n+4$ zig-zag paths and for odd n , there are $n+3$ zig-zag paths. The multiset of boundary vectors of N_{Δ_n} is $\{(1, 0)^2, (-1, \frac{n}{2})^2, (0, -1)^n\}$ in the even case and $\{(1, 0)^2, (-1, n), (0, -1)^n\}$ in the odd case (see Figure 17). We label some of the zig-zag paths as follows:

$$\begin{aligned} \xi_1 &:= w_1, b_1, w_2, b_2, \dots, w_n, b_n, w_1, & [\xi_1] &= (1, 0), \\ \xi_2 &:= w'_1, b'_1, w'_2, b'_2, \dots, w'_n, b'_n, w'_1, & [\xi_2] &= (1, 0), \\ \zeta_i &:= w_i, b'_i, w'_i, b_i, w_i, & [\zeta_i] &= (0, -1), \end{aligned}$$

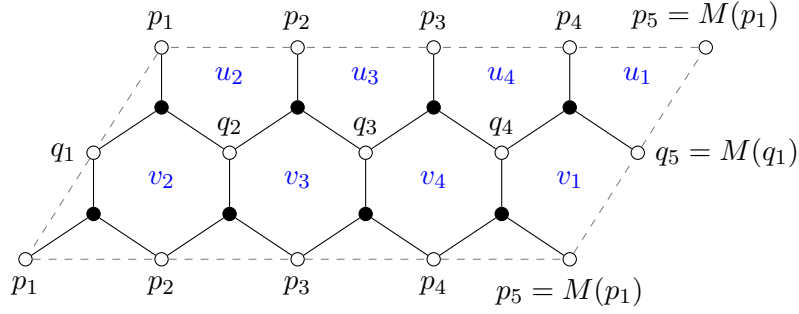


Figure 16. The graph Δ_4 showing the TCD map and face weights.

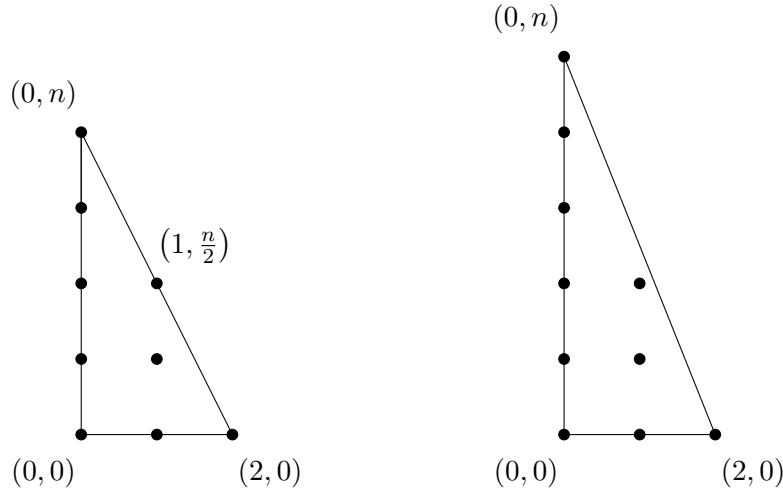


Figure 17. The Newton polygon N_{Δ_n} of Δ_n for even n (left) and odd n (right).

where ζ_i is defined for $i = 1, 2, \dots, n$. Suppose the faces and zig-zag paths of Δ_n are labeled as in Figure 15. The set

$$\{X_1^{\pm 1}, \dots, X_n^{\pm 1}, Y_1^{\pm 1}, \dots, Y_n^{\pm 1}, \chi_{[\zeta_1]}^{\pm 1}, \chi_{[\xi_1]}^{\pm 1}\}$$

is a set of generators for $\mathcal{O}_{\mathcal{L}_{\Delta_n}}$ and the only relation among them is $\prod_{i=1}^n X_i Y_i = 1$. However, it will be more convenient to work with a different set of generators given by

$$\{X_1^{\pm 1}, \dots, X_n^{\pm 1}, \chi_{[\zeta_1]}^{\pm 1}, \dots, \chi_{[\zeta_n]}^{\pm 1}, \chi_{[\xi_1]}^{\pm 1}\}.$$

We will map a subspace of the dimer parameter space $\mathcal{X}_{N_{\Delta_n}}$, defined by prescribing the values of the Casimirs $\chi_{[\zeta_1]}, \dots, \chi_{[\zeta_n]}$, to the AFIT parameter space \mathcal{U}_n . That map will transform each X_i into u_i . As in Section 5.2, there is an extra Casimir $\chi_{[\xi_1]}$ on the GK side that we also fix to be a constant $\lambda \in \mathbb{C}^\times$.

Let $\mathcal{X}_{N_{\Delta_n}, \vec{\alpha}}^\lambda$ (resp. $\mathcal{L}_{\Delta_n, \vec{\alpha}}^\lambda$) denote the Poisson subvariety of $\mathcal{X}_{N_{\Delta_n}}$ (resp. \mathcal{L}_{Δ_n}) where $\chi_{[\xi]} = \lambda$ and

$$\chi_{[\zeta_i]} = \frac{1}{1 - \alpha_i}, \tag{7.1}$$

for all $i \in \{1, 2, \dots, n\}$. The coordinate ring $\mathcal{O}_{\mathcal{L}_{\Delta_n, \vec{\alpha}}}^\lambda$ is generated by $\{X_1^{\pm 1}, \dots, X_n^{\pm 1}\}$. Recall from Section 6 that $\mathcal{U}_n \cong (\mathbb{C} \setminus \{0, -1\})^n$.

Definition 7.1. We define the birational map $\pi_{\vec{\alpha}}: \mathcal{X}_{N_{\Delta_n}, \vec{\alpha}}^\lambda \supset \mathcal{L}_{\Delta_n, \vec{\alpha}}^\lambda \rightarrow (\mathbb{C} \setminus \{0, -1\})^n$ such that

$$\pi_{\vec{\alpha}}^* u_i := X_i, \quad (7.2)$$

for all $i \in \{1, 2, \dots, n\}$.

Recall that $\mathcal{L}_{\Delta_n, \vec{\alpha}}^\lambda$ is a Zariski-dense open subset of $\mathcal{X}_{N_{\Delta_n}, \vec{\alpha}}^\lambda$. Definition 7.1 means that the map $\pi_{\vec{\alpha}}$ is the unique rational map such that, for $[\text{wt}] \in \mathcal{L}_{\Delta_n, \vec{\alpha}}^\lambda$,

$$\pi_{\vec{\alpha}}([\text{wt}]) = (X_1([\text{wt}]), \dots, X_n([\text{wt}])).$$

Lemma 7.2. We have $\pi_{\vec{\alpha}}^* v_i = Y_i$ for all $i \in \{1, 2, \dots, n\}$.

Proof. It follows from $X_i Y_i = \frac{\chi_{[\zeta_{i-1}]}}{\chi_{[\zeta_i]}}$ and the equations (6.6) and (7.1). ■

Next, we check the following.

Proposition 7.3. The map $\pi_{\vec{\alpha}}$ is Poisson.

Proof. The functions X_1, X_2, \dots, X_n are local coordinates on $\mathcal{X}_{N_{\Delta_n}, \vec{\alpha}}^\lambda$. The only nonzero Poisson brackets on $\mathcal{X}_{N_{\Delta_n}, \vec{\alpha}}^\lambda$ in these coordinates are

$$\{X_i, X_{i+1}\} = X_i X_{i+1}, \quad i = 1, 2, \dots, n.$$

We compute that

$$\pi_{\vec{\alpha}}^* \{u_i, u_{i+1}\}_{\mathcal{U}_n} = \pi_{\vec{\alpha}}^* (u_i u_{i+1}) = X_i X_{i+1} = \{X_i, X_{i+1}\} = \{\pi_{\vec{\alpha}}^* u_i, \pi_{\vec{\alpha}}^* u_{i+1}\}. \quad \blacksquare$$

Let $(p, q, M) \in \mathcal{U}_n$ and let $[\text{wt}] \in \mathcal{X}_{N_{\Delta_n}, \vec{\alpha}}^\lambda$ be such that $u^{-1} \circ \pi_{\vec{\alpha}}([\text{wt}]) = (p, q, M)$. We choose edge weights representing $[\text{wt}]$ and Kasteleyn signs as in Figure 15. Note that we have

$$|W(\Delta_{n, \mathbb{A}})| - |B(\Delta_{n, \mathbb{A}})| = 2.$$

Let $P: W(\Delta_{n, \widehat{\mathbb{A}}}) \rightarrow \mathbb{CP}^1$ denote the twisted TCD map associated to $[\text{wt}]$. The graph $\Delta_{n, \widehat{\mathbb{A}}}$ is a union of infinitely many copies of the building block graph K_i , $i \in \mathbb{Z}$. We label the vertices of $\Delta_{n, \widehat{\mathbb{A}}}$ as in Figure 15.

Lemma 7.4. We have $P_{w_i} = p_i$ and $P_{w'_i} = q_i$ for all $i \in \mathbb{Z}$, up to a common projective transformation.

Proof. The polygons p and q are determined up to projective transformations by the cross-ratios (6.3) and (6.4). Using Lemma 4.3, we see from (7.2) and Lemma 7.2 that the P_w have the same cross-ratios. ■

The TCD map for $n = 4$ is shown in Figure 16.

Corollary 7.5. The monodromy matrix of the twisted TCD map P coincides with the monodromy matrix M of the pair of polygons (p, q) .

We now compute this monodromy matrix. The Kasteleyn matrix of K_i is

$$K_{K_i}(w) = \left[\begin{array}{cc|cc} 1 & 0 & 0 & 0 \\ 0 & 1 & 0 & 0 \\ \hline 0 & 0 & 1 & 0 \\ 0 & 0 & 0 & 1 \\ \hline 1 & \frac{1}{u_{i+1}} & -1 & 0 \\ (1 - \alpha_i)w & \frac{1}{u_{i+1}} & 0 & 1 \end{array} \right]$$

so that

$$\Pi_{K_i}(w) = \begin{bmatrix} 1 & \frac{1}{u_{i+1}} \\ (1 - \alpha_i)w & \frac{1}{u_{i+1}} \end{bmatrix} = \frac{1}{u_{i+1}} \begin{bmatrix} u_{i+1} & 1 \\ u_{i+1}(1 - \alpha_i)w & 1 \end{bmatrix}.$$

By Proposition 3.2, the monodromy matrix is $\Pi(1)$, where

$$\Pi(w) = \Pi_{H_1}(w)\Pi_{H_2}(w) \cdots \Pi_{H_n}(w).$$

We have $\det \Pi_{K_i}(w) = \frac{1-w(1-\alpha_i)}{u_{i+1}}$, so we get

$$\det \Pi(1) = \frac{\alpha_{[n]}}{u_{[n]}}. \quad (7.3)$$

The following lemma is elementary.

Lemma 7.6. *Suppose M is a 2×2 matrix and $P(z) = \det(zI + M)$ is its characteristic polynomial. Then $P(z) = z^2 + \text{tr } Mz + \det M$.*

Let $P(z, w)$ denote the characteristic polynomial of Δ_n , normalized so that it has its Newton polygon as on the left picture of Figure 17 with the vertex in the bottom left corner corresponding to the monomial 1, and such that the coefficient of z^2 is $u_{[n]}$. To find the normalization explicitly, we know from Theorem 3.6 and Lemma 7.6 that $P(z, w)$ is up to normalization equal to $\det(zI + \Pi(w)) = z^2 + \text{tr } \Pi(w)z + \det \Pi(w)$, which is equal to

$$z^2 + z \frac{1}{u_{[n]}} \text{tr} \prod_{i=1}^n \begin{bmatrix} u_{i+1} & 1 \\ u_{i+1}(1 - \alpha_i)w & 1 \end{bmatrix} + \frac{1}{u_{[n]}} \prod_{i=1}^n (1 - w(1 - \alpha_i)),$$

so

$$P(z, w) = u_{[n]}z^2 + z \text{tr} \prod_{i=1}^n \begin{bmatrix} u_{i+1} & 1 \\ u_{i+1}(1 - \alpha_i)w & 1 \end{bmatrix} + \prod_{i=1}^n (1 - w(1 - \alpha_i)).$$

Let $H_{(1,k)}$ denote the coefficient of zw^k in $P(z, w)$ for $k = 0, \dots, \lfloor \frac{n+1}{2} \rfloor$, so that when $k \in \{1, 2, \dots, \lfloor \frac{n+1}{2} \rfloor - 1\}$, they are the Hamiltonians of the cluster integrable system. Then, we have

$$\sum_{k=0}^{\lfloor \frac{n}{2} \rfloor} H_{(1,k)} w^k = \text{tr} \prod_{i=1}^n \begin{bmatrix} u_{i+1} & 1 \\ u_{i+1}(1 - \alpha_i)w & 1 \end{bmatrix}.$$

Make the substitution $\beta_i = 1 - \alpha_i$ and consider the above expression as a polynomial in $\beta_1, \beta_2, \dots, \beta_n$. Since each $(1 - \alpha_i)$ inside the matrices appears with a w , the homogeneous component of degree k in $\beta_1, \beta_2, \dots, \beta_n$ is $H_{(1,k)} w^k$. The main result of this section is the following simple procedure for converting between the AFIT Hamiltonians [4] and the GK dimer Hamiltonians for Δ_n .

Theorem 7.7. *Let $k \in \{1, 2, \dots, \lfloor \frac{n+1}{2} \rfloor - 1\}$ and let $\alpha_i = \alpha$ for all i . We have*

1. *The homogeneous degree k component of $\sum_{d=0}^{\lfloor \frac{n+1}{2} \rfloor - 1} H_{(1,d)}$ as a polynomial in the variables $\alpha_1, \dots, \alpha_n$ is, up to a sign, equal to*

$$\sqrt{\frac{\alpha_{[n]}}{X_{[n]}}} \pi_{\vec{\alpha}}^* \circ \Lambda_{\vec{\alpha}}^* \left(\frac{F_k(c)}{\sqrt{c_{[n]}}} \right),$$

which is the product of the Casimir $\sqrt{\frac{\alpha_{[n]}}{X_{[n]}}}$ with the pullback of an AFIT Hamiltonian.

2. The homogeneous degree k component of $\sum_{d=0}^{\lfloor \frac{n+1}{2} \rfloor - 1} H_{(1,d)}$ as a polynomial in $1 - \alpha_1, \dots, 1 - \alpha_n$ is the GK dimer Hamiltonian $H_{(1,k)}$.

Proof. Only the first item remains to be proved. By Corollary 7.5, $\Pi(1)$ is conjugated to $\pi_{\vec{\alpha}}^* \circ \Lambda_{\vec{\alpha}}^* M$ in PGL_2 . Since $\frac{1}{\det M} \text{tr}^2 M$ is a PGL_2 -conjugacy invariant, we have

$$\pi_{\vec{\alpha}}^* \circ \Lambda_{\vec{\alpha}}^* \left(\frac{1}{\sqrt{\det M}} \text{tr} M \right) = \pm \frac{1}{\sqrt{\det(\Pi(1))}} \text{tr}(\Pi(1)).$$

Using Theorem 6.4 and (7.3), we get

$$\sqrt{\frac{\alpha_{[n]}}{X_{[n]}}} \sum_{k=0}^{\lfloor \frac{n}{2} \rfloor} (-1)^k \pi_{\vec{\alpha}}^* \circ \Lambda_{\vec{\alpha}}^* \left(\frac{F_k(c)}{\sqrt{c_{[n]}}} \right) = \pm \sum_{k=0}^{\lfloor \frac{n}{2} \rfloor} H_{(1,k)}.$$

Note that the left-hand side is a polynomial in α_i since $\pi_{\vec{\alpha}}^* \circ \Lambda_{\vec{\alpha}}^* \sqrt{c_{[n]}}$ has a factor $\sqrt{\alpha_{[n]}}$ which cancels the same factor in the numerator. Then, the homogeneous component of degree k in the variables $\alpha_1, \alpha_2, \dots, \alpha_n$ on the left is

$$(-1)^k \sqrt{\frac{\alpha_{[n]}}{X_{[n]}}} \pi_{\vec{\alpha}}^* \circ \Lambda_{\vec{\alpha}}^* \left(\frac{F_k(c)}{\sqrt{c_{[n]}}} \right).$$

Finally, note that $X_{[n]} = \frac{\chi_{[\xi_2]}}{\chi_{[\xi_1]}}$ is a Casimir, hence so is $\sqrt{\frac{\alpha_{[n]}}{X_{[n]}}}$. ■

7.2 Cross-ratio dynamics via a semi-local move

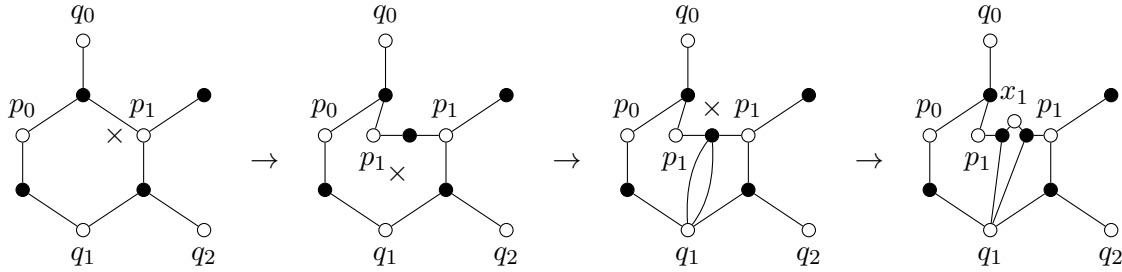


Figure 18. When following the arrows from left to right, this depicts Step 1 of the sequence, namely the insertion of x_1 . The vertices/faces where moves are applied are marked with \times 's.

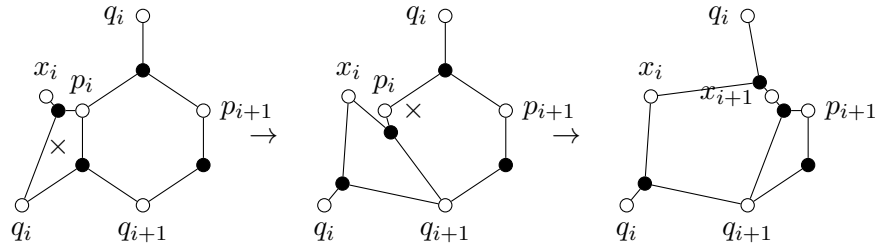


Figure 19. Step 2 in the sequence replacing p_i with x_{i+1} .

We prepare with an observation on multi-ratios.

Lemma 7.8. Assume p, q are nondegenerate twisted n -gons such that p is $\vec{\alpha}$ -related to q . Suppose $x_i, x_{i+1} \in \mathbb{CP}^1$ are two points such that $-\text{cr}(q_i, x_i, q_{i+1}, x_{i+1}) = \alpha_i$. Then,

$$\text{mr}(p_i, q_i, x_i, x_{i+1}, q_{i+1}, p_{i+1}) = -1$$

holds for all $i \in \mathbb{Z}$.

Proof. The lemma follows from the following two equations

$$\begin{aligned} \text{cr}(p_i, q_i, p_{i+1}, q_{i+1}) &= \text{cr}(q_i, x_i, q_{i+1}, x_{i+1}), \\ \text{mr}(p_i, q_i, x_i, x_{i+1}, q_{i+1}, p_{i+1}) &= -\frac{\text{cr}(p_i, q_i, p_{i+1}, q_{i+1})}{\text{cr}(q_i, x_i, q_{i+1}, x_{i+1})}. \end{aligned}$$

■

Now we construct the sequence of moves.

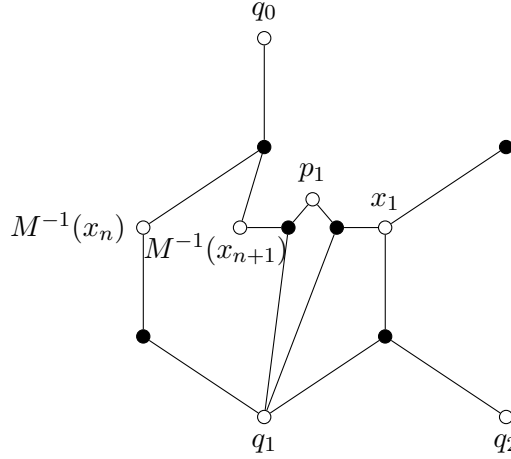


Figure 20. Local configuration near p_1 in Step 3.

Theorem 7.9. Suppose $[\text{wt}] \in \mathcal{X}_{N_{\Delta_n}, \tilde{\alpha}}^\lambda$ is such that $u^{-1} \circ \pi_{\tilde{\alpha}}([\text{wt}]) = (p, q, M)$. Consider the sequence of moves shown in Figures 18, 19, and let μ denote the induced birational map of weights. Then the pair of curves (q, r, M) is $u^{-1} \circ \pi_{\tilde{\alpha}} \circ \mu([\text{wt}])$. In other words, the following diagram commutes:

$$\begin{array}{ccc} \mathcal{X}_{N_{\Delta_n}, \tilde{\alpha}}^\lambda & \xrightarrow{u^{-1} \circ \pi_{\tilde{\alpha}}} & \mathcal{U}_n \\ \mu \downarrow & & \downarrow \nu_{\tilde{\alpha}} \\ \mathcal{X}_{N_{\Delta_n}, \tilde{\alpha}}^\lambda & \xrightarrow{u^{-1} \circ \pi_{\tilde{\alpha}}} & \mathcal{U}_n \end{array}$$

Proof. By Lemma 7.12, it suffices to trace what happens to the twisted TCD map associated to $[\text{wt}]$ through the sequence of moves. We identify \mathbb{A} with the fundamental domain in $\hat{\mathbb{A}}$ containing p_1, \dots, p_n , and the other fundamental domains are denoted $\mathbb{A} + m\gamma_z$, $m \in \mathbb{Z}$. Recall that $P_{w+\gamma_z} = M(P_w)$ for a twisted TCD map. The moves are applied γ_z -periodically in $\hat{\mathbb{A}}$, so we only describe what happens in \mathbb{A} . We proceed in four steps:

1. First, we insert a new point x_1 into the twisted TCD map, which, based on a choice made in Step 3, will turn out to be r_1 ; see Figure 18 for an illustration (in $\mathbb{A} + m\gamma_z$, this means that we insert $M^m(x_1)$). To do this, we begin by using the resplit move to split p_1 into two copies of p_1 and a new black vertex, which we denote b . Then, we add a bigon with vertices b and q_1 , such that the bigon is inside the face also bounded by p_0 and p_1 . In order for this bigon insertion not to change the rest of the TCD map, we require that the weights of the two edges of this bigon sum to 0. Finally, we split b into two new black vertices of degree three while also generating the new white vertex corresponding to x_1 . The result is a version of the graph in the middle of Figure 4 in which all black vertices are trivalent so that we are in the realm of TCD maps.

2. Let $x_i \in \mathbb{CP}^1$ for $i \in \{2, \dots, n+1\}$ be defined by $-\text{cr}(q_i, x_i, q_{i+1}, x_{i+1}) = \alpha_i$. We apply a spider move followed by a resplit that replaces p_i with x_{i+1} ; see Figure 19. When we apply the resplit, (4.1) and Lemma 7.8 imply that the newly created point is x_{i+1} . We apply these moves until we have replaced p_n with a new copy of x_{n+1} .
3. After the moves of Step 2, there is still one copy of p_1 left in the graph. Locally near p_1 , the TCD map looks like Figure 20. This is the same as the rightmost graph in Figure 18, except that the roles of p and x are interchanged. There are two choices of x_1 that make $M^{-1}(x_{n+1}) = x_1$, namely p_1 and r_1 . However, $x_1 = p_1$ makes the weight of the face to the right of the bigon equal to 0, and is therefore disallowed. We then apply the sequence of moves in Step 1 in reverse order to recover the hexagonal graph with p replaced by r .
4. Finally, we translate Δ_n by $\frac{1}{2}\gamma_w$ to interchange q and r . ■

Since the weights of the two edges of a bigon sum to zero, the weight of any dimer cover that uses one of the edges of the bigon is canceled by the weight of the dimer cover that uses the other edge. Therefore, the spectral curve, the Casimirs and the Hamiltonians of the dimer model are unchanged upon inserting a bigon. Since the dimer Casimirs and Hamiltonians are also preserved by the elementary transformations [23, Theorem 4.7], we obtain as a corollary of Theorem 1.4.

Corollary 7.10. *The AFIT Casimirs and Hamiltonians are invariant under cross-ratio dynamics.*

We can now prove Proposition 6.2 on the evolution of the u_i coordinates under cross-ratio dynamics.

Proof of Proposition 6.2. The sequence of moves in Theorem 7.9 is a sequence of local moves on TCD maps starting and ending with a TCD map on Δ_n . It can be seen as a sequence of dimer local moves starting and ending with Δ_n . Up to contractions and expansions of degree 2 vertices, the sequence of dimer local moves is exactly the one described above for the geometric R -matrix transformation. More precisely, the bigon is initially added between the white vertex carrying q_1 and the black vertex resulting from the contraction of the white vertex carrying p_1 . Then, the sequence of n spider moves crosses a string of hexagons and finally the bigon gets deleted at the end of this sequence. Since contractions and expansions of degree 2 vertices do not change the face weights, we deduce that the evolution of the face weights for the sequence in Theorem 7.9 is given by the geometric R -matrix transformation.

Let X'_i and Y'_i be the face weights after applying the birational map μ of Theorem 7.9, which includes in Step 4 a translation by $\frac{1}{2}\gamma_w$. In our case, the face weights of the strip of hexagonal faces crossed by the spider moves are the X_i and they become Y'_i after the transformation, i.e.,

$$(Y'_1, \dots, Y'_n) = \Phi(X_1, \dots, X_n).$$

By Theorem 2.1, we have

$$Y'_i = \frac{\sum_{t=0}^{n-1} \prod_{s=0}^{t-1} X_{i+s}}{\sum_{t=1}^n \prod_{s=1}^t X_{i+s}}.$$

Formula (6.7) follows from the fact that $\pi_\alpha^* v_i = X_i$ and $\pi_\alpha^* u'_i = Y'_i$. ■

We can also use this correspondence with the geometric R -matrix transformation to provide an alternative proof that the cross-ratio dynamics map ν_α is Poisson.

Corollary 7.11. *The map $\nu_{\tilde{\alpha}}$ from \mathcal{U}_n to itself is Poisson for the bracket $\{\cdot, \cdot\}_{\mathcal{U}_n}$.*

Proof. In [27], it is shown that the geometric R -matrix transformation can be rewritten as a composition of cluster mutations for a quiver obtained from the original dimer quiver by adding several edges and vertices. In particular, the Poisson bracket on the space of cluster variables [17] induces on the space of a_i variables the bracket given by $\{a_i, a_{i+1}\} = a_i a_{i+1}$ for every i . Since cluster mutations induce Poisson maps [17], we deduce that the map Φ sending (a_1, \dots, a_n) to (a'_1, \dots, a'_n) is a Poisson map. Alternatively, this result follows from a direct computation on Poisson brackets using formula (2.1).

The Poisson bracket $\{\cdot, \cdot\}_{\mathcal{U}_n}$ on \mathcal{U}_n is given by the same formula (6.5) as the bracket for the a_i . Furthermore, $\nu_{\tilde{\alpha}}$ is given by the composition of the Poisson map Φ with the map transforming each component into its inverse (which is also Poisson), thus $\nu_{\tilde{\alpha}}$ is Poisson. ■

7.3 Other dynamics

In this subsection, we describe all the other integrable dynamics that are defined on the phase space of the cross-ratio dynamics integrable system, called *generalized cluster modular transformations* in [19].

By definition, each side e of the Newton polygon (which we think of as oriented counterclockwise around the boundary of N) corresponds to a subset $\mathcal{Z}_e := \{\beta \in \mathcal{Z} \mid e \in \mathbb{Z}_{>0}[\beta]\}$ of zig-zag paths. Let $|e|_{\mathbb{Z}}$ denote the *integral length* of e , i.e., the number of lattice points in e minus one or equivalently, the number of primitive line segments in e . Let $p: \mathbb{R}^2 \rightarrow \mathbb{T}$ denote the universal covering map of the torus, and let $\tilde{\Gamma}$ denote the biperiodic graph $p^{-1}(\Gamma)$ in \mathbb{R}^2 . Let $\beta_1, \dots, \beta_{|e|_{\mathbb{Z}}}$ denote the zig-zag paths in \mathcal{Z}_e in cyclic order around the torus from right to left. Their lifts to \mathbb{R}^2 form a collection of bi-infinite parallel zig-zag paths $\tilde{\beta}_i$, $i \in \mathbb{Z}$, in $\tilde{\Gamma}$ labeled in order from right to left, such that $p(\tilde{\beta}_i) = \beta_j$, where $1 \leq j \leq |e|_{\mathbb{Z}}$ and $j \equiv i \pmod{|e|_{\mathbb{Z}}}$.

An *extended affine permutation of period k* is a bijection $w: \mathbb{Z} \rightarrow \mathbb{Z}$ such that $w(i+k) = w(i) + k$. Let \hat{S}_k denote the group of extended affine permutations with period k . We will write extended affine permutations w in *window notation* $[w(1), \dots, w(k)]$. Define $\tau := [2, 3, \dots, k, k+1]$, $s_i := [1, 2, \dots, i-1, i+1, i, i+2, \dots, k]$ for $1 \leq i \leq k-1$ and $s_0 = s_k := [0, 2, 3, \dots, k-2, k-1, k+1]$. Then, \hat{S}_k is the group generated by $\tau, s_0, \dots, s_{k-1}$ modulo the relations

$$s_i^2 = 1, \quad s_i s_{i+1} s_i = s_{i+1} s_i s_{i+1}, \quad s_i s_j = s_j s_i \quad \text{if } |i-j| > 1, \quad \tau s_i \tau^{-1} = s_{i+1}.$$

There is a group homomorphism $\text{disp}: \hat{S}_k \rightarrow \mathbb{Z}$ given by $\text{disp}(w) := \frac{1}{k} \sum_{i=1}^k (f(i) - i)$. Given a Newton polygon N , let $E(N)$ denote the set of edges of N . Let L_N denote the kernel of the group homomorphism

$$\prod_{e \in E(N)} \hat{S}_{|e|_{\mathbb{Z}}} \xrightarrow{\sum_{e \in E(N)} \text{disp}} \mathbb{Z},$$

i.e., L_N consists of an extended affine permutation w^e for each edge e of N such that the total displacement $\sum_{e \in E(N)} \text{disp}(w^e)$ is 0.

One of the main results of [19] is that each $w = (w^e)_{e \in E(N)} \in L_N$ determines an automorphism of the cluster Poisson variety \mathcal{X}_N given by a sequence of isotopies, elementary transformations and geometric R -matrix transformations that take a graph Γ to itself, called a generalized cluster modular transformation. Generalized cluster modular transformations are determined by what they do to zig-zag paths and the correspondence is as follows. Each generalized cluster modular transformation ϕ lifts to an $H_1(\mathbb{T}, \mathbb{Z})$ -periodic sequence of isotopies, elementary transformations and geometric R -matrix transformations in $\tilde{\Gamma}$ that take $\tilde{\Gamma}$ to itself. Therefore, each zig-zag path $\tilde{\beta}_i$ of $\tilde{\Gamma}$ ends up at the initial location of a parallel zig-zag path $\tilde{\beta}_j$. Then, $w^e(i) := j$

where e is the edge of N in the direction $[\beta]$. We have an injective group homomorphism (coming from the translation action of $H_1(\mathbb{T}, \mathbb{Z})$)

$$j: H_1(\mathbb{T}, \mathbb{Z}) \hookrightarrow L_N, \quad m \mapsto (\tau_\rho^{(e, m)})_{e \in E(N)},$$

where $\langle \cdot, \cdot \rangle$ denotes the intersection form in \mathbb{T} . Explicitly, identifying $H_1(\mathbb{T}, \mathbb{Z})$ with \mathbb{Z}^2 using the basis (γ_z, γ_w) , if $(a, b), (c, d) \in \mathbb{Z}^2$, then $\langle (a, b), (c, d) \rangle := ad - bc$. The *generalized cluster modular group*, the group of all generalized cluster transformations is isomorphic to the quotient of L_N by the subgroup $j(H_1(\mathbb{T}, \mathbb{Z}))$.

Let $e_{\rightarrow}, e_{\leftarrow}$ and e_{\downarrow} denote the edges of N_{Δ_n} given by the vectors $(2, 0), (-2, n)$ and $(0, -n)$, respectively. For $a \in \{\rightarrow, \leftarrow, \downarrow\}$, we denote the generators of $\widehat{S}_{|e_a|_{\mathbb{Z}}}$ by τ_a and $s_{i,a}$, $0 \leq i \leq |e_a|_{\mathbb{Z}} - 1$. The subgroup $j(H_1(\mathbb{T}, \mathbb{Z})) = \langle \tau_{\leftarrow}^n \tau_{\downarrow}^{-n}, \tau_{\rightarrow}^{-2} \tau_{\leftarrow}^2 \rangle$. The generators of the generalized cluster modular group are

1. $s_{i,\rightarrow}$, $0 \leq i \leq 1$: Let (p, q) be a pair of $\vec{\alpha}$ -related twisted n -gons, and let o (resp. r) denote the other twisted n -gon $\vec{\alpha}$ -related to p (resp. q). Then, $s_{0,\rightarrow}$ (resp. $s_{1,\rightarrow}$) is given by $(p, q) \mapsto (r, q)$ (resp. (p, o)). Here, we are indexing the two horizontal zig-zag paths so that the zig-zag path containing the points of p gets label 1 and the one containing the points of q gets label 2 (see the left hand side of Figure 2).
2. $s_{i,\downarrow}$ for $i = 0, 1, \dots, n-1$: Given a pair of $\vec{\alpha}$ -related twisted n -gons (p, q) , let $s_i \cdot \vec{\alpha}$ be defined by $(s_i \cdot \vec{\alpha})_j := \alpha_{s_i(j)}$. It is not difficult to see that there is a unique $(s_i \cdot \vec{\alpha})$ -related pair of twisted n -gons (p', q') such that $p'_k = p_k$ and $q'_k = q_k$ if $k \neq i+1$. The transformation is $(p, q) \mapsto (p', q')$.
3. Only when n is even, $s_{i,\leftarrow}$, $0 \leq i \leq 1$: There is a graph automorphism exchanging the zig-zag paths in directions $(1, 0)$ and $(-1, \frac{n}{2})$ which sends (p, q) to (p', q') , where

$$p'_k = \begin{cases} p_k & \text{if } k \text{ is odd,} \\ q_k & \text{if } k \text{ is even,} \end{cases} \quad q'_k = \begin{cases} q_k & \text{if } k \text{ is odd,} \\ p_k & \text{if } k \text{ is even.} \end{cases}$$

Note that (p', q') is a pair of $\vec{\alpha}'$ -related twisted n -gons where $\alpha'_i := \frac{1}{\alpha_i}$ and the monodromy is the same as (p, q) . Under this automorphism, $s_{i,\leftarrow}$ becomes $s_{i,\rightarrow}$.

4. $\tau_{\rightarrow} \tau_{\leftarrow}^{-1}$: This is the transformation $(p, q) \mapsto (q, p)$.
5. $\tau_{\leftarrow} \tau_{\downarrow}^{-1}$: Given a twisted n -gon p , let $\text{shift}(p)$ be the twisted n -gon defined by $\text{shift}(p)_i := p_{i+1}$. The transformation is $(p, q) \mapsto (\text{shift}(p), \text{shift}(q))$.

In terms of the generators above, Theorem 7.9 says that cross-ratio dynamics is the generalized cluster modular transformation $\tau_{\rightarrow} \tau_{\leftarrow}^{-1} s_{1,\rightarrow}$. The above discussion shows that there are other integrable discrete dynamics on the same space whose interactions with each other can be written down explicitly as the relations in the generalized cluster modular group. The most interesting one occurs when n is even where, if we conjugate cross-ratio dynamics by the automorphism in item 3, we get a generalized cluster modular transformation that we call *switch dynamics*.

Let us mention the interpretation of the three geometrically non-trivial operations above in terms of discrete integrable systems. Recall from the beginning of Section 1.3 that a solution of the cross-ratio dynamics system may be seen as a map $f: \mathbb{Z}^2 \rightarrow \mathbb{CP}^1$, such that $f_{i,0} = p_i$ and $f_{i,1} = q_i$. We view each row as a twisted n -gon and the four vertices on the boundary of any *quad*, i.e., (1×1) -square, are required to satisfy the cross-ratio condition $\text{cr}(f_{i,j}, f_{i,j+1}, f_{i+1,j}, f_{i+1,j+1}) = \alpha_i$. Then, cross-ratio dynamics corresponds to a vertical translation by one unit in \mathbb{Z}^2 . A priori, there is a one-parameter family of choices for r (resp. o) such that the cross-ratios formed by the quads between q and r (resp. o and p) are α_i , but after imposing the monodromy condition in the twisted case, there is only one choice.

Similarly, switch dynamics is related to the corresponding *discrete equation of Toda type* [7] of the cross-ratio dynamics system. The Toda type equation is a lattice equation satisfied by the even (resp. odd) parity vertices of a solution of the cross-ratio dynamics system. Thus, the even (resp. odd) vertices of the cross-ratio dynamics system satisfy an equation independently of the odd (resp. even) vertices. Moreover, a solution of the Toda type equation on the even (resp. odd) vertices can be extended to a solution of the cross-ratio dynamics system, but there is a one-parameter family of such extensions on \mathbb{Z}^2 . Again, upon imposing the monodromy condition in the twisted case, the one-parameter family reduces to only two extensions. Given one extension, there is thus exactly one other such extension, and this defines switch dynamics by alternately choosing the other odd (resp. even) extension.

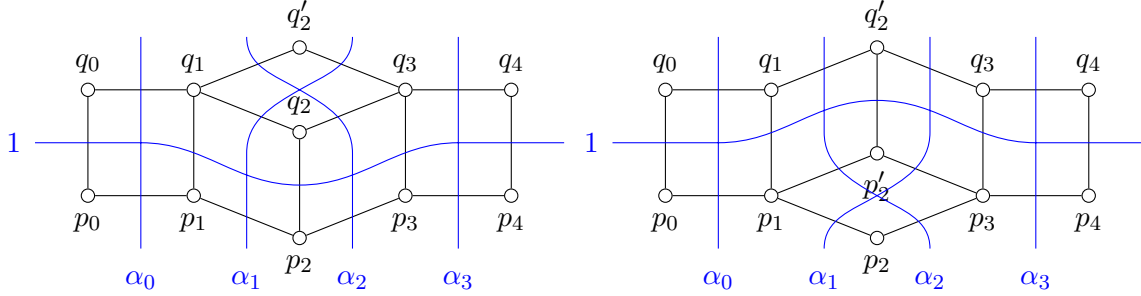


Figure 21. Illustration of $s_{1,\downarrow}$ around the cube formed by $p_1, p_2, p_3, p'_2, q_1, q_2, q_3$ and q'_2 . On these pictures, we are requiring that the cross-ratio of the four points around any quad be equal to the ratio of the parameters attached to the two blue lines crossing the quad. The three blue lines with parameters α_1, α_2 and 1 cycle around the cube.

Finally, $s_{i,\downarrow}$ corresponds to introducing a “fault” in the lattice; see Figure 21. On that figure we start with the points $p_1, p_2, p_3, q_1, q_2, q_3$ satisfying the two cross-ratio equations corresponding to the two front faces of the cube. We then compute q'_2 using the equation $\text{cr}(q_2, q_1, q_3, q'_2) = \alpha_2/\alpha_1$ corresponding to the top face. There are three possible ways to compute p'_2 , using any equation corresponding to one of the three hidden faces of the cube. They actually give the same result and this fact is called 3D-consistency of the cross-ratio system [7].

7.4 Square TCD map

For n even, consider the graph Γ_n in \mathbb{T} for which a fundamental domain is obtained by gluing the cylinder graphs G_i shown on the left side of Figure 22 for $i \in \{1, 2, \dots, \frac{n}{2}\}$ in the order $G_1 G_2 \cdots G_{\frac{n}{2}}$, so that w_{2n+1} is identified with w_1 and w_{2n+2} with w_2 (see the left side of Figure 23 for Γ_6). Similarly, for odd n , let Γ_n be obtained by gluing the graphs $G_1 G_2 \cdots G_{\frac{n-3}{2}} G_{\frac{n-1}{2}} G_n^{\text{odd}}$ from left to right and identifying w_{2n+1} with w_1 and w_{2n+2} with w_2 (see the right side of Figure 23 for Γ_5). Here G_n^{odd} is the graph represented on the right picture of Figure 22.

We label some of the zig-zag paths of Γ_n as follows:

$$\begin{aligned} \xi_1 &:= w_1, b_1, w_2, b_2, \dots, w_n, b_n, w_1, & [\xi_1] &= (1, 0), \\ \xi_2 &:= w'_1, b'_1, w'_2, b'_2, \dots, w'_n, b'_n, w'_1, & [\xi_2] &= (1, 0), \\ \zeta_{2i-1} &:= w_{2i}, b_{2i-1}, w'_{2i}, b'_{2i-1}, w_{2i}, & [\zeta_{2i-1}] &= (0, 1), \\ \zeta_{2i} &:= w_{2i}, b'_{2i-1}, w'_{2i}, b_{2i-1}, w_{2i}, & [\zeta_{2i}] &= (0, -1), \end{aligned}$$

where $i \in \{1, 2, \dots, \lfloor \frac{n}{2} \rfloor\}$, and for n odd, we also define $\zeta_n := w_1 b_n w'_1 b'_n w_1$ where $[\zeta_n] = (0, 1)$. Using the basis (γ_z, γ_w) , we identify $H_1(\mathbb{T}, \mathbb{Z})$ with \mathbb{Z}^2 . Then, the Newton polygon of Γ_n is

$$N_{\Gamma_n} = \begin{cases} \text{Convex-hull}\{(0, 0), (2, 0), (0, \frac{n}{2}), (2, \frac{n}{2})\} & \text{if } n \text{ is even, (Figure 24, left),} \\ \text{Convex-hull}\{(0, 0), (2, 0), (0, \frac{n-1}{2}), (2, \frac{n+1}{2})\} & \text{if } n \text{ is odd (Figure 24, right).} \end{cases}$$

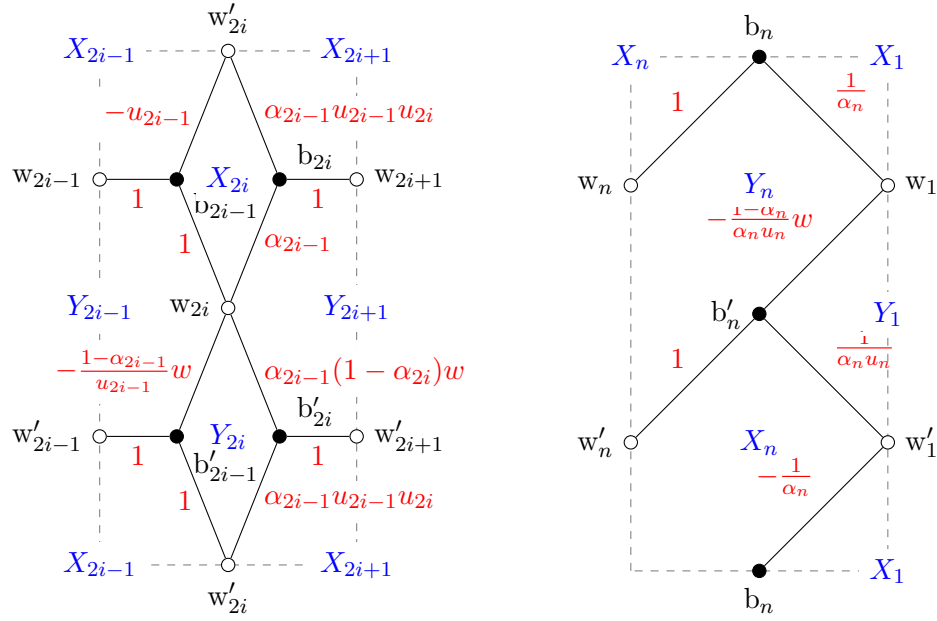


Figure 22. The building block graphs G_i and G_n^{odd} .

For any n , the faces of Γ_n are labeled by their face weights X_i, Y_i for $i \in \{1, 2, \dots, n\}$ as shown in Figure 22. A set of generators for the coordinate ring $\mathcal{O}_{\mathcal{L}_{\Gamma_n}}$ is given by

$$\{X_1^{\pm 1}, \dots, X_n^{\pm 1}, \chi_{[\zeta_1]}^{\pm 1}, \dots, \chi_{[\zeta_n]}^{\pm 1}, \chi_{[\xi_1]}^{\pm 1}\}.$$

Let $\lambda \in \mathbb{C}^\times$ and let $\mathcal{X}_{N_{\Gamma_n}, \vec{\alpha}}^\lambda$ (resp. $\mathcal{L}_{\Gamma_n, \vec{\alpha}}^\lambda$) denote the Poisson subvariety of $\mathcal{X}_{N_{\Gamma_n}}$ (resp. \mathcal{L}_{Γ_n}), where $\chi_{[\xi_1]} = \lambda$ and

$$\chi_{[\zeta_k]} := \begin{cases} 1 - \alpha_k & \text{if } k \text{ is odd,} \\ \frac{1}{1 - \alpha_k} & \text{if } k \text{ is even,} \end{cases}$$

where $k \in \{1, 2, \dots, n\}$. The coordinate ring $\mathcal{O}_{\mathcal{L}_{\Gamma_n, \vec{\alpha}}}^\lambda$ is generated by $\{X_1^{\pm 1}, \dots, X_n^{\pm 1}\}$. We define the birational map

$$\pi_{\vec{\alpha}}: \mathcal{X}_{N_{\Gamma_n}, \vec{\alpha}}^\lambda \supset \mathcal{L}_{\Gamma_n, \vec{\alpha}}^\lambda \rightarrow (\mathbb{C} \setminus \{0, -1\})^n$$

by $\pi_{\vec{\alpha}}^* u_i := X_i$ for all $i \in \{1, 2, \dots, n\}$. Similarly to Lemma 7.2 and Proposition 7.3, $\pi_{\vec{\alpha}}^* v_i = Y_i$ for all $i \in \{1, 2, \dots, n\}$ and $\pi_{\vec{\alpha}}$ is Poisson.

Let $(p, q, M) \in \mathcal{U}_n$ and let $[\text{wt}] \in \mathcal{X}_{N_{\Gamma_n}, \vec{\alpha}}^\lambda$ be such that

$$u^{-1} \circ \pi_{\vec{\alpha}}([\text{wt}]) = (p, q, M).$$

The left picture of Figure 22 shows edge weights and Kasteleyn signs. Let $P: W(\Gamma_{n, \hat{\mathbb{A}}}) \rightarrow \mathbb{CP}^1$ denote the twisted TCD map associated to $[\text{wt}]$. We label the vertices of $\Gamma_{n, \hat{\mathbb{A}}}$ as in Figure 22.

Lemma 7.12. *We have (see Figure 23) $P_{w_i} = p_i$ and $P_{w'_i} = q_i$ for all $i \in \mathbb{Z}$, up to a common projective transformation. The monodromy matrix of the twisted TCD map P coincides with the monodromy matrix M of the pair of polygons (p, q) .*

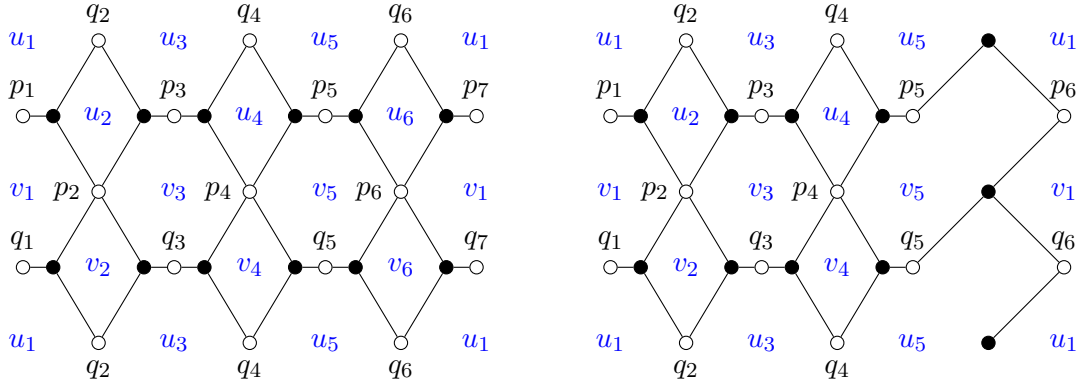


Figure 23. The relevant bipartite graphs to describe a pair of curves of length $n = 6$ (left) and $n = 5$ (right). Here the top and the bottom sides of each graph are identified, yielding the cylinder graphs $\Gamma_{6,\mathbb{A}}$ and $\Gamma_{5,\mathbb{A}}$. If we additionally identify the left and right sides of each graph, we obtain the torus graphs Γ_6 and Γ_5 . In blue we indicate how the face weights are related to the coordinates on the space of pairs of $\vec{\alpha}$ -related twisted polygons.

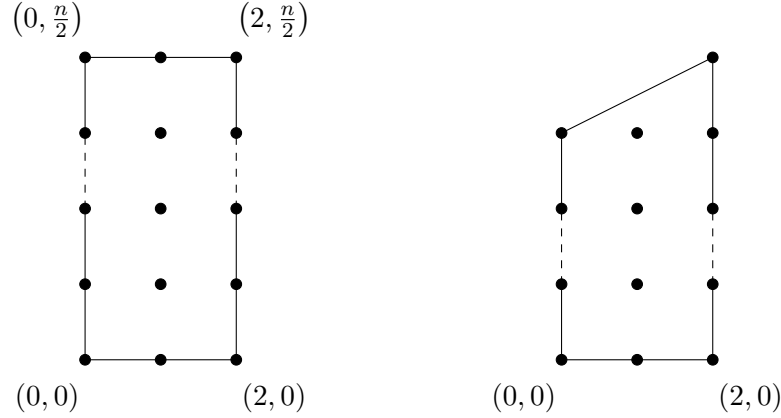


Figure 24. The Newton polygon N_{Γ_n} of Γ_n for even n (left) and odd n (right).

The Kasteleyn matrix of G_i is

$$K_{G_i}(w) = \left[\begin{array}{cc|cc} 1 & 0 & 0 & 0 \\ 0 & 1 & 0 & 0 \\ \hline 0 & 0 & 1 & 0 \\ 0 & 0 & 0 & 1 \\ \hline \alpha_{2i-1}u_{2i-1}u_{2i} & \alpha_{2i-1}u_{2i-1}u_{2i} & 1 & -u_{2i-1} \\ \alpha_{2i-1}(1-\alpha_{2i})w & \alpha_{2i-1} & -\frac{1-\alpha_{2i-1}}{u_{2i-1}}w & 1 \end{array} \right]$$

so that

$$\begin{aligned} \Pi_{G_i}(w) &= \frac{\alpha_{2i-1}}{(1-\alpha_{2i-1})w-1} \begin{bmatrix} u_{2i-1}(u_{2i} + (1-\alpha_{2i})w) & u_{2i-1}(1+u_{2i}) \\ (1-\alpha_{2i})w + u_{2i}(1-\alpha_{2i-1})w & 1 + u_{2i}(1-\alpha_{2i-1})w \end{bmatrix}, \\ \det \Pi_{G_i}(w) &= \left(\frac{\alpha_{2i-1}}{(1-\alpha_{2i-1})w-1} \right) ((1-\alpha_{2i})w-1)\alpha_{2i-1}u_{2i-1}u_{2i}, \\ \det \Pi_{G_i}(w) &= \alpha_{2i-1}\alpha_{2i}u_{2i-1}u_{2i}. \end{aligned}$$

Similarly, we compute

$$\begin{aligned}\Pi_{G_n^{\text{odd}}}(w) &= \frac{\alpha_n}{(1 - \alpha_n)w - 1} \begin{bmatrix} 1 & (1 - \alpha_n)w \\ u_n & u_n \end{bmatrix}, \\ \det \Pi_{G_n^{\text{odd}}}(w) &= \frac{\alpha_n}{(1 - \alpha_n)w - 1} (-\alpha_n u_n), \\ \det \Pi_{G_n^{\text{odd}}}(1) &= \alpha_n u_n.\end{aligned}$$

Therefore, for all n , we get

$$\det \Pi(1) = \alpha_{[n]} u_{[n]}.$$

Let $P(z, w)$ denote the characteristic polynomial of Γ_n , normalized so that

$$\det(zI + \Pi(w)) = \frac{\alpha_{\text{odd}}}{\prod_{i \text{ odd}} ((1 - \alpha_i)w - 1)} P(z, w).$$

Let $H_{(1,k)}$ denote the coefficient of zw^k in $P(z, w)$ for $k = 0, \dots, \frac{n}{2}$, so that when $k \in \{1, 2, \dots, \frac{n}{2} - 1\}$, they are the Hamiltonians of the cluster integrable system. Then, we have

$$\sum_{k=0}^{\frac{n}{2}} H_{(1,k)} w^k = \frac{\prod_{i=1}^{\frac{n}{2}} ((1 - \alpha_{2i-1})w - 1)}{\alpha_{\text{odd}}} \text{tr } \Pi(w).$$

Since each $(1 - \alpha_i)$ inside each of the matrices whose product is $\Pi(w)$ appears with a w , the homogeneous component of degree k in $1 - \alpha_1, 1 - \alpha_2, \dots, \alpha_n$ is $H_{(1,k)} w^k$.

Theorem 7.13. *Let $k \in \{1, 2, \dots, \lfloor \frac{n+1}{2} \rfloor - 1\}$ and let $\alpha_i = \alpha$ for all i . We have:*

1. *The homogeneous degree k component of $\sum_{d=0}^{\lfloor \frac{n}{2} \rfloor} H_{(1,d)}$ as a polynomial in the variables $\alpha_1, \dots, \alpha_n$ is, up to a sign, equal to*

$$\sqrt{X_{[n]} \alpha_{[n]}} \pi_{\vec{\alpha}}^* \circ \Lambda_{\vec{\alpha}}^* \left(\frac{F_k(c)}{\sqrt{c_{[n]}}} \right),$$

which is the product of the Casimir $\sqrt{X_{[n]} \alpha_{[n]}}$ with the pullback of an AFIT Hamiltonian.

2. *The homogeneous degree k component of $\sum_{d=0}^{\lfloor \frac{n}{2} \rfloor} H_{(1,d)}$ as a polynomial in $1 - \alpha_1, \dots, 1 - \alpha_n$ is the dimer Hamiltonian $H_{(1,k)}$.*

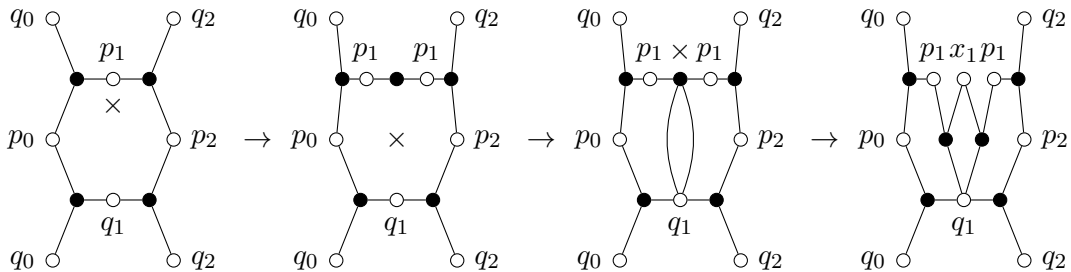


Figure 25. Step 1: Insertion of x_1 .

As in Theorem 7.9, we have the following.

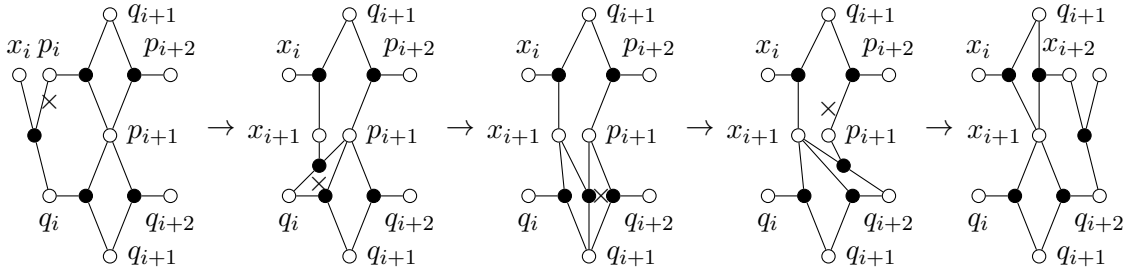


Figure 26. Step 2: Replacing (p_i, p_{i+1}) with (x_{i+1}, x_{i+2}) .

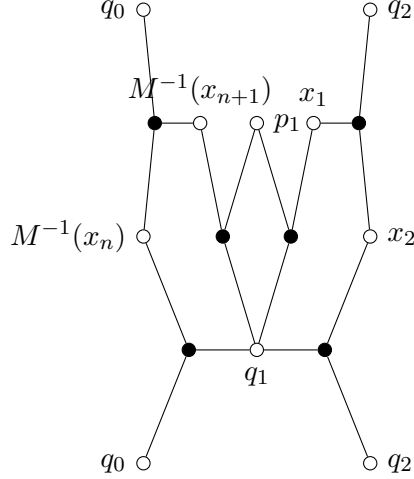


Figure 27. Step 3: Local configuration near p_1 after Step 2. Apply Step 1 backwards to obtain Γ_n .

Theorem 7.14. Suppose $[\text{wt}] \in \mathcal{X}_{N_{\Gamma_n}, \vec{\alpha}}^\lambda$ is such that $u^{-1} \circ \pi_{\vec{\alpha}}([\text{wt}]) = (p, q, M)$. Consider the sequence of moves shown in Figures 25, 26 and 27, and let μ denote the induced birational map of weights. Then, the following diagram commutes:

$$\begin{array}{ccc}
 \mathcal{X}_{N_{\Gamma_n}, \vec{\alpha}}^\lambda & \xrightarrow{u^{-1} \circ \pi_{\vec{\alpha}}} & \mathcal{U}_n \\
 \mu \downarrow & & \downarrow \nu_{\vec{\alpha}} \\
 \mathcal{X}_{N_{\Gamma_n}, \vec{\alpha}}^\lambda & \xrightarrow{u^{-1} \circ \pi_{\vec{\alpha}}} & \mathcal{U}_n
 \end{array}$$

We now explain how the sequence in Theorem 7.14 is related to geometric R -matrices. Let $n \geq 2$. We first transform the graphs Γ_n into graphs $\tilde{\Gamma}_n$ as follows. Recall that Γ_n possesses two zig-zag paths with homology $(1, 0)$, the path ξ_1 which goes through all the white vertices carrying the q_i 's and the path ξ_2 which goes through all the white vertices carrying the p_i 's. We modify the path ξ_2 by contracting all the 2-valent white vertices carrying points of the form p_{2i-1} with $1 \leq 2i-1 \leq n$ (this concerns every white vertex carrying a point of the form p_{2i-1} except in the odd n case the trivalent white vertex which carries p_1) and we horizontally expand all the white vertices carrying points of the form p_{2i} with $1 \leq 2i \leq n$, in such a way that each of the two new white vertices created by such an expansion is connected to one black neighbor in ξ_1 and to another black neighbor in ξ_2 . We call $\tilde{\Gamma}_n$ the graph obtained from this procedure. Using the terminology of [9], this corresponds to putting the 2-loop graph Γ_n in its 1-expanded form. We have depicted $\tilde{\Gamma}_6$ on Figure 28.

The sequence in Theorem 7.14 is a sequence of local moves on TCD maps starting and ending with a TCD map on Γ_n . It can be seen as a sequence of dimer local moves starting and ending

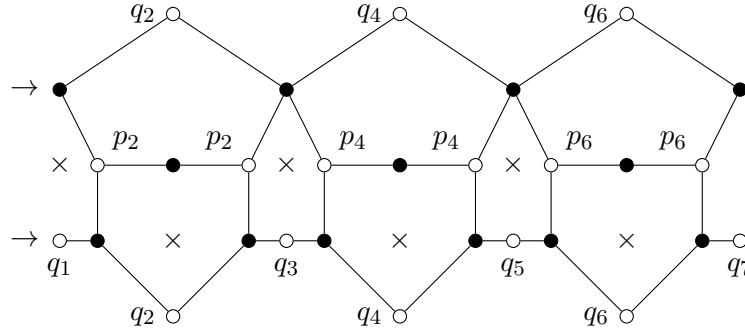


Figure 28. The graph $\tilde{\Gamma}_6$. The two arrows on the left indicate the two endpoints to which a bigon is attached and the stars indicate the string of hexagonal faces traversed by spider moves before coming back to the starting point and deleting the bigon.

with Γ_n . Since the transformation of Γ_n into $\tilde{\Gamma}_n$ only involves contractions and expansions of degree 2 vertices, the sequence can be turned into a sequence of dimer local moves starting and ending with $\tilde{\Gamma}_n$. Up to contractions and expansions of degree 2 vertices, the latter sequence of dimer local moves is exactly the one described above for the geometric R -matrix transformation.

A Schur complement

Suppose $M = \begin{bmatrix} A & B \\ C & D \end{bmatrix}$ is a $(p+q) \times (r+q)$ block matrix with D an invertible $q \times q$ matrix. Let $V := \text{coker } M$. Let e_i denote the i th basis column vector, and let $v_i \in V$ denote the image of e_i under the cokernel map. Let $M/D := A - BD^{-1}C$ denote the Schur complement.

Theorem A.1 (Schur determinant formula [43]). *If M is a square matrix ($p = r$), then we have*

$$\det(M) = \det(D) \det(M/D).$$

Theorem A.2. *$\text{coker } M/D \cong \text{coker } M$, and under this identification the cokernel map of M/D is $e_i \mapsto v_i$ for $i = 1, \dots, p$.*

Proof. After a change of basis, M takes the block diagonal form $\begin{bmatrix} M/D & 0 \\ 0 & D \end{bmatrix}$,

$$M = \begin{bmatrix} I & BD^{-1} \\ 0 & I \end{bmatrix} \begin{bmatrix} M/D & 0 \\ 0 & D \end{bmatrix} \begin{bmatrix} I & 0 \\ D^{-1}C & I \end{bmatrix}.$$

Since D is invertible, we have $\text{coker } D = 0$. Therefore, we have

$$\text{coker } M \cong \text{coker } M/D \oplus \text{coker } D \cong \text{coker } M/D.$$

Under the change of basis $\begin{bmatrix} I & BD^{-1} \\ 0 & I \end{bmatrix}$ of \mathbb{C}^{p+q} , we have

$$e_i \mapsto \begin{bmatrix} I & BD^{-1} \\ 0 & I \end{bmatrix}^{-1} e_i = e_i \quad \text{for } i = 1, 2, \dots, p,$$

from which we see that the cokernel map of M/D , when we identify $\text{coker } M/D$ with $\text{coker } M = V$, is given by $e_i \mapsto v_i$. ■

Acknowledgements

TG thanks Nick Ovenhouse for discussions about networks in a cylinder. SR thanks Ivan Izmistiev for discussions on cross-ratio dynamics during a visit at TU Wien, Anton Izosimov for comments on Newton polygons in the first version of this paper and Rei Inoue for exchanges on the geometric R -matrix. NA was supported by the Deutsche Forschungsgemeinschaft (DFG) Collaborative Research Center TRR 109 “Discretization in Geometry and Dynamics” and by the ENS-MHI chair funded by MHI. NA and SR were partially supported by the Agence Nationale de la Recherche, Grant Number ANR-18-CE40-0033 (ANR DIMERS). SR was also partially supported by the CNRS grant Tremplin@INP, which funded a visit of NA to Paris-Saclay.

References

- [1] Affolter N., Glick M., Pylyavskyy P., Ramassamy S., Vector-relation configurations and plabic graphs, *Selecta Math. (N.S.)* **30** (2024), 9, 55 pages, [arXiv:1908.06959](#).
- [2] Affolter N., Glick M., Ramassamy S., Triple crossing diagram maps and multiple cluster structures, in preparation.
- [3] Affolter N.C., Discrete differential geometry and cluster algebras via TCD maps, Ph.D. Thesis, Technische Universität Berlin, 2023, [arXiv:2305.02212](#).
- [4] Arnold M., Fuchs D., Izmistiev I., Tabachnikov S., Cross-ratio dynamics on ideal polygons, *Int. Math. Res. Not.* **2022** (2022), 6770–6853, [arXiv:1812.05337](#).
- [5] Berenstein A., Kazhdan D., Geometric and unipotent crystals, *Geom. Funct. Anal.* (2000), special issue, 188–236, [arXiv:math.QA/9912105](#).
- [6] Bobenko A., Pinkall U., Discrete isothermic surfaces, *J. Reine Angew. Math.* **475** (1996), 187–208.
- [7] Bobenko A.I., Suris Yu.B., Integrable systems on quad-graphs, *Int. Math. Res. Not.* **2002** (2002), 573–611, [arXiv:nlin.SI/0110004](#).
- [8] Bobenko A.I., Suris Yu.B., Discrete differential geometry. Integrable structure, *Grad. Stud. Math.*, Vol. 98, American Mathematical Society, Providence, RI, 2008, [arXiv:math.DG/0504358](#).
- [9] Chepuri S., Plabic R-matrices, *Publ. Res. Inst. Math. Sci.* **56** (2020), 281–351, [arXiv:1804.02059](#).
- [10] Cimasoni D., Reshetikhin N., Dimers on surface graphs and spin structures. II, *Comm. Math. Phys.* **281** (2008), 445–468, [arXiv:0704.0273](#).
- [11] Eager R., Franco S., Schaeffer K., Dimer models and integrable systems, *J. High Energy Phys.* **2012** (2012), no. 6, 106, 25 pages, [arXiv:1107.1244](#).
- [12] Etingof P., Geometric crystals and set-theoretical solutions to the quantum Yang–Baxter equation, *Comm. Algebra* **31** (2003), 1961–1973, [arXiv:math.QA/0112278](#).
- [13] Fock V.V., Goncharov A.B., Cluster ensembles, quantization and the dilogarithm, *Ann. Sci. Éc. Norm. Supér.* **42** (2009), 865–930, [arXiv:math.AG/0311245](#).
- [14] Fock V.V., Marshakov A., Loop groups, clusters, dimers and integrable systems, in Geometry and Quantization of Moduli Spaces, *Adv. Courses Math. CRM Barcelona*, Birkhäuser, Cham, 2016, 1–66, [arXiv:1401.1606](#).
- [15] Fomin S., Zelevinsky A., Cluster algebras. IV. Coefficients, *Compos. Math.* **143** (2007), 112–164, [arXiv:math.RA/0602259](#).
- [16] Gekhtman M., Shapiro M., Tabachnikov S., Vainshtein A., Integrable cluster dynamics of directed networks and pentagram maps, *Adv. Math.* **300** (2016), 390–450, [arXiv:1406.1883](#).
- [17] Gekhtman M., Shapiro M., Vainshtein A., Cluster algebras and Poisson geometry, *Mosc. Math. J.* **3** (2003), 899–934, [arXiv:math.QA/0208033](#).
- [18] Gekhtman M., Shapiro M., Vainshtein A., Poisson geometry of directed networks in an annulus, *J. Eur. Math. Soc.* **14** (2012), 541–570, [arXiv:0901.0020](#).
- [19] George T., Ramassamy S., Discrete dynamics in cluster integrable systems from geometric R -matrix transformations, *Comb. Theory* **3** (2023), 12, 29 pages, [arXiv:2208.10306](#).
- [20] Glick M., The pentagram map and Y -patterns, *Adv. Math.* **227** (2011), 1019–1045, [arXiv:1005.0598](#).
- [21] Glick M., Pylyavskyy P., Y -meshes and generalized pentagram maps, *Proc. Lond. Math. Soc.* **112** (2016), 753–797, [arXiv:1503.02057](#).

- [22] Glick M., Rupel D., Introduction to cluster algebras, in *Symmetries and Integrability of Difference Equations, CRM Ser. Math. Phys.*, Springer, Cham, 2017, 325–357, [arXiv:1803.08960](#).
- [23] Goncharov A.B., Kenyon R., Dimers and cluster integrable systems, *Ann. Sci. Éc. Norm. Supér.* **46** (2013), 747–813, [arXiv:1107.5588](#).
- [24] Hertrich-Jeromin U., Introduction to Möbius differential geometry, *London Math. Soc. Lecture Note Ser.*, Vol. 300, Cambridge University Press, Cambridge, 2003.
- [25] Hertrich-Jeromin U., McIntosh I., Norman P., Pedit F., Periodic discrete conformal maps, *J. Reine Angew. Math.* **534** (2001), 129–153, [arXiv:math.DG/9905112](#).
- [26] Inoue R., Lam T., Pylyavskyy P., Toric networks, geometric R -matrices and generalized discrete Toda lattices, *Comm. Math. Phys.* **347** (2016), 799–855, [arXiv:1504.03448](#).
- [27] Inoue R., Lam T., Pylyavskyy P., On the cluster nature and quantization of geometric R -matrices, *Publ. Res. Inst. Math. Sci.* **55** (2019), 25–78, [arXiv:1607.00722](#).
- [28] Izosimov A., Dimers, networks, and cluster integrable systems, *Geom. Funct. Anal.* **32** (2022), 861–880, [arXiv:2108.04975](#).
- [29] Izosimov A., Polygon recutting as a cluster integrable system, *Selecta Math. (N.S.)* **29** (2023), 21, 31 pages, [arXiv:2201.12503](#).
- [30] Kajiwara K., Noumi M., Yamada Y., Discrete dynamical systems with $W(A_{m-1}^{(1)} \times A_{n-1}^{(1)})$ symmetry, *Lett. Math. Phys.* **60** (2002), 211–219, [arXiv:nlin.SI/0106029](#).
- [31] Kang S.-J., Kashiwara M., Misra K.C., Miwa T., Nakashima T., Nakayashiki A., Affine crystals and vertex models, in *Infinite Analysis, Part A, B (Kyoto, 1991)*, *Adv. Ser. Math. Phys.*, Vol. 16, World Scientific Publishing, River Edge, NJ, 1992, 449–484.
- [32] Kashiwara M., Nakashima T., Okado M., Tropical R maps and affine geometric crystals, *Represent. Theory* **14** (2010), 446–509, [arXiv:0808.2411](#).
- [33] Kasteleyn P.W., Dimer statistics and phase transitions, *J. Math. Phys.* **4** (1963), 287–293.
- [34] Khesin B., Soloviev F., The geometry of dented pentagram maps, *J. Eur. Math. Soc.* **18** (2016), 147–179, [arXiv:1308.5363](#).
- [35] Lam T., Pylyavskyy P., Inverse problem in cylindrical electrical networks, *SIAM J. Appl. Math.* **72** (2012), 767–788, [arXiv:1104.4998](#).
- [36] Lam T., Pylyavskyy P., Total positivity in loop groups, I: Whirls and curls, *Adv. Math.* **230** (2012), 1222–1271, [arXiv:0812.0840](#).
- [37] Lam T., Pylyavskyy P., Crystals and total positivity on orientable surfaces, *Selecta Math. (N.S.)* **19** (2013), 173–235, [arXiv:1008.1949](#).
- [38] Lester J.A., Triangles. II. Complex triangle coordinates, *Aequationes Math.* **52** (1996), 215–245.
- [39] Nijhoff F., Capel H., The discrete Korteweg–de Vries equation, *Acta Appl. Math.* **39** (1995), 133–158.
- [40] Ovenhouse N., Non-commutative integrability of the Grassmann pentagram map, *Adv. Math.* **373** (2020), 107309, 56 pages, [arXiv:1810.11742](#).
- [41] Ovsienko V., Schwartz R., Tabachnikov S., The pentagram map: a discrete integrable system, *Comm. Math. Phys.* **299** (2010), 409–446, [arXiv:0810.5605](#).
- [42] Ovsienko V., Schwartz R.E., Tabachnikov S., Liouville–Arnold integrability of the pentagram map on closed polygons, *Duke Math. J.* **162** (2013), 2149–2196, [arXiv:1107.3633](#).
- [43] Schur J., Über Potenzreihen, die im Innern des Einheitskreises beschränkt sind, *J. Reine Angew. Math.* **147** (1917), 205–232.
- [44] Schwartz R., The pentagram map, *Experiment. Math.* **1** (1992), 71–81.
- [45] Schwartz R.E., Discrete monodromy, pentagrams, and the method of condensation, *J. Fixed Point Theory Appl.* **3** (2008), 379–409, [arXiv:0709.1264](#).
- [46] Soloviev F., Integrability of the pentagram map, *Duke Math. J.* **162** (2013), 2815–2853, [arXiv:1106.3950](#).
- [47] Springer T.A., Linear algebraic groups, 2nd ed., *Mod. Birkhäuser Class.*, Birkhäuser, Boston, MA, 2008.
- [48] Thurston D.P., From dominoes to hexagons, in *Proceedings of the 2014 Maui and 2015 Qinhuaangdao Conferences in Honour of Vaughan F.R. Jones’ 60th Birthday*, *Proc. Centre Math. Appl. Austral. Nat. Univ.*, Vol. 46, Australian National University, Canberra, 2017, 399–414, [arXiv:math.CO/0405482](#).
- [49] Weinreich M.H., The algebraic dynamics of the pentagram map, *Ergodic Theory Dynam. Systems* **43** (2023), 3460–3505, [arXiv:2104.06211](#).